Master Thesis
TVVR 17/5016

Evaluation of Seasonal Inflow Forecasting to Support Multipurpose Reservoir Management

A case study for the Upper Maule River Basin, Chile

Johan Visser

LUNDS UNIVERSITET
Lunds Tekniska Högskola

Division of Water Resources Engineering
Department of Building and Environmental Technology
Lund University

Evaluation of Seasonal Inflow Forecasting to Support Multipurpose Reservoir Management

A case study for the
Upper Maule River Basin, Chile

By:
Johan Visser

Master Thesis

Division of Water Resources Engineering
Department of Building & Environmental Technology
Lund University
Box 118
221 00 Lund, Sweden

Water Resources Engineering
TVVR-17/5016
ISSN 1101-9824

Lund 2017
www.tvrl.lth.se

Master Thesis
Division of Water Resources Engineering
Department of Building & Environmental Technology
Lund University

Title:	Evaluation of Seasonal Inflow Forecasting to Support Multipurpose Reservoir Management: A case study for the Upper Maule River Basin, Chile
Supervisor:	Magnus Persson - Department of Water Resources Engineering
Supervisor:	Michael Butts - Department of Water Resources, DHI Denmark
Examiner:	Rolf Larsson - Department of Water Resources Engineering
Language:	English
Year:	Spring 2017
Keywords:	Seasonal Forecasting, Reservoir Management, Ensemble Streamflow Prediction, Downscaling, Maule
Cover Photo:	Upper Maule River Basin © DHI

Abstract

Seasonal hydrological forecasts of future streamflow volumes can provide water resources managers with valuable information to improve long-term water resources planning and water use efficiency. The latest generation of coupled ocean-atmosphere general circulation models provides an opportunity for the prediction of hydroclimatic variables (e.g. precipitation, streamflow; soil moisture) at long lead times, which is central to water resources management, agriculture and disaster planning. However given the inherent uncertainty and the large-scale resolution of climate model forecasts compared to the catchment scale, there is a need to evaluate their accuracy and value for water management. This study systematically evaluates several seasonal hydrological forecasting options for a mountainous catchment in central Chile, to assess seasonal reservoir inflow forecast skill in comparison with conventional seasonal hydrological forecasting. We find, in comparison with resampled historical precipitation forecasts, that bias-corrected seasonal precipitation and temperature forecasts from the latest global climate models can improve the accuracy and skill of inflow forecasts during the high-rainfall season (April-October) forecasts with periods of above-average rainfall typically associated with the El Niño-Southern Oscillation (ENSO). For reservoir managers, this improvement in forecast skill provides valuable information related to aid long-term planning of water resources management and hydropower production. Due to greater predictability of predominantly snowmelt-based inflow during the low-rainfall season (October-April), accurate simulation of initial hydrological conditions such as reservoir water levels and accumulated snow, can provide accurate seasonal hydrological forecasts for longer lead times with the use of forecasted precipitation and temperature data. However, the improvements in inflow forecast accuracy and skill, during the low-rainfall season, are marginal when compared with an Extended Streamflow Prediction (ESP) approach.

Acknowledgements

This thesis has been produced during my scholarship period at Lund University, thanks to a Swedish Institute scholarship. I would like to give my sincerest gratitude to the Swedish Institute for providing me with this incredible opportunity as well as their continuous support throughout my journey.

I would like to thank my supervisor, Michael Butts, who provided me with the opportunity to conduct my thesis work at DHI, Denmark. Thank you for all of your guidance, input and support throughout this project. You have provided me with an incredible learning experience that I am sincerely grateful for.

Specials thanks to Helle Planteig for her friendly help and support through all of the administrative processes required to get a non-EU citizen working behind a computer in Denmark. I am indebted to Jacob Larsen for all his help in the configuration and running of MIKE Workbench. Thank you for helping me navigate the maize of projects files and your willingness to always help out on the multiple occasions I got stuck. Even through persistent model errors and a hard drive crash, your approach was always friendly and patient.

Special thanks to Peter Godiksen for introducing me to R and all of his support during the project. Many thanks to Roar Jensen for providing me with information on the project background and the configuration of the hydrological models. To my fellow interns at DHI, Suba, Michael and Adib, thank you for friendship and making our time together in the ‘garage’ so enjoyable.

Thank you to my supervisor at LTH, Magnus Persson, for all of your valuable input and support during this project. Many thanks to Rolf Larsson for his review and contribution to the improvement of this report.

Finally, to my parents and girlfriend back home in South Africa, thank you for all of your love and support during my time abroad. Knowing I have such a strong support system back home, provided me with tremendous motivation and focus to take on this challenge, and you therefore have a big share in this achievement.

Summary

Seasonal hydrological forecasts of future streamflow volumes can provide water resources managers with valuable information to improve long-term water resources planning and water use efficiency. The latest generation of Coupled Ocean-atmosphere General Circulation Models (CGCMs) provides an opportunity for the prediction of hydroclimatic variables (e.g. precipitation, streamflow; soil moisture) at long lead times, which is central to water resources management, agriculture and disaster planning. However given the inherent uncertainty and the large-scale resolution of climate model forecasts compared to the catchment scale, there is a need to evaluate their accuracy and value for water management at catchment scale, which is the scale at which water is managed.

This study systematically evaluates several seasonal hydrological forecasting options for a mountainous catchment in central Chile, to assess potential seasonal forecast skill improvement and added value over conventional seasonal hydrological forecasting approaches. Accurate prediction of seasonal inflows to the Colbún Reservoir, a large multipurpose dam located at the outlet of the Upper Maule River Basin, would provide valuable information to aid planning of long-term water resources management and hydropower generation.

Conventional climatology-and hydrological based seasonal forecast approaches are expressed through the methods of using resampled long-term observed inflow records to Colbún Reservoir, as well as through Extended Streamflow Prediction (ESP) using metrological forcing of resampled historical catchment precipitation records. Seasonal hydrological forecasting options based on the combined use of an ESP approach with meteorological forecasts from the latest CGCMs are evaluated against conventional methods. A combined ESP and CGCM seasonal hydrological forecasting system is used to assess multiple forecast options consisting of varied meteorological forecast variables, statistical downscaling procedures and hydrological model configurations.

Previous work indicates a high level of precipitation predictability in the study region due to the effects of El Niño-Southern Oscillation (ENSO) and streamflow predictability because of storage of water in the snow pack. As the catchment's rainfall season occurs in the austral winter, followed by a snowmelt period in spring, the study evaluates the potential improvement of seasonal hydrological forecast skill with the use of reforecast precipitation and temperature (snowmelt) data sourced from the coupled ocean-atmosphere dynamical forecast system, ECMWF-System 4. The application and impact of a linear statistical downscaling method is assessed to correct systematic biases in ECMWF-System 4 forecast ensembles due to forecast model limitations such as computational demands, limited observational data for initial conditions, and approximation of physical processes,

Seasonal streamflow forecasts for selected years are generated using a suite of hydrological models and data processing tools. The conceptual NAM rainfall-runoff

model is used for catchment runoff generation. Output from the NAM model is used as input into the river basin management and planning tool MIKE HYDRO Basin. MIKE HYDRO Basin is used to represent the rivers, reservoirs, water users and water diversions in the Upper Maule River Basin. The incorporation of Data Assimilation (DA) of streamflow and reservoir levels to observed levels, and its impacts on seasonal inflow forecast accuracy, is assessed. MIKE Workbench is used for the establishment of model links between the NAM and MIKE HYDRO Basin models and the configuration of forecast simulations and automated workflows.

A number of forecast verification methods are used to evaluate seasonal hydrological forecast performance in terms of forecast bias against observed values, and forecast accuracy compared to conventional ESP based seasonal forecast approaches. Results of seasonal inflow forecast over the high-rainfall season (April-October) indicate seasonal forecast improvement in terms of model bias and forecast skill with the use of bias corrected forecasted precipitation data. An increased seasonal forecast model bias and reduction in forecast skill however occurs during periods of below-average precipitation, due to the overestimation of seasonal precipitation based on the use long-term monthly average bias correction scaling factors. A general reduction in seasonal forecast accuracy is observed after lead month 2. Average percentage volume errors at the end of the 7-month high-rainfall season forecast period were calculated as 12.6% for bias corrected CGCM based seasonal inflow forecast versus 19.5% for an ESP based approach using resampled historical precipitation.

Results for seasonal inflow forecasts over the low-rainfall season (October-April) indicate a large overall reduction in model bias compared to high-rainfall season forecasts, due to increased predictability of predominantly snowmelt based inflow. Introduction of bias corrected temperature forecasts resulted in small decrease of forecast model bias and increase in forecast accuracy. The use of bias corrected precipitation data results in increased forecast skill for above-average precipitation years, but overestimations of precipitation during periods of below-average precipitation. A general reduction in seasonal forecast skill is observed after lead month 2. Average percentage volume errors at the end of the 7-month low-rainfall season forecast period were calculated as 7.3% for bias corrected CGCM based seasonal inflow forecast versus 7.6% for a for an ESP based approach using resampled historical precipitation.

Data Assimilation (DA) of reservoir levels and streamflows over the hindcast periods, provides improved forecast accuracy and skill predominantly over the initial forecast lead months. For simulation periods where a good match between simulated and observed records are been obtained, Data Assimilation (DA) of reservoir levels and streamflow provides limited forecast improvement over the hindcast and forecast period. Although inclusion of DA provides a more accurate representation of initial hydrological conditions and total accumulated inflow volume at Time of Forecast (ToF), simulation model biases can however still be present in the forecast period.

The study shows that the use of bias corrected seasonal precipitation and temperature forecasts from the latest global climate models over resampled historical

meteorological data, can improve seasonal hydrological forecast accuracy and skill over periods of above-average rainfall typically associate with the El Niño-Southern Oscillation (ENSO). For reservoir managers, this improvement in forecast skill provides valuable information related to potential hydrological effects of ocean–atmosphere teleconnections, to aid long-term planning of water resources management and hydropower production. Due to increased predictability of predominantly snowmelt-based inflow during the low-rainfall season, accurate simulation of initial hydrological conditions such as reservoir water level and accumulated snow, can provide accurate low-rainfall seasonal hydrological forecasts for long lead times with the use of forecasted precipitation and temperature data. Increases in forecast accuracy and skill over an ESP based approach was however marginal.

It is recommended that additional seasonal inflow forecasts based on the combined ESP and CGCM model approach be conducted for additional forecast periods and historical years to evaluate forecast performance under varied hydrological conditions. Analysis of additional statistical downscaling methods such as quantile mapping is recommended due to high annual variability of catchment precipitation. Incorporation of DA of snow measurements is also recommended for more accurate representation of the snowpack volume, due to its important role is the hydrological cycle of the study area.

Acronyms and Abbreviations

Term	Description
BC	Bias Correction
CGCM	Coupled ocean-atmosphere General Circulation Models
DA	Data Assimilation
ENSO	El Niño-Southern Oscillation
ECMWF	European Centre for Medium range Weather Forecasting
ECOMS	European Climate Observations, Modelling and Services initiative
EoS	End of Simulation
GCM	General Circulation Model / Global Climate Model
IHC	Initial Hydrologic Conditions
LS	Linear Scaling
MAP	Mean Annual Precipitation
MAR	Mean Annual Runoff
masl	meters above sea level
MW	Megawatt
NAM	Nedbør Afstrømnings Model
ONI	Oceanic Niño Index
RCM	Regional Climate Model
RPS	Ranked Probability Score
RPSS	Ranked Probability Skill Score
S4	System 4
SoS	Start of Simulation
SST	Sea Surface Temperature
SVZ	Southern Volcanic Zone
ToF	Time of Forecast
UDG	User Data Gateway
UMRB	Upper Maule River Basin

Table of Contents

List of Figures

List of Tables

Appendices

1 Introduction

1.1 Background

The effective and equitable management of conflicting water user demands such as domestic water supply, hydropower generation, and agriculture, can provide substantial economic benefits to ensure energy, food, and water security. For water managers, accurate predictions of future streamflow volumes can provide valuable information to aid decision-making and management of a valuable and limited resource.

Seasonal or long-range forecasting of precipitation and streamflow, has been incorporated into many water resources projects, with particular application to reservoir management (Gelfan, et al., 2015; Arenaa, et al., 2015; Dixon & Wilby, 2015). With the aid of hydrological modelling and optimisation tools, seasonal forecasted meteorological variables such as precipitation and temperature, can be incorporated into existing hydrological models to provide an estimation of future streamflows under a variety of historical conditions or climate change scenarios (Etkin, 2009).

The reliability and accuracy of seasonal streamflow forecasts depend on a number of factors, including the hydrological model configuration and calibration as well as the skill and resolution of climate variable forecasts. In a study across Europe, Bierkens & Beek (2009) found that seasonal forecasting skill is highly dependent on the correct simulation of initial catchment conditions related to water storages such as soil moisture and surface water storage.

Continent- or country scale seasonal hydrological forecasting systems however usually do not incorporate water related infrastructure at local scale such as reservoirs, canals, river diversions and major water users. In regions with high seasonal and interannual variability in runoff, artificial surface water storages such as dams are constructed to increase the seasonal carry-over storage and increase water security. There is thus an opportunity to investigate the potential use of seasonal hydrological forecasting systems at a local scale to provide valuable information to local water managers and water users.

In some regions of the world, local seasonal and interannual weather patterns can be greatly affected by large-scale atmospheric circulation patterns known as teleconnections (Rivera, et al., 2012). The latest seasonal forecasting systems in operation are based on Coupled Global Circulation Models (CGCMs) primarily consisting of a coupled ocean-atmosphere dynamic simulation model. These latest forecasting models are able to better simulate slowly varying teleconnections signals in a climate system that contains memory, such as sea surface temperature (SST), which is related to the relatively high heat storage capacity of water (MacLachlan, et al., 2015). While the effects of large-scale teleconnections on regional and local weather can vary greatly in intensity and duration, early detection of potential

teleconnection development can provide valuable information related to early estimations of seasonal precipitation and associated runoff.

This study evaluates the use of seasonal hydrological forecasting in the Upper Maule River Basin located in central Chile. The Colbún Reservoir, situated at the outlet of the basin, is a large multipurpose dam supplying water for hydropower generation and large scale irrigation. Western South America is subject to considerable inter-annual climate variability due to El Niño-Southern Oscillation (ENSO), thus forecasting of inter-annual streamflow variations associated with ENSO would provide an opportunity to optimise water management decisions based on seasonal predictions (Rivera, et al., 2012). An initial study by DHI (2011) indicated a high level of rainfall predictability in the study region related to the effects of the ENSO as well as seasonal streamflow predictability based on the volume of the basin's snow pack. Accurate seasonal inflow forecasts can therefore provide valuable information to reservoir managers to improve long-term water resources planning and water use efficiency.

1.2 Objectives

The main objective of this project work is to explore the added value associated with the use of seasonal hydrological forecasts for long-term decision-making in reservoir operation for the Upper Maule River Basin in central Chile. To determine the added value of seasonal hydrological forecasts for decision-making in reservoir operation, the project will systematically evaluate the potential increase in seasonal forecast accuracy and skill of several seasonal hydrological forecasting options over conventional climatology based approaches.

As the basin's rainfall season occurs in the austral winter, followed by a snowmelt period in spring, the study will evaluate the value of forecasting precipitation and temperature (snowmelt) or both, for predicting reservoir inflows. The ability of the latest generation of CGCMs to capture the effects of global climate patterns such as ENSO would be examined, as well the corresponding impacts on rainfall and hydrology. Due to the varied reliability of seasonal precipitation forecasts with geographical location and scale, the value of using these forecasts for small scale hydrological forecasting will be assessed.

The sources and contributions of uncertainty in seasonal hydrological forecasts are identified and potential methods to reduce uncertainty will be examine through 1) Data Assimilation (DA) of reservoir levels and streamflows, and 2) bias correction of meteorological forecast data with the used of observed data.

The objectives of this study can be summarised to the evaluation of following points:

- The added value associated with the use of seasonal forecasts for long-term decision-making in reservoir operation for the Upper Maule River Basin in central Chile.

- Climate-model based seasonal forecast model performance against conventional climatology-and hydrological based forecast seasonal approaches;
- The ability of the latest generation of global climate-ocean models to capture the effects of global climate patterns such as ENSO are examined for this study area;
- The added value of forecasting precipitation and temperature (for snowmelt) and both, for predicting reservoir inflows and water resource management;
- The improvement of initial hydrological conditions and seasonal forecast performance through incorporation of DA of reservoir levels and streamflows;
- Evaluation of bias correction of meteorological forecast data and its effect on seasonal forecast performance.

2 Seasonal Forecasting

2.1 Background

A key element in achieving sustainable and risk based water resources management, is forecasting the future condition of surface water resources (Sudheer, et al., 2014). Accurate prediction of future hydrological states can provide valuable information to aid water resources mangers in the efficient operation of water related infrastructure and mitigation of the effects of natural disasters and climate variability.

A hydrological forecast is an estimation of the future states of hydrological variables. Hydrological forecasts typically aim to convert meteorological observations and forecasts into estimates of future river flows (Sene, 2010). Forecasting techniques can include rainfall-runoff hydrological models as well as hydrodynamic flow routing models. Additional model components can be required for water quality applications, and for inducing catchment specific features such reservoirs, wetlands, water users and snowmelt.

The prediction of future hydrological states can be categorized based on the forecast horizon. WMO (2009) provides the following classification for hydrological forecasts:

a) Short-term hydrological forecasts, which cover a period of up to two days;
b) Medium-range hydrological forecasts, which apply to a period ranging from 2 to 10 days;
c) Long-range hydrological forecasts, which refer to a period exceeding 10 days.

Seasonal hydrological forecasting aims to predict the future states of hydrological variables (e.g. streamflow, soil moisture) at monthly to seasonal time scales (Yuan, et al., 2015). Seasonal hydrological forecasting, also referred to as long-term hydrological forecasting, is essential for the forecast and mitigation of persistent hydrological phenomena such as droughts. Successful performance of seasonal forecasts systems requires accurate representation of initial catchment conditions (e.g. streamflow, soil moisture, snow cover) that contain memory in hydrological systems, as well as skilful seasonal forecasts of meteorological forcing variables (e.g. precipitation and temperature) used in hydrological models (Shukla & Lettenmaier, 2011; Yuan, et al., 2015).

2.2 Benefits and Limitations

Accurate and reliable seasonal hydrological forecasts can provide valuable information to water resources mangers and provide large potential socioeconomic benefits to interrelated sectors such as water, health, energy, agriculture and food security. Hydrological extremes such as floods and droughts can have severe and long lasting socioeconomic impacts on affected areas. Improved streamflow predictions can aid in the reductions of losses associated with hydrological extremes events, to

the extent of flood and drought mitigated through management of water resources stored in reservoirs (Wood & Lettenmaier, 2006). In years with non-occurrence of hydrological extreme events, accurate seasonal hydrological forecasts can still provide potential economic benefits. Yao and Georgakakos (2001) found that reliable inflow forecasts and adaptive decision systems can substantially benefit reservoir performance, with the potential to increase hydropower revenues through incorporation of climate information in hydrological forecasts. Brumbelow & Georgakakos (2001) showed the potenial benefits of improved hydrological forecast related to the mananagement of agricultural water supply.

Despite the potential benefits of improved seasonal forecasting systems, the majority of operational hydrological forecasting systems of long lead times are based on methods and data sources that have been in place for over 50 years (Wood & Lettenmaier, 2006). One of the contributing factors is that long-term meteorological predictability is quite limited. Shorter-term meteorological forecasts based on atmospheric modelling have skill for approximate time horizons of two weeks (Higgins, 2015), potentially providing only a marginal improvement over long-term climatic averages. Climate and weather forecast skill has however improved significantly over recent decades due to technological advancement in computational power, increased model spatial and temporal resolution and improved observation capabilities for boundary model forcing such as sea surface temperature (SST) (Wood & Lettenmaier, 2006). Hydrological modelling improvements have however been more limited due to the physical processes that control runoff generation contain longer memory and are more spatially varied than those that control weather and climate (Wood & Lettenmaier, 2006; Goddard, et al., 2001).

The majority of seasonal hydrological forecast are limited to forecast lead times of 1 to 3 months, primarily due to the limited skill of meteorological forecasts at longer lead times. The successful performance of seasonal hydrological forecast systems is therefore highly reliant on the accuracy of meteorological forecasts and the accurate representation of initial catchment conditions that contain memory related to for example, the land surface moisture states (Shukla & Lettenmaier, 2011).

Wood & Lettenmaier (2008) showed that seasonal streamflow volumes for northern Californian regions with high snow pack accumulation could be forecasted with reasonable accuracy for lead times up to five months. Forecast accuracy was found to be related to the physically constrained evolution of initial land surface moisture states, from snow accumulation in the winter wet season and melting in spring. Relating snowpack volumes to the subsequent spring and summer runoff through regression methods has been used for decades (Pagano & Garen, 2004). Forecasts made following drier summer periods do not include the snowpack volumes that influences hydrological fluxes. Therefore, seasonal hydrological forecasts over these dry seasons are more dependent on initial soil moisture conditions and accuracy of meteorological forecasts (Maurer & Lettenmaier, 2003).

2.3 Uncertainty in forecasts

The primary objective of seasonal hydrological forecasting is to provide predicted future streamflows of sufficient accuracy at a maximum lead time. This allows for water resources managers and users to take appropriate action to mitigate losses and increase water use efficiency (WMO, 2009). Shukla & Lettenmaier (2011) indicated that the two key factors limiting seasonal hydrological forecast skill are (1) uncertainties in the Initial Hydrological Conditions (IHC) associated with uncertainties in hydrological model prediction skill and meteorological forcing over the hindcast period; and (2) climate forecast skill over the forecast period.

Meteorological forecasts have been seen as the main source of uncertainty in hydrological forecast systems for some years due to the attempt to essentially model a chaotic atmosphere. With regards to hydrological models, there are four main sources of uncertainty related to deterministic flow modelling, which are (1) random or systematic errors in the model inputs or boundary condition data; (2) random or systematic errors in the recorded output data; (3) uncertainty due to sub-optimal parameter values; and (4) errors due to incomplete or biased model structure (Beven & Freer, 2001; Madsen, 2003; Butts, et al., 2004).

Numerous attempts have however been made by researchers in the hydrological and climate communities to reduce the uncertainties associated with seasonal hydrological forecasting. For example, various researchers have investigated methods for assimilating observed hydrological data (e.g. streamflow, reservoir level, snow cover) to improve the IHCs for seasonal hydrological forecast (Shukla & Lettenmaier, 2011; Wood & Lettenmaier, 2006; Clark, et al., 2006). The latest generation of coupled atmosphere-ocean-land general circulation models (CGCMs) can also improve the accuracy of seasonal meteorological forecasts over periods where meteorological forcing variables play a significant role in runoff generation compared to IHC.

2.4 Current methods

Traditional seasonal hydrological forecasting approaches are based on time series modelling, by relating large-scale climate indices such as Sea Surface Temperature (SST) and/or local IHC with hydrological predictands (Yuan, et al., 2015). With the increased use of conceptual and distributed hydrological models, seasonal hydrological forecast with the aid of such models became popular. One example is the Extended Streamflow Prediction (ESP), also known as Ensemble Streamflow Prediction, which was first introduced by the US National Weather Service (NWS) in 1977 and still used in modern streamflow forecasting systems (Twedt, 1977; Najafi, et al., 2012).

An ESP based forecast system initialises a hydrological model with current IHC's, and runs forecast simulations based on resampled long-term historical records of observed meteorological forcing variables such as precipitation and temperature. The ESP approach can be useful over certain seasonal periods where long term memory of land surface moisture states (e.g. soil moisture, snow cover, reservoirs) have an

strong influence on forecast accuracy. ESP based seasonal forecast skill however decreases significantly over most regions of the world after a period of 1 month (Shukla, et al., 2013). Therefore, the seasonal predictability of meteorological forcing variables has to be taken into account for long-term hydrological forecasting systems.

Coupled ocean-atmosphere general circulation models (CGCMs) are the main sources of seasonal precipitation forecasts by some of the main operational meteorological centres, including the European Centre for Medium-Range Weather Forecasts (ECMWF) and the United States (US) National Centers for Environmental Prediction (NCEP). In recent years, there has been great improvement in model physics, data inputs, and computational power of CGCMs (Peng, et al., 2014). CGCM forecasts are typically produced as probabilistic based ensembles through multiple model initializations of different initial conditions and physical parameterizations, to account for various uncertainties. Limitations of CGCMs such as computational demands, limited observational data for initial conditions, and approximation of physical processes, can lead to systematic biases in model output ensemble spreads (Molteni, et al., 2011).

Multiple statistical and dynamical downscaling techniques have been developed to overcome such model biases. Statistical downscaling methods establish a statistical relationship between a local observed variable (predictand) and a larger scale variable modelled by a CGCM (predictor) (Wetterhall, et al., 2012; Bárdossy & Pegram, 2011). Dynamical downscaling uses output data from a CGCM as boundary conditions for a smaller scale Regional Climate Model (RCM) which induced multiple feedback processes related to radiation and water balances.

The continuous development and improvement of CGCMs for seasonal climate predictions has however improved the understanding and representation of ocean–atmosphere teleconnections such as El Niño-Southern Oscillation (ENSO), as well a land–atmosphere coupling that form the basis of seasonal climate forecasts (Yuan, et al., 2015). Consequently the combined use of an ESP approach with meteorological forecasts from CGCMs, has received more attention over recent years (Mo & Lettenmaier, 2014; Yuan, et al., 2013).

A combined ESP and CGCM seasonal hydrological forecast system typically consists of initialization procedures, pre-processing statistical or dynamical downscaling procedures, hydrological models, and hydrological post-processing procedures. While combined forecasting systems may share similar initialization procedures to ESP, the key difference is the use of climatic variable forecasts from CGCM over the seasonal forecast period. The selection and configuration of seasonal hydrological forecast model components and climatic variable inputs is therefore of key importance to ensure an ensemble forecast of sufficient skill.

3 Study Area

3.1 Introduction

The Upper Maule River Basin is located in central Chile within the 7th Maule Region, one of Chile 15 first order administrative divisions. The region derives its name from the 240 km long Maule River draining westwards from the Andes, bisecting the Region before draining into the Pacific Ocean, just north of the city of Constitución (see *Figure 3-1*). The total surface area of the Maule River Basin is approximately 20,295 km^2. The local climate is temperate humid (Mediterranean) characterized by dry summers and high rainfall during the austral winter months (Pizarro-Tapia, et al., 2014).

The Maule River is an important source of water and alluvial soils used for agricultural practices in parts of the Central Valley situated between the foothills of the Andes mountain range and the parallel coastal mountain range. The Region's economy is largely driven by forestry and agriculture, led by commercial winemaking developed from traditional activity along the Maule Valley. The Maule River provides inflow for five hydropower generating plants in the region through a series of reservoirs, run-of-river and tunnel diversions. The Maule River is also of great historic importance, as it demarcated the southern limits of the Inca Empire (Cobo & Hamilton, 1979).

This study will focus on the Upper Maule River Basin, a subcatchment of the larger Maule River Basin, which constitutes the drainage area upstream of the Colbún Reservoir to the headwaters of the Maule River along the Andes mountain range and border with Argentina.

3.2 Topography

The Upper Maule River Basin encapsulates the 5741 km^2 area upstream, predominantly to the east and southeast, of the Colbún Reservoir at an elevation of 425 masl (see *Figure 3-2*). The basin area is enclosed by mountain ranges that form part of the Southern Volcanic Zone (SVZ) of the Andean Volcanic Belt. The eastern catchment divide, approximately 75 km east from the Colbún Reservoir, is created by the Andes mountain range ridgeline at an approximation elevation of 3000 masl. This ridgeline also forms the national border between Chile and Argentina. The highest elevation in the catchment is the summit of the stratovolcano *Descabezado Grande* (3953 masl), located approximately 40 km east from the Colbún Reservoir in the northern edge of the catchment and the SVZ. The majority of the catchment extends upstream in a south-southeast direction forming the drainage basin of the Melado River, forming a southern and south-western catchment divide at an elevation of approximately 2200 masl.

3.3 Drainage

The Maule River originates at Laguna de Maule, located in proximity to the Argentinean border at an elevation of 2163 masl (see *Figure 3-2*). From the headwaters, the river drains westward and is joined on its right bank by rivers Puelche, Cipreses and Claro. Near the confluence with the Claro River, the Maule River is joined on its left bank by the Meldo River, a major tributary originating from Laguna Dial located near the southern boundary of the basin. A short distance downstream of this major confluence, the Maule River flows into the 1420 million m^3 capacity Colbún reservoir, forming the controlled outlet of the Upper Maule River Basin.

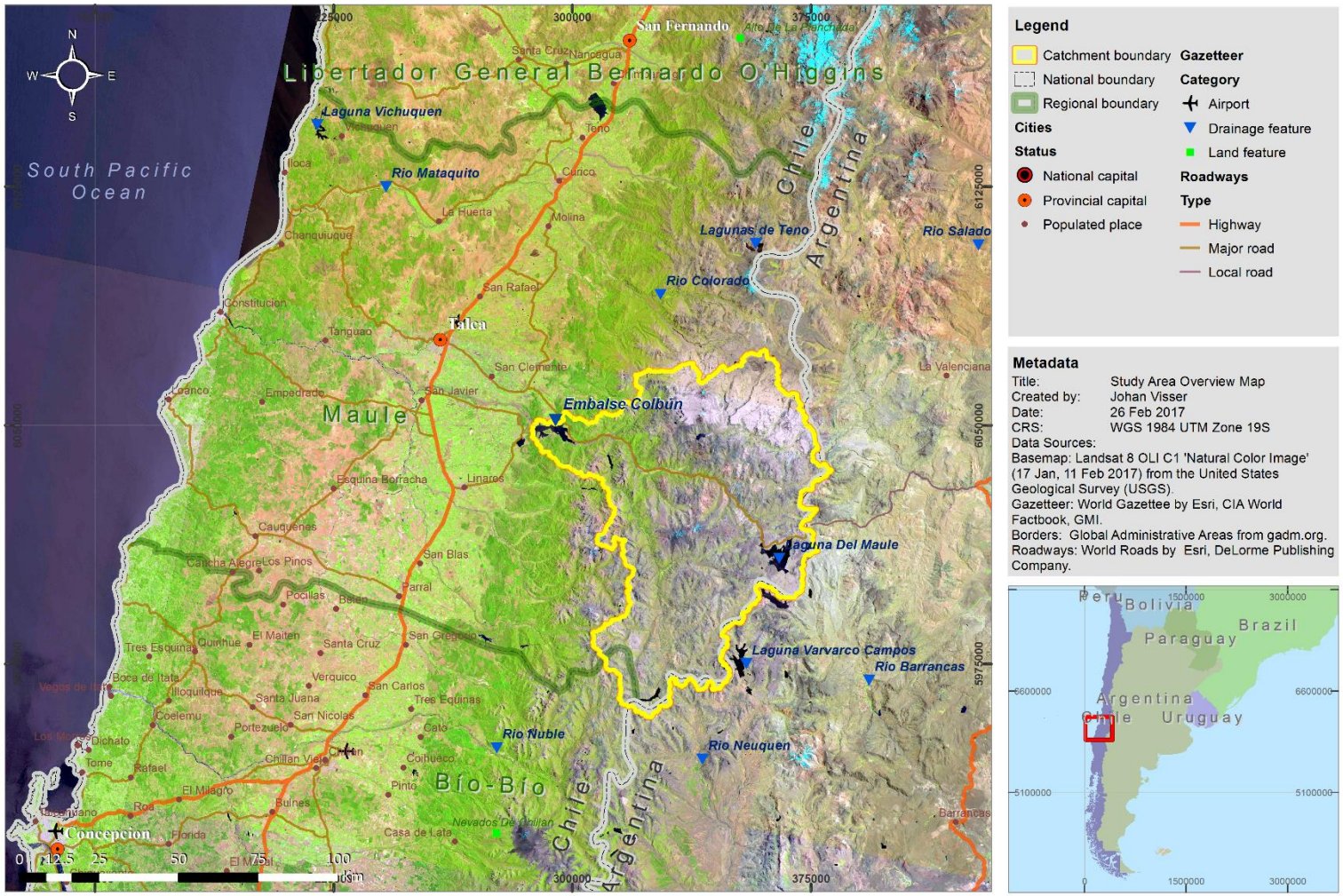

Figure 3-1 | Study Area Overview Map

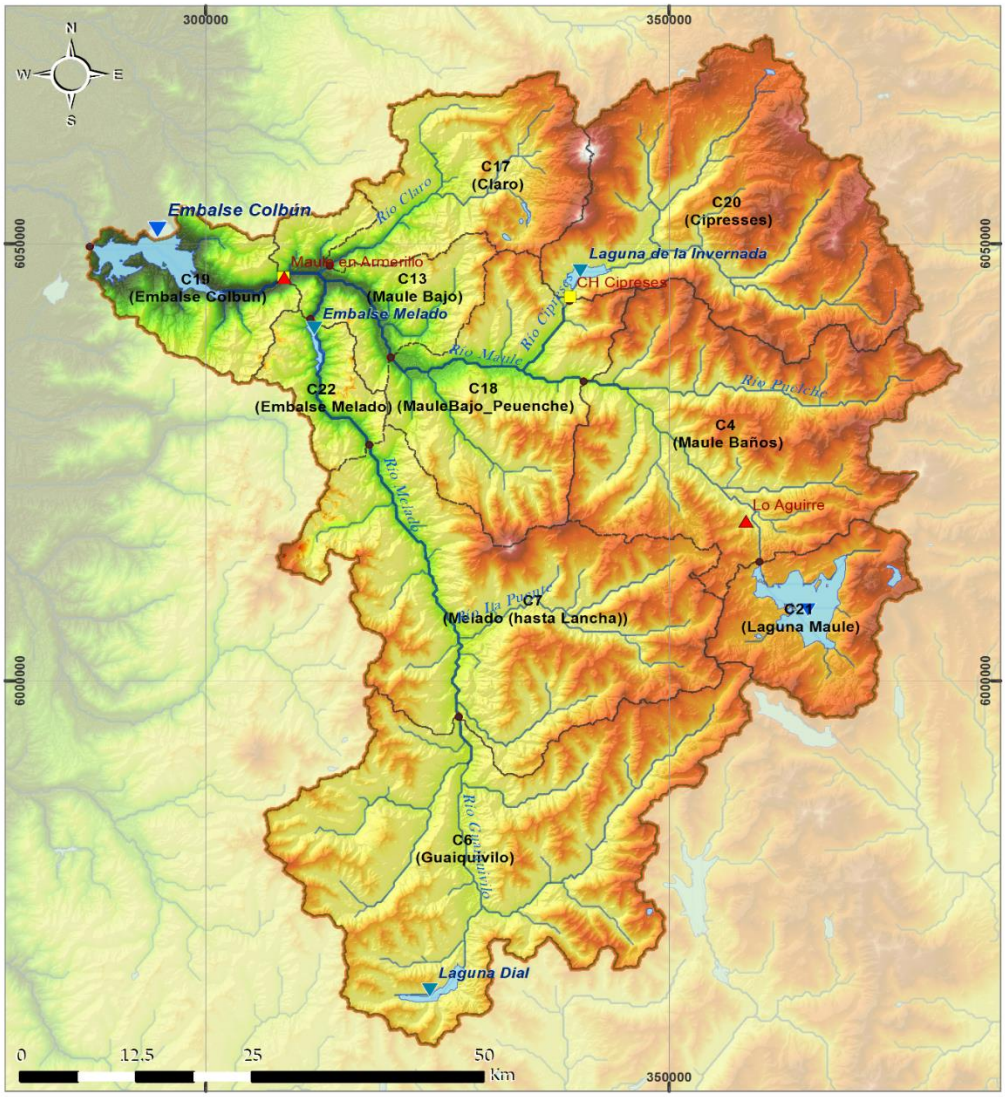

Legend

- Catchment boundary
- Stream network
- Subbasin boundary
- Subbasin outlet
- Lake/Reservoir

Gazetteer

Category

- Drainage feature
- Rainfall Station
- Temperature Station

Elevation (masl)

Value

- High : 4000
- Low : 400

Metadata

Title:	Subbasin Map
Created by:	Johan Visser
Date:	04 March 2017
CRS:	WGS 1984 UTM Zone 19S

Data Sources:
DEM: SRTM 1 Arc-Second Global from the United States Geological Survey (USGS);
Stream Network: HydroSHEDS (Lehner, B. et al., 2008);
Lakes: HydroLAKES (Messager, M.L., et al., 2016). Data from hydrosheds.org;
Gazetteer: World Gazettee by Esri, CIA World Factbook, GMI.

Figure 3-2 | Upper Maule River Basin Drainage Map

4 Data Collection and Review

4.1 Previous work

DHI was contracted by Chilean utility company, Colbún S.A., to establish a real-time modelling system for both short-term and long-term forecasting of inflows to the Colbún Reservoir (DHI, 2011). Colbún S.A. is a power generation company in Chile, with a countrywide energy generating capacity of approximately 3279 MW from a mix of sources. The forecast modelling system was developed and put into operation in 2011 for one of Colbún S.A.'s larger hydropower plants, namely the 474 MW Colbún hydropower station located in the Upper Maule River Basin. Water resources in the basin are shared with upstream power producers as well as with extensive irrigation schemes.

The implemented modelling system, which is also used in this study, is based on the NAM rainfall-runoff model and the river- and reservoir regulation model, MIKE HYDRO Basin (see *Table 4-1*). The seasonal forecast model for Colbún S.A. is based on historical flows and rainfall until time of forecast, and then using the Extended Streamflow Prediction (ESP) method based on historical rainfall to predict a range of future streamflow. The system enabled Colbún S.A. to safely operate the reservoir during forecasted flood events and optimise energy generation more effectively, reducing potential downstream property damage and loss of life.

Table 4-1 | Colbún S.A. Forecast Model Components

Rainfall-Runoff Model	NAM
Reservoir- and River Regulation Model	MIKE Basin
Real-time Modelling System	MIKE IPO

Hydrological data and relevant information for the study area was largely collected from established DHI project models and accompanying reports (DHI, 2011; Panthi, 2016). Collected data was reviewed based on its intended application for seasonal forecasting and is discussed in following sections. Information about the configuration and operation of the hydrological models and forecasting system is discussed in *Chapter 5.3*.

4.2 Precipitation

Precipitation in the Upper Maule River Basin is highly seasonal, with the onset of rainfall season starting in April and reaching a maximum around June. In this study, referral to the hydrological year therefore implies the 12-month period from 01 April to 31 March. The large majority of precipitation in the basin occurs within the austral winter months from May to August. Following this period, precipitation decreases and a significantly lower amount of precipitation is experienced through the spring

and summer period from September to March. *Figure 4-1* presents the average monthly precipitation per hydrological year for rainfall station *Armerillo*, located approximately 7 km upstream of the Colbún Reservoir (see *Figure 3-2*).

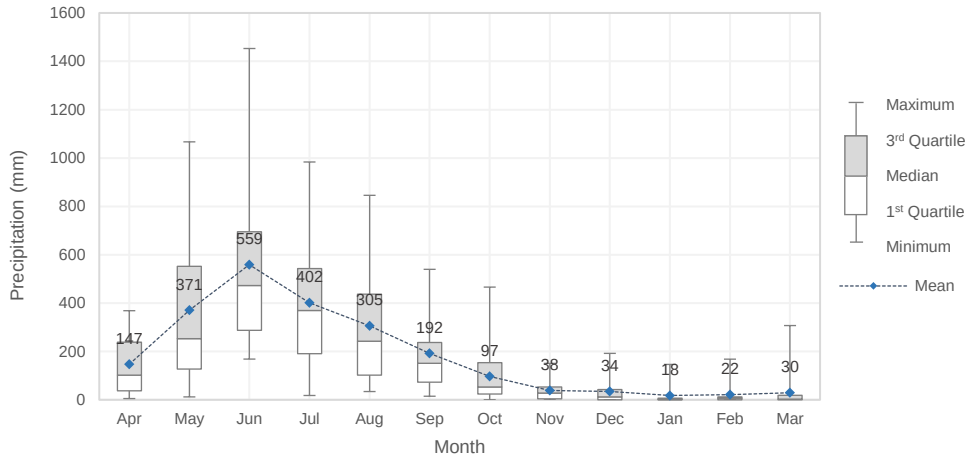

Figure 4-1 | Rainfall station Armerillo average monthly precipitation (1991-2008)

The average annual precipitation for the *Armerillo* station is approximately 2200 mm. From *Figure 4-1* it can be seen that greatest amount of precipitation and variability occurs during the austral winter months, with considerable annual variation occurring during the peak precipitation months of May and June. After this period, a steady decrease in average monthly rainfall occurs until the month of February. A small increase occurs in March, followed by a significant increase in average monthly precipitation occurs during April, at the onset of the hydrological year.

4.2.1 Spatial distribution of precipitation

Due to limited availability of observed rainfall data, catchment precipitation files for the established NAM model subcatchments were largely based on the *Armerillo* (509 masl) and *Cipreses* (933 masl) rainfall station records. The shorter records of additional stations and their locations, predominantly in the valleys, provided limited additional information on rainfall distribution and variation with elevation. In addition to rainfall measurements, snow pack observations are available for a number of mountain stations in the study area (see *Figure 4-2*). Information on rainfall and snow data availability for the study area can be found within the original hydrology project report (DHI, 2011).

Additional information on the spatial distribution of precipitation in the study area was obtained from the NASA Tropical Rainfall Measuring Mission (TRMM). Satellite based precipitation data at a 27 x 27 km grid cell resolution was obtained for

the period between 2005 and 2010. This data was primarily used on a qualitative basis and limited comparisons to the ground observations during the low-rainfall season (Oct-Mar) were made.

Based on the available information, catchment precipitation files were produced for each established subcatchment of the study area for the period between 1991 and 2011. Mean Annual Precipitation (MAP) values per subcatchment are presented in *Table 4-2* and the spatial distribution of mean annual rainfall is shown in *Figure 4-2*.

Table 4-2 | NAM model and subbasin average rainfall per hydrological year (Apr-Mar)

Subbasin no.	Name	Area	Mean Annual Precipitation (MAP)
-	-	km²	mm
C17	Claro	400.9	1911
C20	Cipresses	867.1	1257
C19	Embalse Colbun	268.0	1083
C22	Embalse Melado	142.2	1904
C6	Guaiquivilo	1155.1	1218
C21	Laguna Maule	308.7	1106
C13	MauleBajo I	505.8	1751
C18	Maule Bajo II	255.4	1751
C4	Maule Baños	861.85	1086
C7	Melado	976.0	1419
	Total	**5741.0**	

From *Figure 4-2* it can be seen than annual precipitation varies significantly throughout the Upper Maule River Basin. Higher annual precipitation is experienced towards the north-western region of the basin. Increased precipitation in this region is due to the orographic effect of Andes mountain range, with the associated rain shadow effect decrease precipitation towards to east. The *Armerillo* rainfall gauge location (see *Figure 4-2*) appears to be located at the region of highest annual rainfall in the basin.

Precipitation towards to southern end of the basin also decreases. Possibly due to the protective mountain ridgeline on the western edge of the basin. There are also only a limited number of precipitation stations in the eastern and southernmost areas of the basin. Thus, estimations of precipitation distribution at higher altitudes in the basin elevation are highly uncertain.

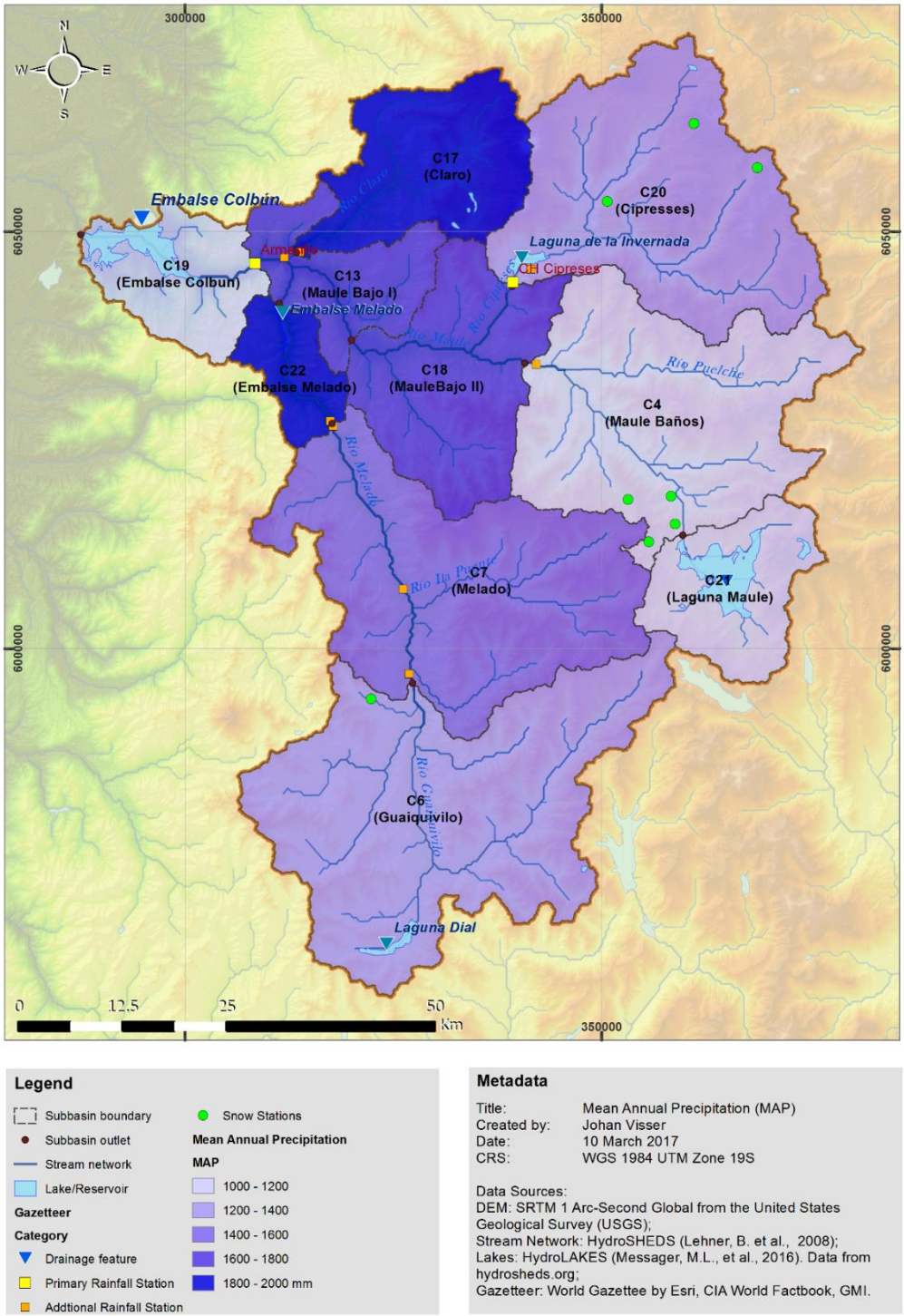

Legend

- Subbasin boundary
- Subbasin outlet
- Stream network
- Lake/Reservoir

Gazetteer

Category

- Drainage feature
- Primary Rainfall Station
- Addtional Rainfall Station
- Snow Stations

Mean Annual Precipitation

MAP

- 1000 - 1200
- 1200 - 1400
- 1400 - 1600
- 1600 - 1800
- 1800 - 2000 mm

Metadata

Title:	Mean Annual Precipitation (MAP)
Created by:	Johan Visser
Date:	10 March 2017
CRS:	WGS 1984 UTM Zone 19S

Data Sources:
DEM: SRTM 1 Arc-Second Global from the United States Geological Survey (USGS);
Stream Network: HydroSHEDS (Lehner, B. et al., 2008);
Lakes: HydroLAKES (Messager, M.L., et al., 2016). Data from hydrosheds.org;
Gazetteer: World Gazettee by Esri, CIA World Factbook, GMI.

Figure 4-2 | Mean Annual Precipitation (MAP) per subcatchment

4.3 Streamflow

Information on streamflow gauge location, data availability and subcatchment calibration can be found in the hydrological analysis report (DHI, 2011). The model calibration has focused on the overall performance in terms of inflow water balance and seasonal distribution of inflow to the Colbún Reservoir. Calibration of inflow to the Colbún Reservoir is discussed in *Section 5.3.3*. *Figure 4-3* presents the observed average monthly-accumulated inflow to Colbún Reservoir for the period between 1991 and 2011.

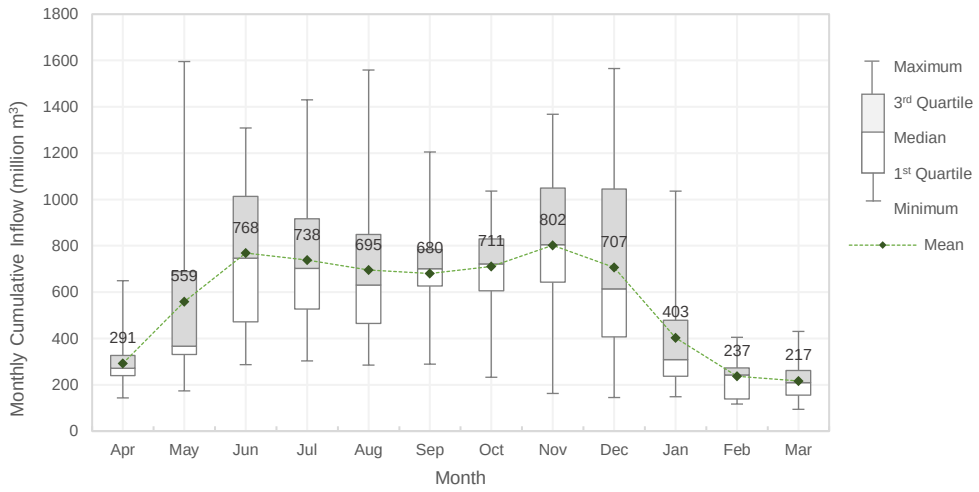

Figure 4-3 | Colbún Reservoir average monthly observed inflow (1991-2011)

When compared to the average monthly precipitation pattern in *Figure 4-1*, the corresponding monthly-accumulated flow volume in *Figure 4-3* shows a quite different monthly distribution. *Figure 4-3* indicates a corresponding increase in catchment runoff during the onset of the rainfall season in April. Peak inflow to the reservoir occurs during the peak precipitation month of June. In the subsequent months from July to October, inflow volumes decreases only slightly with reduced annual variability, despite a significant decrease in average precipitation. An increase in inflow volumes is seen during the months of November and December, with large annual variability during the month of December. After this period, a large decrease in inflow volumes occurs in the months from Jan to March.

The shape of the inflow hydrograph in *Figure 4-3* indicates that snowmelt accumulation- and snowmelt processes play an important part in annual water balance Upper Maule River Basin. As the majority of precipitation in the basin occurs during the winter months, significant snow accumulation occurs at higher altitudes in the basin. By mid-winter, up to roughly 80% of the basin can be covered in snow (DHI,

2011). The subsequent spring melting period provides a substantial contribution to the total annual runoff in the catchment. The snow pack therefore constitutes a valuable natural seasonal water storage. A comparison of seasonal snow cover extent in the basin during the summer and winter periods is presented in *Figure 4-4.*

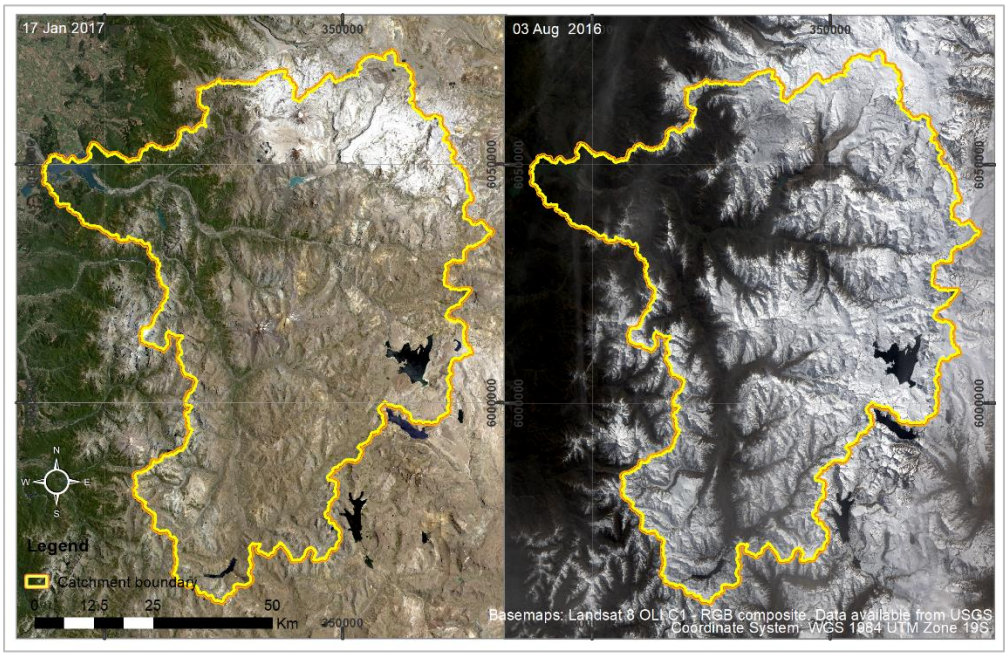

Figure 4-4 | Upper Maule River Basin snow cover extent comparison for summer (left: January 2017) and winter periods (right: August 2016)

Figure 4-3 also indicates great annual inflow variability occur during the months of November and December. With average low rainfall during this period, the runoff variability during this period could be attributed to annually varied snow cover depth/extent as well as timing of the snowmelt peak.

Figure 4-5 presents a comparison of the average monthly precipitation for the *Armerillo* rainfall station and observed inflow to the Colbún Reservoir. Average observed monthly temperature for the *LoAguirre* temperature station, located approximately 5 km downstream of *Laguna del Maule* at elevation of 1981 masl (see *Figure 3 2*) , is also presented.

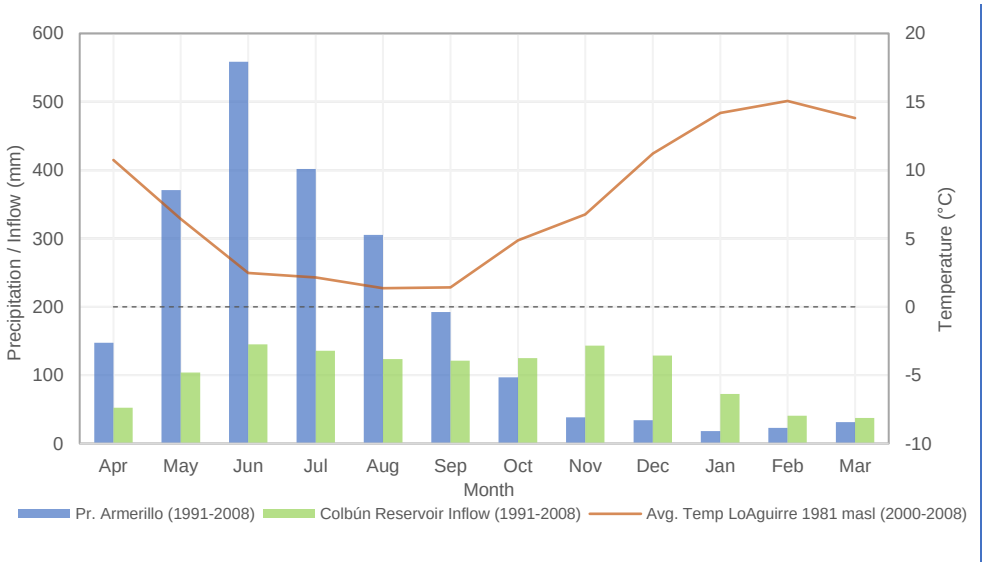

Figure 4-5 | Comparison of monthly- precipitation, Colbún Reservoir inflow and air temperature.

Figure 4-5 shows that the increase in average monthly inflow to the Colbún reservoir can be attributed to the increase in average temperature. As the *LoAguirre* temperature station is located at 1981 masl, the portion of the basin located at higher elevations is expected to exhibit lower average temperatures with increasing elevation. The temperature increase occurring between September and October initiates the snowmelt period and an increase in reservoir inflow. The temperature variability during this period therefore plays an important role in the timing and intensity of the snowmelt period. Following this period, inflow to the Colbún Reservoir reaches a peak average inflow volume in November, after which average inflow subsides with increasing temperatures and diminishing snow cover depth.

4.4 Temperature and Evaporation

As snow accumulation and melting has a significant influence on the annual hydrograph of the Upper Maule River Basin, correct modelling of temperature distribution in the catchment is of key importance. Due to limited observed temperature data availability, temperature distribution in the catchment was primarily based on two temperature stations namely, *MauleArmerillo* (430 masl) and *LoAguirre* (1981 masl) (see *Figure 3-1*). The use of these two stations allowed for the establishment of a temperature-elevation relationship and the creation of temperature times series files for 200 m elevation zones. Population of historical time series per elevation zone was based on the following sequence:

1. If observations from both stations were available, the temperature of each elevation zone is calculated by linear interpolation/extrapolation based on the available station data;

2. If data is only available for one station, the available data and a standard lapse rate is used to calculate the elevation zone temperatures;
3. If no data exist for a particular date, a long-term average temperature is used based on the elevation zone and historical observed data.

Due to limited availability, reference evapotranspiration (ET_0) data for the study area was sourced from the FAO CLIMWAT database (FAO, 2017). A relationship between average monthly reference evapotranspiration and elevation was established based on station in proximity to the study area. Subcatchment were assigned average monthly reference evapotranspiration values based on their average catchment elevation.

Figure 4-6 presents the average monthly air temperature for the *LoAguirre* temperature station for the period between 2000 and 2010. This station was primarily used in the creation of temperature files for elevation zones, due to the availability of good quality hourly data.

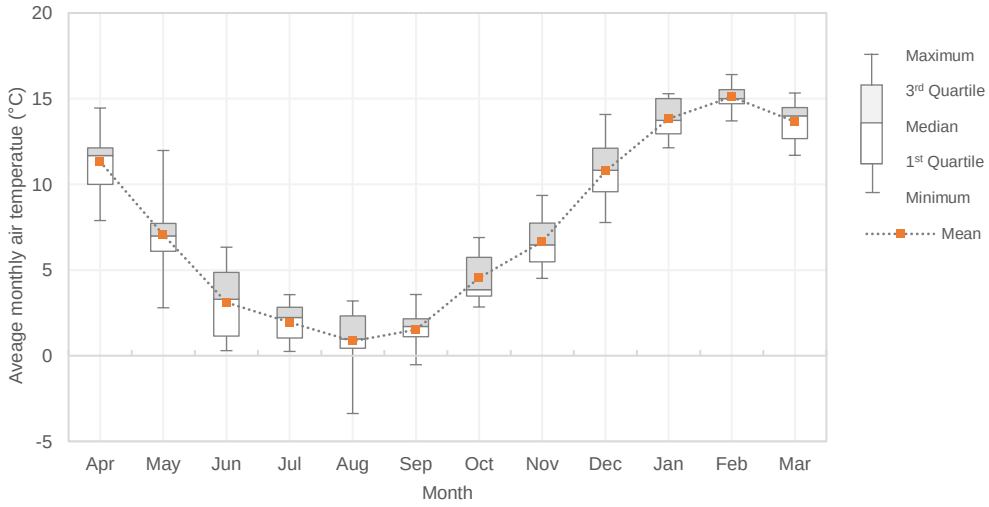

Figure 4-6 | Temperature station LoAguirre average monthly air temperature (2000-2010)

Figure 4-6 indicates a relative increased temperature variability during the months of June and August. Increased temperatures during this time could contribute to larger percentages of precipitation falling as rainfall, thus reducing the snow cover depth and associated snowmelt-generated runoff during the spring period. The opposite is also true for colder temperatures during over the austral winter months with potential temporary delay of the snowmelt period and associated reservoir inflow.

Figure 4-7 presents a comparison of average monthly temperatures for the *MauleArmerillo* (430 masl) and *LoAguirre* (1981 masl) temperature stations. The

comparison provides information on the distribution of average monthly temperatures with regards to elevation in the basin.

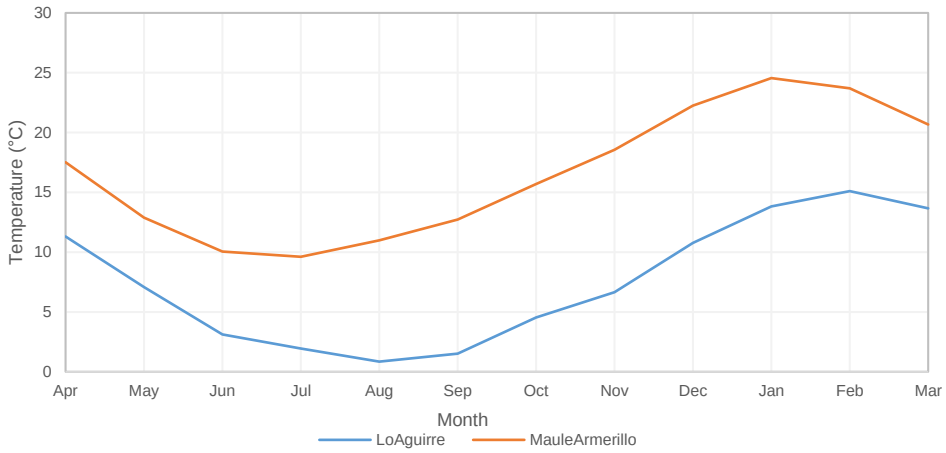

Figure 4-7 | Average monthly temperature for LoAguirre and MauleArmerillo stations (2000-2010)

Figure 4-7 indicates that the higher altitude *LoAguirre* station experiences minimum and maximum average temperatures approximately one month after the lower altitude *MauleArmerillo* station. The annual temperature variation for both stations is approximately 15°C between summer and winter periods. The *LoAguirre* station experiences a prolonged colder period over the winter months with slower response to increasing temperatures during spring month of September. Indicating a potential slower snowmelt response from higher altitudes in the basin.

4.5 Annual variability of precipitation and runoff

To gain more information on the interannual climate variability of the Upper Maule Basin, annual totals of area-weighted catchment average precipitation and observed inflow were compared. *Figure 4-8* presents a comparison of total annual catchment-based precipitation and total inflow to the Colbún Reservoir per hydrological year (Apr-Mar).

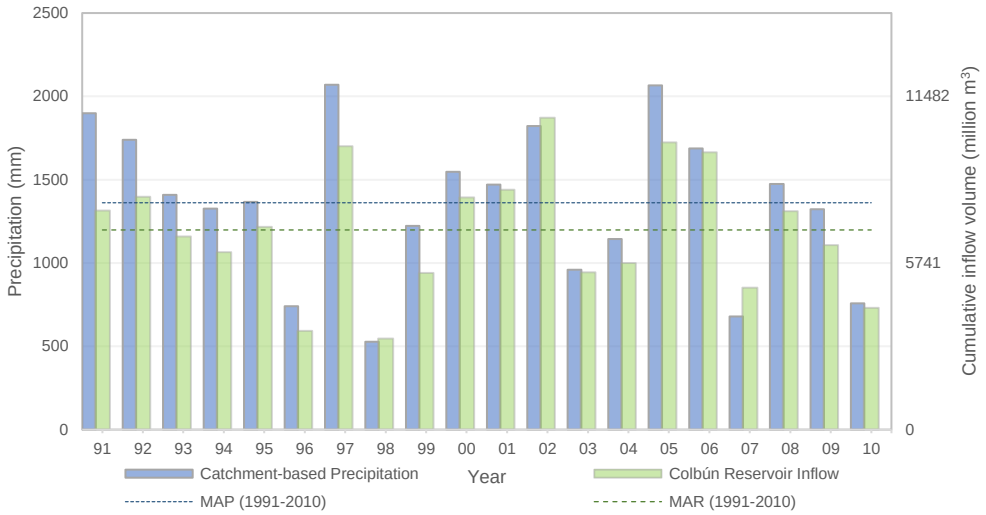

Figure 4-8 | Total annual catchment-based precipitation and Colbún Reservoir inflow

From *Figure 4-8*, a large interannual variability in catchment precipitation and total runoff can be noted. Hydrological years with significantly below average total precipitation and correspondingly significantly low runoff are seen as the hydrological years 1996, 1998 and 2007. At the opposite end of the spectrum, substantial precipitation occurs in during 1997, 2002 and 2005. The largest annual cumulative inflow to the Colbún Reservoir occurs during 2002, although higher precipitation was observed in 1997 and 2005. Various factors could have contributed to this result, including the drier preceding years experienced in 1996 and 2004 as well as varying snowmelt contributions.

4.6 El Niño-Southern Oscillation

El Niño-Southern Oscillation (ENSO) events are coupled ocean-atmosphere phenomenon, with El Niño and La Niña at opposite warming and cooling phases. The ENSO cycle is a scientific term that describes fluctuating temperatures between the atmosphere and the ocean in the equatorial pacific, approximately between the International Date Line and the west coast of South America (Solomon, et al., 2007; NOAA, 2016).

El Niño involves the warming phase of the ENSO, resulting in the weakening of a usually strong SST gradient across the equatorial Pacific, with associated changes in ocean circulation. The closely linked atmospheric counterpart to ENSO, the Southern Oscillation (SO), involves changes in trade winds, tropical circulation and precipitation. Historically, El Niño events occur about every 3 to 7 years and typically alternate between the cooling La Niña phase with below average temperatures. El Niño and La Niña phase usually last for 9 to 12 months, but extensive phases may last

for multiple years. Associated changes in the trade winds, atmospheric circulation, precipitation and associated warming of the atmosphere can cause widespread changes in the climate system that last several months, leading to significant socio-economic losses (Met Office UK , 2016; NOAA, 2016).

The El Niño (La Niña) is characterised by a time-series of the monthly SST anomalies in a region of the central equatorial Pacific. The Niño 3.4 region (5°S - 5°N, 120°W - 170°W) is one of several used to monitor SST changes in the tropical Pacific (see *Figure 4-9*). El Niño (La Niña) phases are characterized by a five consecutive 3-month running mean of SST anomalies in the Niño 3.4 region that is above (below) the threshold of +0.5°C (-0.5°C) (NOAA, 2017; Met Office UK , 2016). This standard of measurement is known as the Oceanic Niño Index (ONI). The thresholds values for El Niño and La Niña phases can be broken down further as presented in *Table 4-3*.

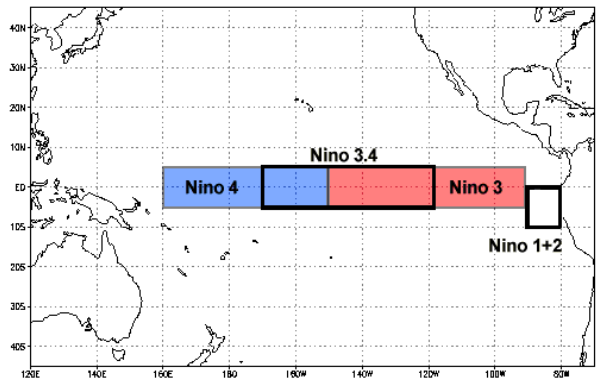

Figure 4-9 | Nino regions for STT anomaly measurements in tropical Pacific (NOAA, 2017)

Table 4-3 | El Niño/La Niña event threshold categories and associated STT anomalies in Niño 3.4 region (Williams & Null, 2015)

Event threshold category	El Niño SST anomaly (°C)	La Niña SST anomaly (°C)
Weak	0.5 to 0.9	- 0.5 to -0.9
Moderate	1.0 to 1.4	-1.0 to -1.4
Strong	1.5 to 1.9	-1.5 to -1.9
Very Strong	≥ 2.0	≤ -2.0

Figure 4-10 shows SST anomalies in Pacific Ocean during a strong La Niña (December 1988) and a very strong El Niño (December 1997). During ENSO events, the changes in sea surface temperature result in changes in atmospheric circulation, which through atmospheric dynamics can extend well beyond the Pacific region. Due to the varied seasonal timing, location and intensity ENSO related effects, statistical

analysis of past ENSO events can produced empirical relationships between measured climatological variables and local associated impacts. An important feature of the ENSO cycle is that its evolution is predictable several months in advance, thus allowing mitigation measures to be introduced to reduce negative effects as well as taking advantage of potential favourable effects. The accurate prediction and simulation of ENSO effects is therefore highly dependent on the use of accurate initial model conditions to represent state of the ocean-climate system (Met Office UK , 2016).

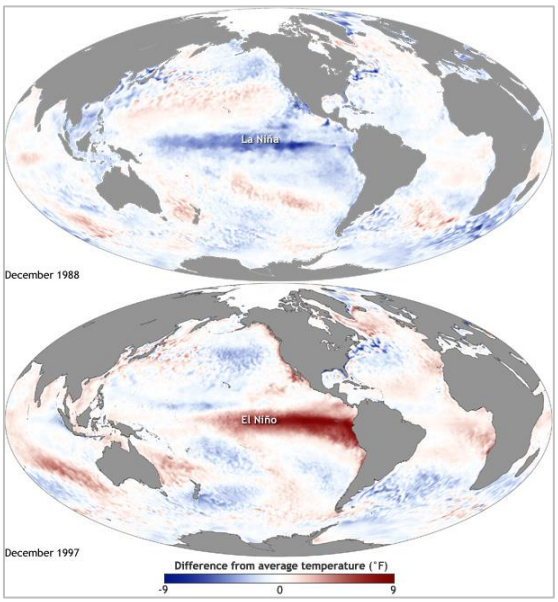

Figure 4-10 | Sea surface temperature anomaly in the Pacific Ocean during a strong La Niña (top, December 1988) and very strong El Niño (bottom, December 1997). Maps by NOAA Climate.gov, based on data provided by NOAA (NOAA, 2014)

4.6.1 ENSO Influence on Study Area

Western South America is subject to considerable interannual variability due to ENSO, leading to above-average precipitation in western South America during El Niño phases, and opposite conditions during cooling La Niña phases (Rivera, et al., 2012). In a study to investigate the seasonality of ENSO-related rainfall variability in central Chile, Montecinos et al. (2000) found that during El Niño warming phases, there is a inclination for the occurrence of above-average precipitation between 30° and 35°S in the austral winter winter (June-July-August, and from 35° to 38°S in late spring (October-Novemeber). Following El Niño phases, a rainfall deficit is typically observed from around 38° to 41°S during the following summer (January-February-March), when El Niño reaches its maximum development. The Upper Maule River Basin is situated between approximately 35.3° and 36.3° S, and is therefore situated in an area which could potentially expect above-average rainfall over the seaonal

period between June and November, during El Niño warming phases. Montecinos et al. (2000) also found that the opposite rainfall anomalies are characteristic during La Niño cooling phases, resulting in below-average precipititon in the indentified latteral zones. However, not all warm (cold) phases were found to lead to wet (dry) conditions, which could be explained by intraseasonal variations in the related circulation patterns as a result of the nonlinear behavior of the ocean-atmosphere system (Montecinos, et al., 2000; Rivera, et al., 2012).

Based on a cluster analysis of 43 stream gages located in south central and southern Chile (34°-40°S), Rubio-Álvarez & McPhee (2010) indicated two major geographical zones can be considered homogeneous from the point of view of water availability variation. These zones include on one hand the greater Maule River basin and its tributaries (north) and the rivers located within the Itata, Biobío, Imperial, and Valdivia river basins (south). The study found significant correlation with climatic indexes at different spatial and temporal scales, with ENSO influence being stronger at the northern sub-region, and notably the Antarctic Oscillation (AAO) and the Pacific Decadal Oscillation (PDO) correlation with summer flows in the southern subregion. *Figure 4-11* presents a monthly flow regime comparison for the Maule River during El Niño and normal years, based on a 36 year long observed Armerillo station streamflow record.

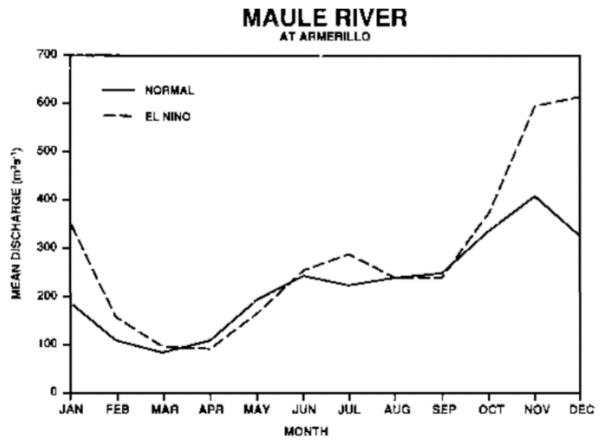

Figure 4-11 | Mean Monthly Flows of Maule River at Armerillo comparing regimes in El Niño and normal years (Waylen, et al., 1993)

From *Figure 4-11* it can be seen that significantly higher monthly average flows are experienced during the period from October to February during years warming El Niño phases. Associated above-average precipitation over the winter months lead to increased snow accumulation during the austral winter periods, thus resulting in increased average monthly streamflow during the spring snowmelt period.

A possible explanation for interannual variability in catchment precipitation could be related to the influence of ENSO phases and timing. *Table 4-4* presents the total annual catchment-based precipitation and Colbún reservoir inflow for hydrological years from 1991 to 2010. Annual runoff percentage is calculated based on the total

runoff divided by the total precipitation. Recorded El Niño and La Niña phases based on the Oceanic Niño Index (ONI) are indicated per occurring year. El Niño (La Niña) phases are characterized by five consecutive 3-month rolling mean of SST anomalies above (below) threshold values of +0.5 °C (-0.5 °C).

Table 4-4 | Total catchment-based precipitation and Colbún Reservoir inflow per hydrological year.

Year	Catchment-based Precipitation	Colbún Reservoir Inflow	ONI Phase
	mm	mm	-
1991	1899	7542	Moderate El Niño
1992	1740	8022	
1993	1408	6651	
1994	1327	6113	Weak El Niño
1995	1367	6985	Weak La Niña
1996	741	3406	
1997	2070	9759	Very strong El Niño
1998	528	3138	Moderate La Niña
1999	1223	5397	Moderate La Niña
2000	1547	7998	Weak La Niña
2001	1470	8268	
2002	1821	10743	Moderate El Niño
2003	960	5415	
2004	1143	5736	Weak El Niño
2005	2065	9895	
2006	1688	9549	Weak El Niño
2007	679	4892	Moderate La Niña
2008	1474	7522	
2009	1323	6357	Moderate El Niño
2010	759	4194	Moderate La Niña
Average	**1362**	**6879**	

From *Table 4-4*, a correlation between annual precipitation totals and ONI phases can be seen, with above-average precipitation totals occurring in years with El Niño occurrences such as 1991, 1997 and 2002. A corresponding correlation regarding below-average precipitation can be seen for years with recorded La Niña occurrences such as 1998, 1999 and 2007.

Above average rainfall recorded during the 2005 hydrological year is not by the associated with an active El Niño warming phase, but could have been influenced by the weak El Niño which occurred towards the end of 2004. Similarly, below average rainfall occurring in 1996 is not associated with an active La Niña cooling phase. The relationship between the ONI and precipitation in the Upper Maule Basin was therefore investigated further.

Figure 4-12 and *Figure 4-13* present comparative time series plots of monthly cumulative- precipitation (Armerillo) and inflow to the Colbún reservoir, to a 3-month

rolling mean SST anomaly for the Niño 3.4- and Niño 1+2 Regions. As a comparison of observed values is preferred, the precipitation record of the *Armerillo* rainfall station is used for the comparison in *Figure 4-12*, as it was found to be the most reliable observed precipitation record during the hydrological analysis (DHI, 2011).

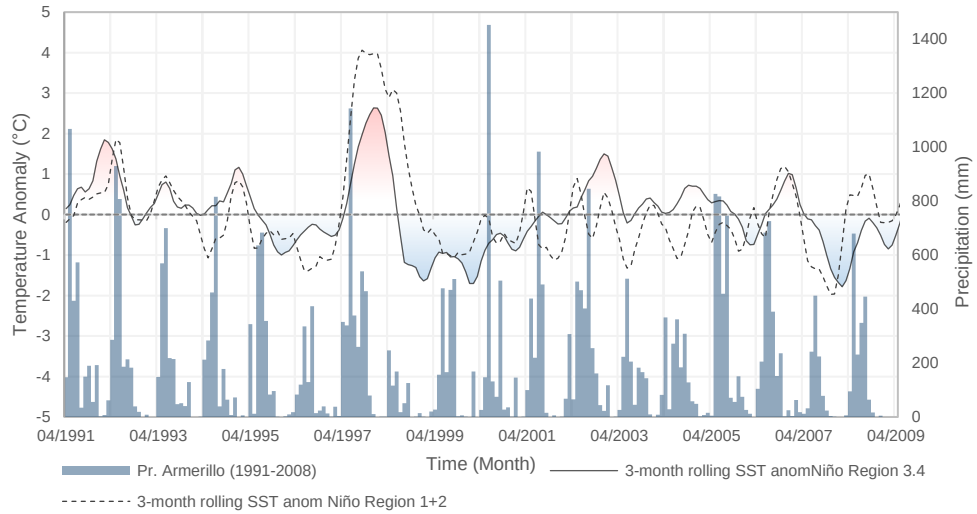

Figure 4-12 | Monthly accumulated precipitation (Armerillo) vs 3-month rolling mean SST temperature anomaly for Niño Region 3.4 and Niño Region 1+2

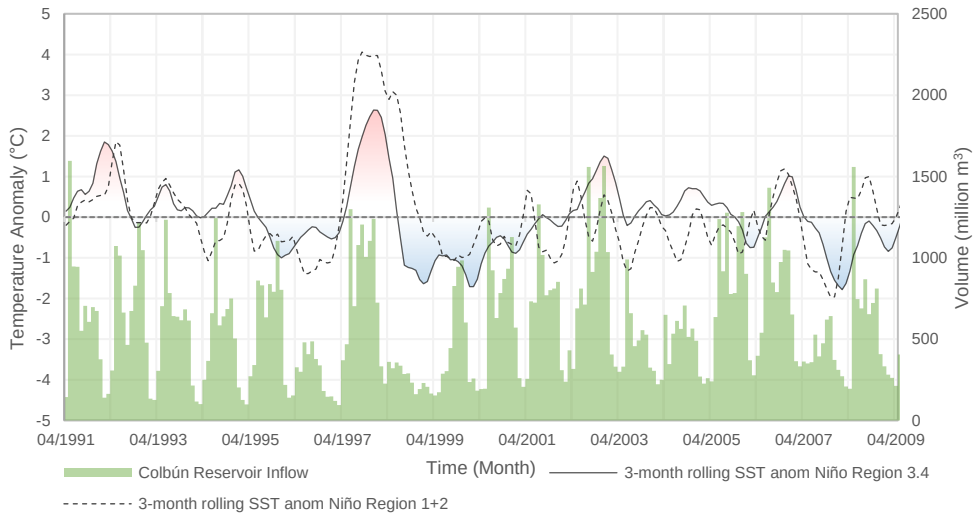

Figure 4-13 | Monthly accumulated Colbún Reservoir inflow vs 3-month rolling mean SST temperature anomaly for Niño Region 3.4 and Niño Region 1+2

From *Figure 4-12* and *Figure 4-13* it can be seen that total accumulated precipitation and reservoir inflow appear to follow similar developments compared to SST anomalies in Niño Region 3.4- and Region 1+2. Positive SST temperature anomalies in Niño Regions 3.4- and Region 1+2 generally correspond to an increase in annual accumulated precipitation and reservoir inflow over the study area. Similarly, negative SST anomalies in these regions appear correspond to lower accumulated precipitation and reservoir inflow.

Extremely high precipitation in 1997 and correlates well to an established strong El Niño phase and associated strong positive SST anomalies in Niño 3.4- and Niño 1+2 Regions over this time period.

Lower recorded precipitation and inflow during the 1996, 2003 and 2004 hydrological years appear to be better correlated to negative SST anomalies in Niño Region 1+2 than compared to higher recorded SST anomalies in Niño Region 3.4. This potential improved correlation could provide reasoning for low precipitation periods occurring outside of establish ONI phases as found in *Table 4-4*.

A steady increase in annual accumulated inflow can be noted for the period from 1998 to 2002 with a corresponding increasing trend in mean SST anomalies for both Niño Regions. High cumulative rainfall and inflow for the 2005 hydrological year however does not correspond to a period of substantial SST anomalies, but is situated between two weak El Niño phases.

4.6.2 Variation in precipitation and streamflow regimes

Monthly precipitation and flow regime comparisons were conducted for years with El Niño/La Niña phases compared to long-term average values, to assess the influence of ENSO on the temporal distribution of precipitation and runoff in the study area.

4.6.2.1 Precipitation

The total monthly catchment-based precipitation for hydrological years with of *moderate*- to *very strong* El Niño and La Niña occurrences are presented in *Figure 4-14* and *Figure 4-15* respectively.

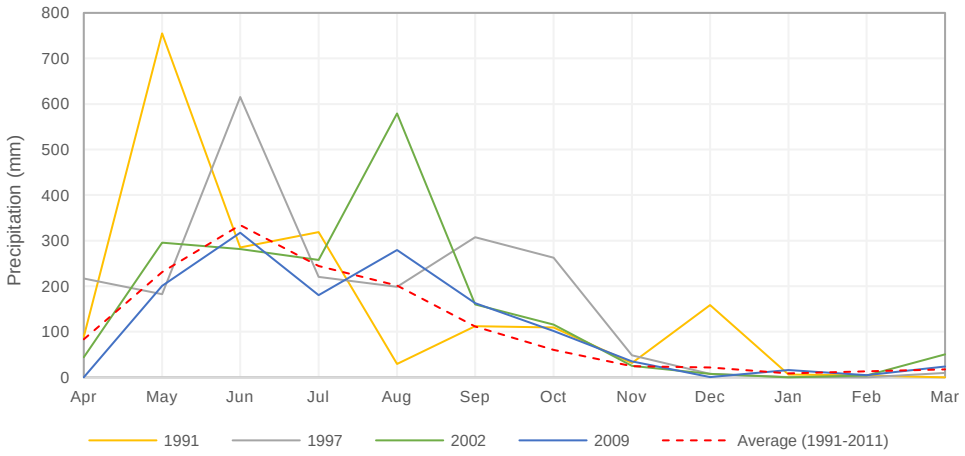

Figure 4-14 | Catchment-based total monthly precipitation for years with recorded Moderate to Very strong El Niño occurrences

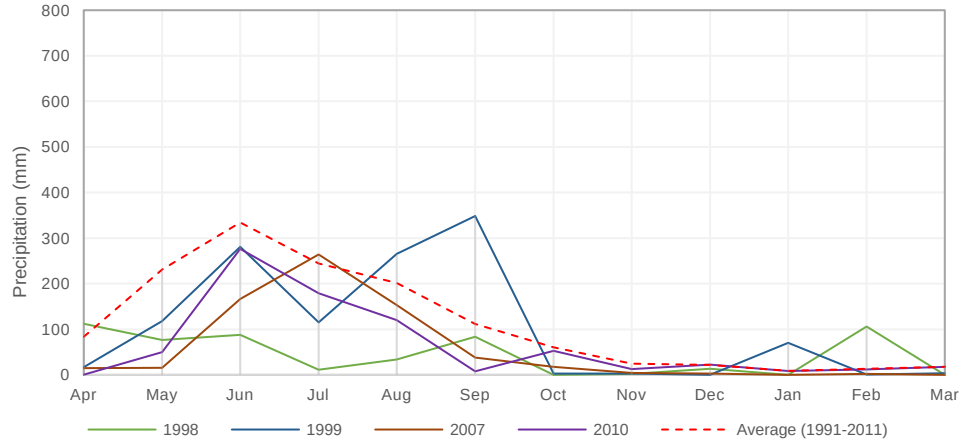

Figure 4-15 | Catchment-based total monthly precipitation for years with recorded Moderate La Niña occurrences

Figure 4-14 indicates above average precipitation is experienced in period between May and Aug for years with El Niño occurrences, During 1997 and 2009, above average precipitation was also experienced during the period from August to October. This corresponds temporal distribution of increased precipitation corresponds to information provided in Section 4.6.1. The increased precipitation and warmer temperatures during the austral winter provides early snowmelt runoff as well as

additional snowpack volume at higher altitudes. This leads to increased early season runoff and additional runoff during the spring melting period.

Figure 4-15 indicates a substantial reduction in total austral winter precipitation during La Niña occurrences, with significant reductions experienced during the period from April to June. A severe reduction in annual precipitation is experienced during 1998. Increased rainfall is however experienced in 1999 during the months of August and September. This however could be attributed to an increase in oceanic temperatures during the latter end of a moderate La Niña phase.

4.6.2.2 Colbún Reservoir Inflow

A similar average monthly flow regime comparison as shown in (*Figure 4-11*) was conducted based on observed inflow record to the Colbún Reservoir. Average monthly flow values for years with recorded *moderate* to *very Strong* El Niño/ La Niña are presented in *Figure 4-16* and *Figure 4-17* .

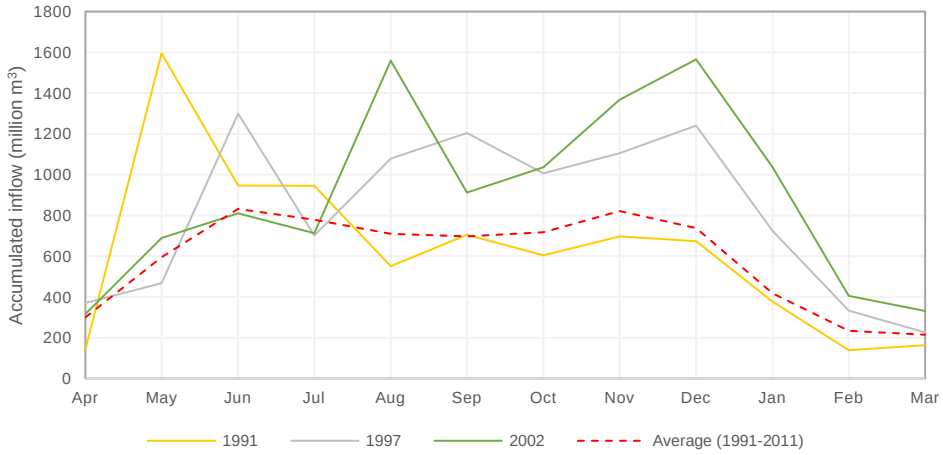

Figure 4-16 | Colbún Reservoir average monthly inflow for years with recorded moderate to very strong El Niño occurrences

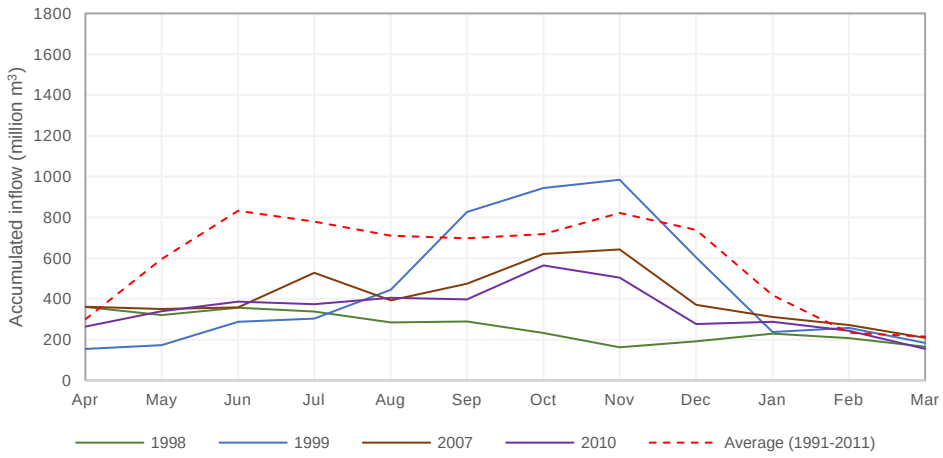

Figure 4-17 | Colbún Reservoir average monthly inflow for years with recorded moderate to very strong La Niña occurrences

Figure 4-16 indicates above average monthly inflow to the Colbún Reservoir was experienced for the period from August to February during El Niño occurrence years. This can be attributed to the increased precipitation during the preceding high-rainfall season and resultant increase in snowmelt contribution during spring. Above-average inflows were experienced in May during the 1991 *moderate* El Nino, with for the remainder of the hydrological year.

Figure 4-17 indicates a severe reduction in monthly average inflow to the Colbún Reservoir for years with La Niña occurrences. Above-average inflow during the spring period of 1999, is due to above-average precipitation experienced over this period (see *Figure 4-15*). Reduced precipitation over the austral winter period can therefore be seen to lead to a clear reduction in snowmelt-based runoff during spring.

4.6.3 Relationship between seasonal precipitation and runoff

As indicated in *Sections 4.2* and *Figure 4-5*, inflow volumes to the Colbún Reservoir during the low-rainfall season (Oct-Apr) appears to be highly dependent on total precipitation over the austral winter period. The accurate estimation of snow cover depth and distribution in the catchment during the high-rainfall season (Apr-Oct) would therefore provide valuable information in the estimation of future low-rainfall season inflow. *Figure 4-18* presents a comparison of total accumulated low-rainfall

season inflow to the Colbún Reservoir vs total accumulated catchment precipitation during the preceding high-rainfall season.

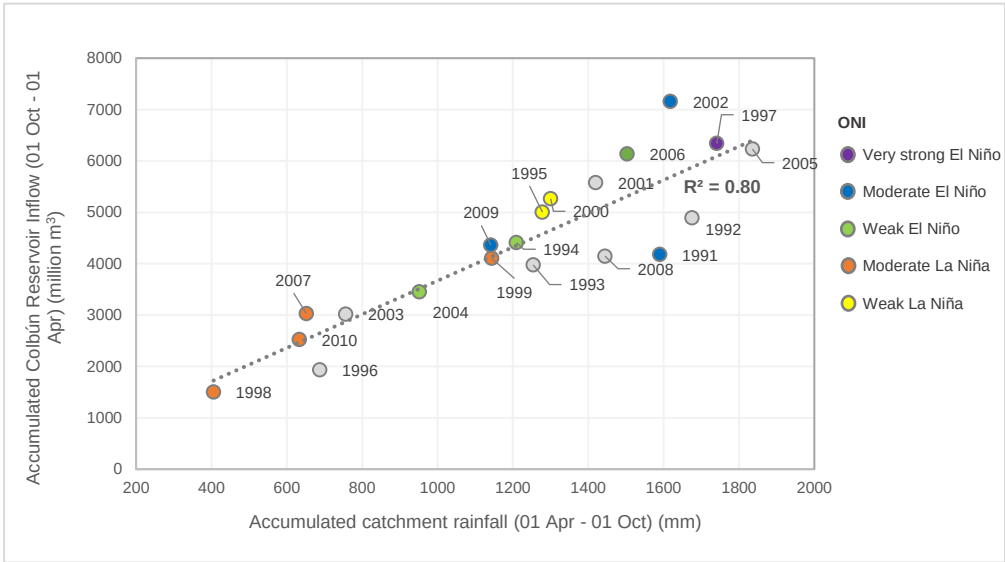

Figure 4-18 | Accumulated low-rainfall season Colbún Reservoir inflow vs preceding high-rainfall season accumulated catchment precipitation

Figure 4-14 illustrates a good correlation between low-rainfall season Colbún Reservoir inflow and preceding high-rainfall season accumulated catchment precipitation. This indicates that if high-rainfall season catchment precipitation can be accurately measured or estimated, an initial estimation of accumulated low-rainfall season inflow to the Colbún Reservoir could potentially be made. Variable basin regulation and climatic patterns, amongst other factors, however can have a significant effect on produced runoff and accumulated inflow.

Figure 4-14 also indicates that hydrological years similar recorded ONI phases tend to group together in areas of similar precipitation and associated runoff. This is evident for hydrological years with lower than 900 mm of accumulated catchment precipitation, where *moderate* La Niña phases were recorded for 3 of the 5 years. The remaining two years, 1996 and 2003, were found to have larger recorded negative SST anomalies in Niño Region 1+2, compared to the Niño Region 3.4.

Deviations from these groupings of similar ONI phases such as for *moderate* El Niño phases in 2002, 2004 and 2006, could possibly be attributed to the catchment conditions of the preceding season. High precipitation and runoff during the 2001 hydrological year for example, could have significantly increased surface- and groundwater storage levels in the catchment as well a snow cover depth. High precipitation in 2002 could therefore have fallen on a ‘wet’ catchment with a higher runoff percentage, thus limiting the amount of runoff reduction. A similar scenario is

evident for the high precipitation/high inflow year of 1997, preceded by a below-average precipitation year of 1996. The role of groundwater-, surface water- and snow storage could therefore be of key importance in the estimation of seasonal runoff.

4.7 Global Climate Model data

The European Climate Observations, Modelling and Services initiative (ECOMS) is responsible for the coordination of activities surrounding three ongoing European projects (EUPORIAS, SPECS and NACLIM) (UCMG, 2016). Multiple activities in these projects require seasonal forecasts from the latest forecasting systems (e.g., ECMWF - System 4, NCEP - CFSv2 or UKMO - GloSea5) for a reduced number of datasets and variables. Information can be obtained from data providers, but resulting formats and aggregations may not be identical, requiring post processing before use. Data access to certain datasets may also not be straightforward to separate data use policies.

To aid data management, the Santander Meteorology Group at the University of Cantabria developed the ECOMs User Data Gateway (UDG) in order to facilitate seasonal forecasting data access to end users (UCMG, 2016). The UDG provides an efficient platform for users to retrieve required seasonal forecasting datasets for a study region. The use of R has been adopted for a number of tasks in mentioned projects for processes such as forecast validation and downscaling. An R package called loadeR.ECOMS was developed by the Santander Meteorology Group for data exploration and access as well as additional functionalities (Santander Meteorology Group, 2017).

This study uses monthly ensembles of ECMWF- System 4 precipitation (variable *tp*) and near-surface air temperature (variable *tas*) reforecasts. The System 4 coupled ocean-atmosphere forecasting system is described in more detail in *Section 5.1.3*. The period from 1991 to 2010 is used for all System 4 based datasets employed in this study based on the matching availability of observed data for the study area. *Figure 4-19 and Figure 4-20* show the System 4 mean seasonal accumulated precipitation and near-surface air temperature for a 15-member seasonal forecast ensemble over central Chile and the demarcated study area. Seasonal periods are indicated by a three month period acronyms e.g. MAM representing the autumn months of March-April-May.

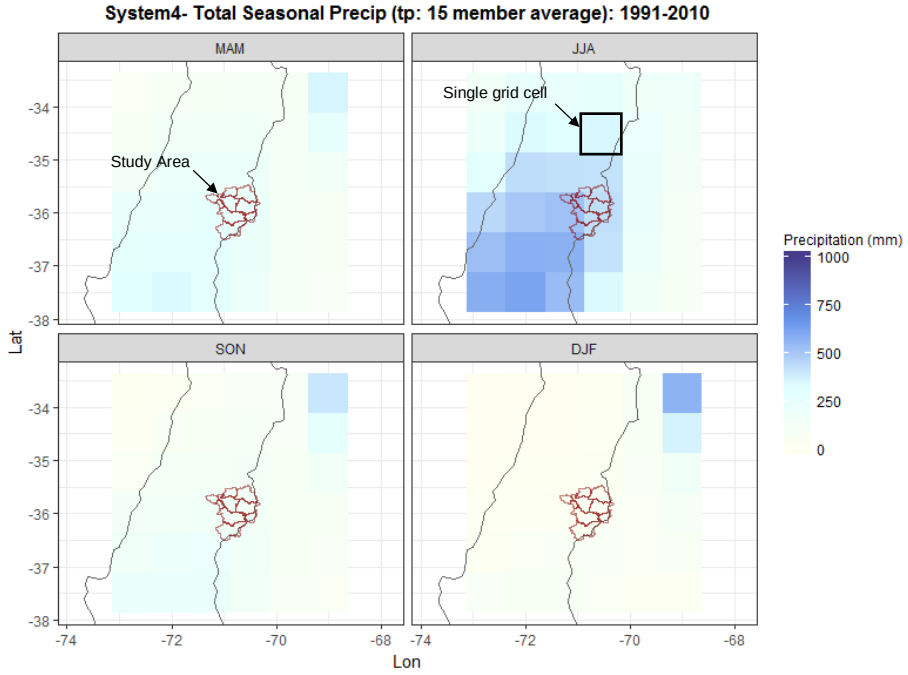

Figure 4-19 | System 4_seasonal 15: Average accumulated seasonal precipitation (1991-2010)

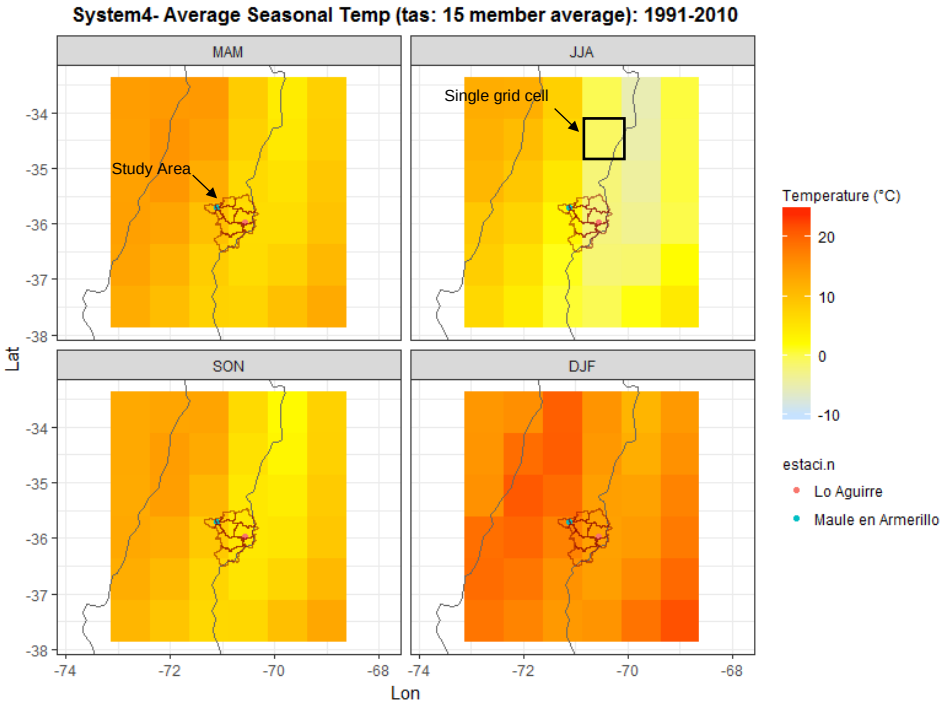

Figure 4-20 | System 4_seasonal 15: Average seasonal near-surface air temperature (1991-2010)

Similar to observed precipitation records (see *Section 4.2), Figure 4-19* indicates a high seasonality in annual System 4 precipitation totals with considerably higher average accumulated precipitation over the austral winter period. Investigating the spatial distribution of seasonal precipitation, the clear impact of the Andes mountain range is shown with a sharp reduction in precipitation east of the Argentinean border. A clear increase in annual precipitation is also evident from north to south over the study area, increasing further towards the southern regions of Chile. The average accumulated catchment-based observed precipitation for the winter season (1991-2010) was calculated as 774 mm. The value can be compared to System 4 winter precipitation values in *Figure 4-19* of approximately 450 mm, which indicates a large underestimation of seasonal accumulated precipitation by the System 4 based grid cells.

System 4 seasonal temperature distribution shown in *Figure 4-20,* presents a similar seasonal distribution compared to observed temperature records *(see Figure 4-6).* The effects of the increased average elevation over the Andes mountain range is clearly evident, resulting in decreased temperatures over this region. A closer comparison of System 4 grid cell resolution and study area size is shown *Figure 4-21* and *Figure 4-22.* These figures presents the System 4 total seasonal precipitation and temperature for a 15-member seasonal forecast ensemble initialized every 3 months starting 01 March 2002.

From *Figure 4-21* it can be seen that the Upper Maule River Basin is situated over six System 4 precipitation grid cells, with the majority of the basin located over two cells. Examination of *Figure 4-21 and Figure* 4-22 reveals a distinct change cell values from east to west. The change indicates the System 4 simulated interface between the Maule valley foothills and Andes mountain range. A clear decrease in grid cell precipitation and temperature values can be seen for cells west of this interface.

Due to the relative coarse nature of the System 4 grid data compared the basin size, System 4 data assignment to subbasins was not solely based on the grid cell it was located in. For seasonal forecast simulations, System 4 precipitation grid data for the forecast period in question was downloaded for the study area extent with a 0.75° degree buffer, using the loadeR.ECOMS package in R. Forecast precipitation grid data was then assigned to each subbasin using bilinear interpolation of the gridded dataset to centroid location of each subbasins. Thus resulting in unique forecast precipitation time series for each defined subbasin. For temperature data, System 4 temperature grid data was then assigned to the *LoAguirre* and *MauleArmerillo* temperatures stations using bilinear interpolation of the gridded dataset to known location of each station.

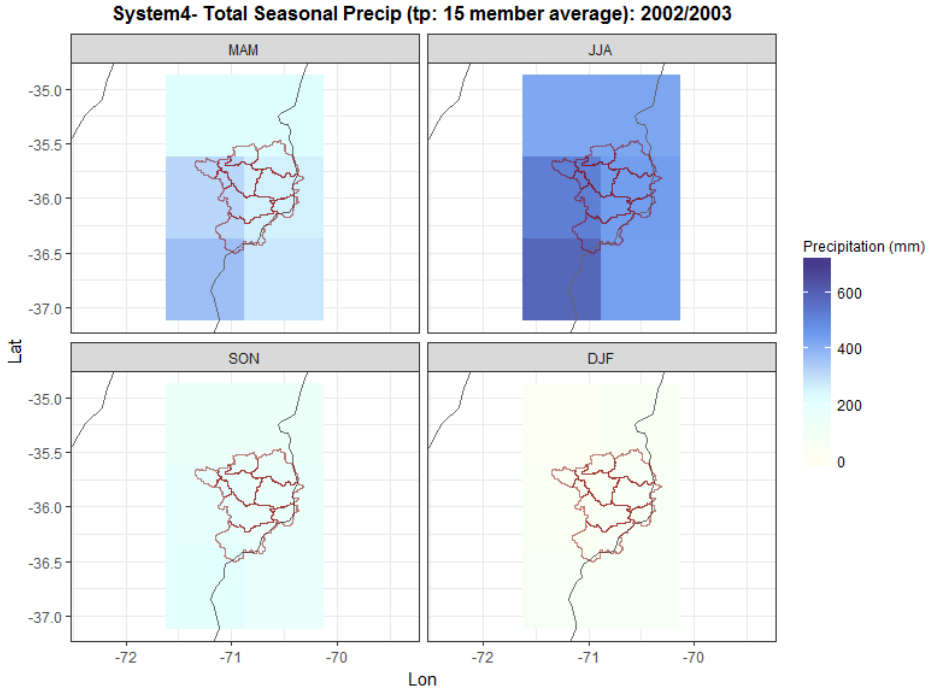

Figure 4-21 | System 4_seasonal 15: Accumulated seasonal precipitation 2002/2003

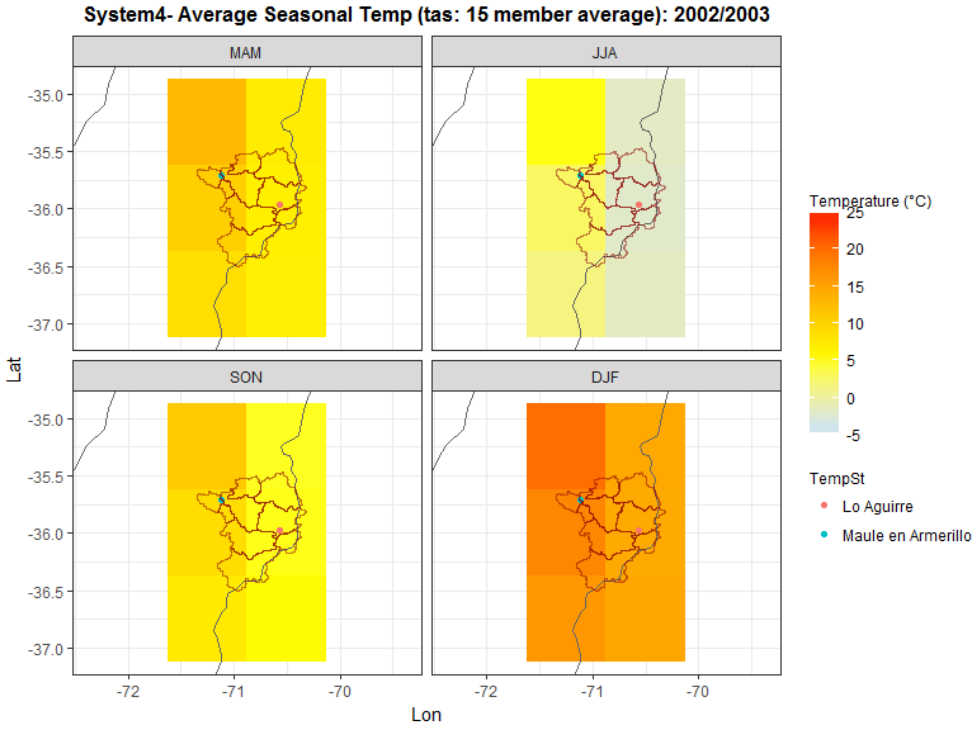

Figure 4-22 | System 4_seasonal 15: Average seasonal near-surface air temperature 2002/2003

5 Methodology

5.1 Workflow

Figure 5-1 presents the main steps in the study methodology and the related workflow processes based on the two types of meteorological forcing data used in this study. Each step and related processes are discussed in detail in this chapter.

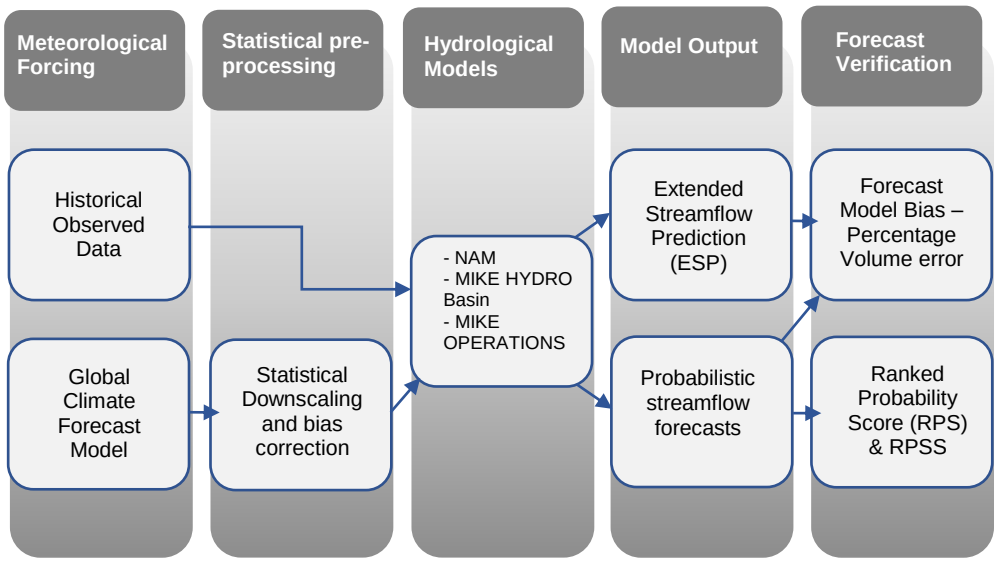

Figure 5-1 | Study categorical workflow and related processes

5.1.1 Analysis Year Selection

Due to time constraints, seasonal forecasts were conducted and analysed for selected years based on available hydrological data. Four consecutive years of 2002, 2003, 2004 and 2005 were selected to represent a range of climatic conditions experienced over this time period (see *Figure 4-8*). In total, seven seasonal forecast time periods would be used for forecast option comparison as presented in *Table 5-1*. System 4 forecast ensembles were available once a month for forecasting, but two sets of forecasts for each year are examined here. These were selected to cover periods of critical conditions in reservoir systems, when forecasted inflow information would be most valuable to reservoir managers, such as estimated precipitation during winter and then snowmelt contribution during spring. Two annual start dates, or Time of Forecast (ToF), were therefore selected representative of the start of the high-rainfall season (01 April) and the start of the low-rainfall season (01 October). Seasonal forecast would consist of a 6-month hindcast period up to the ToF, followed by a 7-month forecast period.

Table 5-1 | Seasonal forecast simulation dates for selected analysis years

	Simulation time period	Start of Simulation (SoS)	Time of Forecast (ToF)	End of Simulation (EoS)
High-rainfall Season	1	2001-10-01	2002-04-01	2002-10-31
	2	2002-10-01	2003-04-01	2003-10-31
	3	2003-10-01	2004-04-01	2004-10-31
	4	2004-10-01	2005-04-01	2005-10-31
Low Rainfall Season	5	2002-04-01	2002-10-01	2003-04-30
	6	2003-04-01	2003-10-01	2004-04-30
	7	2004-04-01	2004-10-01	2005-04-30

Figure 5-2 compares the monthly precipitation and Colbún Reservoir inflow over the selected period (01 April 2002 - 31 October 2005), together with the average monthly temperature for the *LoAguirre* temperature station.

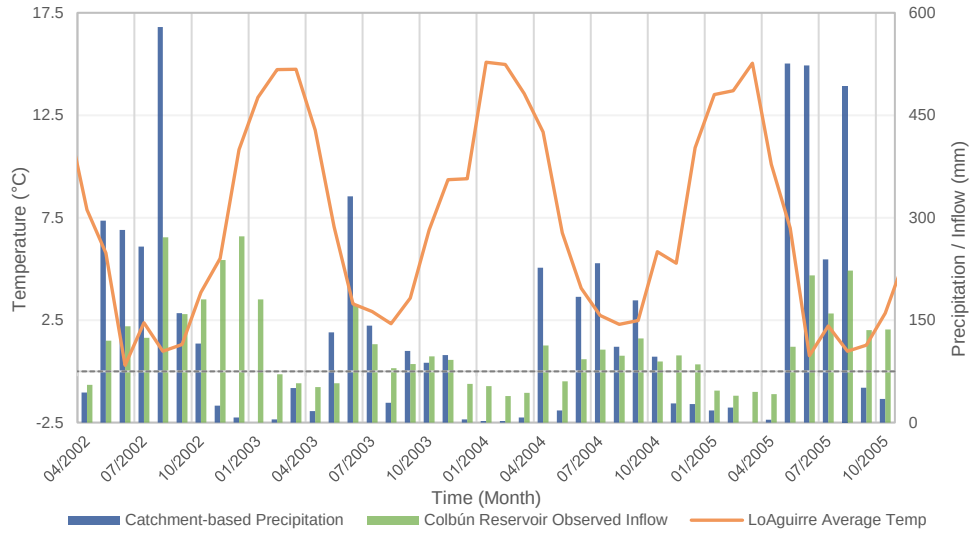

Figure 5-2 | Observed monthly catchment-based precipitation, Colbún Reservoir inflow and LoAguirre temperature for selected analysis period (01 Apr 2002 – 31 Oct 2005)

Figure 5-2 shows the high precipitation occurring during the 2002 and 2005 high-rainfall seasons, as well as the increased inflow during the subsequent low-rainfalls seasons. *Figure 5-2* also indicates that above-average temperatures were experienced during the 2003 and 2004 austral winter periods, as well as for the 2003 spring period. This increase in temperature could potentially have resulted in a reduction in snow accumulation over the winter period and an earlier onset of the snowmelt period. Additional hydrological analysis of selected study years can be found in Appendix A.

5.1.2 Selected Seasonal Forecasting Options

In total, 10 sets of forecasts options were carried out for seasonal inflow forecast performance evaluation and comparison. A short description of forecast options and associated model configuration and input datasets is provided below. Explanations of forecasting option concepts are describe in the following sections of this chapter. A summary table of the selected seasonal forecast options in presented in *Table 5-2*.

Seasonal Forecast Options:

1. Historical flows until time of forecast (ToF) hereafter Extended Streamflow Prediction (ESP) based on historical discharges. This is referred to here as ESP-Q and is used as a reference case.

2. Historical flows and precipitation up to ToF, hereafter ESP based on historically observed precipitation. This corresponds to the widely used Extended Streamflow Prediction method.

3. Option 2) with Data Assimilation (DA) of reservoir inflows and reservoir water levels up to the time of forecast.

4. Historical flows and precipitation up to ToF, hereafter ESP based on ensemble seasonal System 4 precipitation forecasts.

5. Option 4) with DA of reservoir inflows and reservoir water levels up to the time of forecast.

6. Option 5) with downscaling of precipitation data.

7. Historical flows and precipitation up to ToF, hereafter ESP based on ensemble seasonal System 4 forecast of precipitation and temperature.

8. Option 7) with DA of reservoir inflows and reservoir water levels.

9. Option 8) with downscaling of temperature data only.

10. Option 9) with downscaling of precipitation data, i.e. both precipitation and temperature.

Table 5-2 | Summary of selected Seasonal Forecast options

Forecast Option		Inflows before ToF based on		Inflows after ToF based on						
				Ensemble Streamlow prediction based on						
No.	Name	Historical Streamflows	Historical Precipitation (Rainfall-runoff Model)	Historical Streamflows ESP-Q	Historical Precipitation ESP-P	System 4 forecast variable (15 member ensemble)		Includes DA of discharge and water levels	Includes Downscaling of Precip Data	Includes Downscaling of Temp Data
						Precipitation	Temperature			
1	ESP-Q	x		x						
2	ESP-P		x		x					
3	ESP-P_DA		x		x			x		
4	S4		x			x				
5	S4_DA		x			x		x		
6	S4_DA_BC		x			x		x	x	
7	S4T		x			x	x			
8	S4T_DA		x			x	x	x		
9	S4T_DA_BC		x			x	x	x		x
10	S4TP_DA_BC		x			x	x	x	x	x

5.1.3 ECMWF-System 4

The European Centre for Medium-Range Weather Forecasts' (ECMWF) System 4 operational seasonal forecast system has been operation since November 2011. System 4 is a fully coupled ocean-atmosphere dynamical forecast system. The atmospheric model has a resolution of approx. 0.7° (79 km) in longitude and latitude with 91 vertical levels. The ocean model has a horizontal resolution of 1° in the mid-latitudes with enhanced meridional resolution near the equator, with 42 vertical levels. Initial conditions for the atmospheric and land surface components are obtained from the ECMWF's ERA-Interim reanalysis. System 4 is a probabilistic forecast system meaning ensemble forecasts are generated for each lead time step since the initialization date which potentially shows a better skill than a deterministic forecast system (single value) (Molteni, et al., 2011).

System 4 is has two main types of forecast, namely reforecasts and operational forecasts. Operational forecasts run two different ensemble sizes based on the same mode configuration:

1. A 51-member ensemble initialized at the start of every calendar month with lead times from 0 to 6 months (7-month forecast period)
2. A 15-member ensemble initialized four times a year (01 Feb, 01 May, 01 Aug and 01 Nov) with a forecast range of 13 months.

System 4 seasonal reforecasts (also known as hindcasts) are available for 30 year period from 1981 to 2010. Reforecasts are generated on the first day of each month using the same configuration as real-time forecasts, but has a smaller ensemble size of 15 members and run for 7 months (Molteni, et al., 2011).

Ensembles for each forecast or reforecast are generated by using an ensemble of initial conditions and the use of stochastic physics. At the seasonal timescale, most of the spread in the ensemble is internally generated and the role of initial perturbations is limited. It is however attempted to represent most of the important perturbations to allow a realistic evolution of the ensemble spread through the early part of the forecast (Molteni, et al., 2011).

In this study, the System 4 seasonal reforecast product are used due to dataset's intended use in calibration and verification processes. Reforecast datasets for the meteorological forcing variables precipitation (variable *tp)* and near-surface air temperature (variable *tas*) were downloaded based on monthly initialisations of a 7-month forecast for the period between 1991 and 2010.

5.2 Statistical pre-processing

Due to the coarse resolution typically available from Global Climate Models datasets, a series of dynamic downscaling methods can be used derive higher resolution Regional Climate Models (RCMs) presenting local conditions in higher detail. RCMs however due suffer from similar bias problems as the global-scale models and are exceptionally demanding on computer resources (Hay & Clark, 2003). An alternative is the use of simple statistical downscaling techniques that can be employed to improve global climate model based output (Hay & Clark, 2003; Leung, et al., 2003).

Statistical downscaling techniques develop empirical relationships between features reliably simulated in global-scale models at larger grid size resolution, and surface predictands at sub-grid scales such as precipitation amounts. The disadvantage of statistical downscaling techniques is that empirical relationships must be develop from historical forecasts (also referred to as hindcasts or reforecasts) from the same model used in a real-time operational setting. Temporal stationarity of empirical relationships is thus assumed to translate to future climate forecast (Hay & Clark, 2003; Wetterhall, et al., 2012).

Several sophisticated statistical methods have been developed for downscaling climatic variables. Draw (2016) tested a number of statistical downscaling methods for precipitation forecast from System 4 for a catchment in Spain and found slightly better performance in terms of seasonal inflow forecast accuracy, reliability and bias against observations, using a simple linear downscaling method. For this study, the simple Linear Scaling (LS) method was selected for the statistical downscaling of System 4 based gridded precipitation and temperature forecasts.

5.2.1 Linear Scaling

For bounded variables such as precipitation, the Linear Scaling (LS) method scales the modelled variable value by multiplying it with the ratio of the observed and GCM modelled mean values over the control forecast period (also referred to as hindcast period):

$$\hat{z}_{mod}(t,n) = z_{mod}(t,n) \times \frac{\bar{Z}_{obs}(n)}{\bar{Z}_{mod}(n)}$$

(1)

where

$z_{mod}(t,n)$: GCM-modelled variable value at time t for point n in space

$\hat{z}_{mod}(t,n)$: The adjusted GCM based at time t for point n in space

$\bar{Z}$: Denotes the mean- observed (obs) and modelled (mod) values over the hindcast period

The linear scaling method removes GCM variable biases in the mean, but the coefficient of variance of the modelled data is not changed (Lenderink, et al., 2007). For unbounded variables such as temperature, additive adjustments are based on the difference between the mean values of observed and GCM modelled values over the hindcast period:

$$\hat{z}_{mod}(t,n) = z_{mod}(t,n) + (\bar{Z}_{obs}(n) - \bar{Z}_{mod}(n))$$

(2)

The application of the DM to System based precipitation and temperature data for the study area is discussed in the following sections.

5.2.2 Precipitation data bias correction

Long-term average monthly observed- and modelled precipitation values was based on the hindcast period from 1991 to 2009. For this period, System 4 precipitation data was collected for each subbasin based on monthly forecast initializations and a 7-month forecast period. Average System 4 precipitation values were determined as a factor of the month of the year and forecast lead month. *Figure 5-3* presents the average monthly System 4 based precipitation totals per forecast lead month for the *Embalse_Colbún* subbasin (see *Figure 3-2*). Average monthly-observed precipitation of the *Embalse_Colbún* subbasin based precipitation file is presented for comparison.

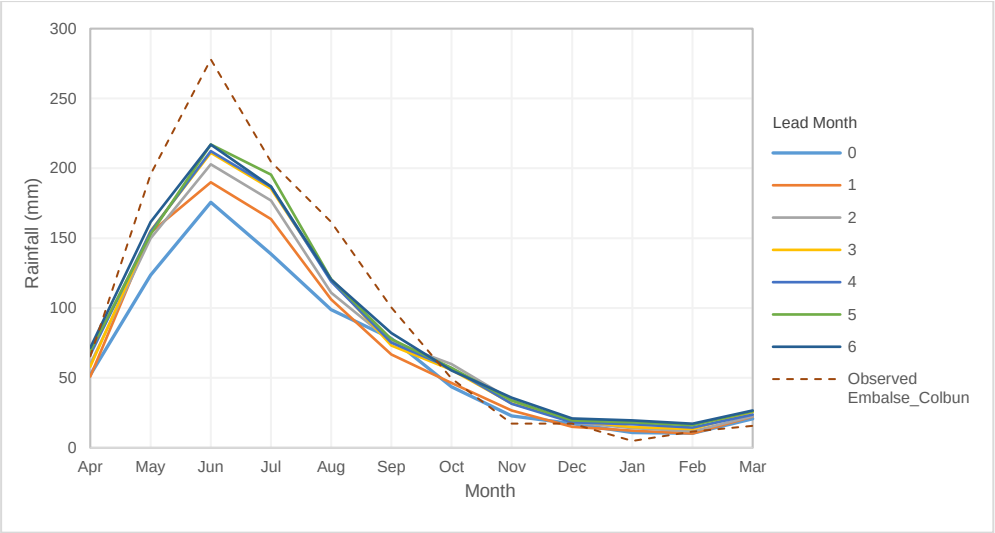

Figure 5-3 | System 4 average monthly forecasted precipitation per lead month for Embalse_Colbún subbasin (1991-2009)

From *Figure 5-3* it can be seen that monthly average total precipitation for System 4 forecast increases with increasing lead month time. Compared to the observed record of the subbasin, System 4 based forecast underestimates total precipitation for the majority of the high-rainfall season (Apr-Oct). Average precipitation forecasts in the low-rainfall season (Oct-Apr) are comparable to observed values.

Monthly scaling factors for subbasins were calculated based on the ratio between the average monthly precipitation values for the observed record, and System 4 data as a factor of forecast lead month. The calculated monthly precipitation scaling factors for the *Embalse_Colbún* subbasin are presented in *Figure 5-4*.

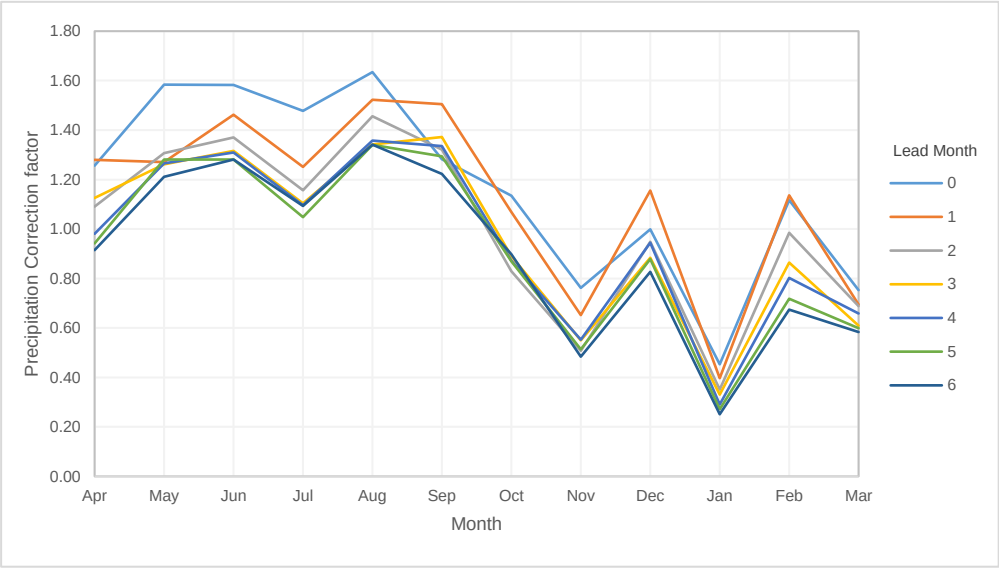

Figure 5-4 | Monthly precipitation scaling factors for System 4 precipitation data per forecast lead month (Embalse_Colbún subbasin)

Figure 5-4 shows precipitation scaling factors greater than 1.0 in the high-rainfall season when System 4 precipitation forecasts underestimate precipitation. Similarly, scaling factors are below 1.0 for periods of overestimation. Scaling factors can also be seen to decrease with increasing lead month time to compensate for increasing bias. Due to the low average observed precipitation totals for the period between November and March, differences between observed and forecasted precipitation totals constitute large percentage error values, resulting in exceptionally low value scaling factors for the months of November, January and March.

Monthly precipitation scaling factors were determined for all subbasins using the same method. These scaling factors were applied to the raw System 4 daily-accumulated 7-month precipitation forecast as collected for each subbasin. The resulting product is a bias corrected 7-month daily time series of forecasted precipitation to be used for meteorological forcing in the hydrological model.

5.2.3 Temperature bias correction

Long-term average observed monthly temperatures were calculated for the available data period from 2000 to 2009. For this period, System 4 temperature forecast data was collected for the *LoAguirre* and *MauleArmerillo* temperature stations. System 4 temperature data was based on monthly forecast initializations and a 7-month forecast period. Average System 4 temperature values were determined as a factor of the month of the year and forecast lead month. *Figure 5-5* presents the average monthly

System 4 temperatures per forecast lead month for the *LoAguirre* station location. The average observed monthly temperatures for the *LoAguirre* station has been added for comparison.

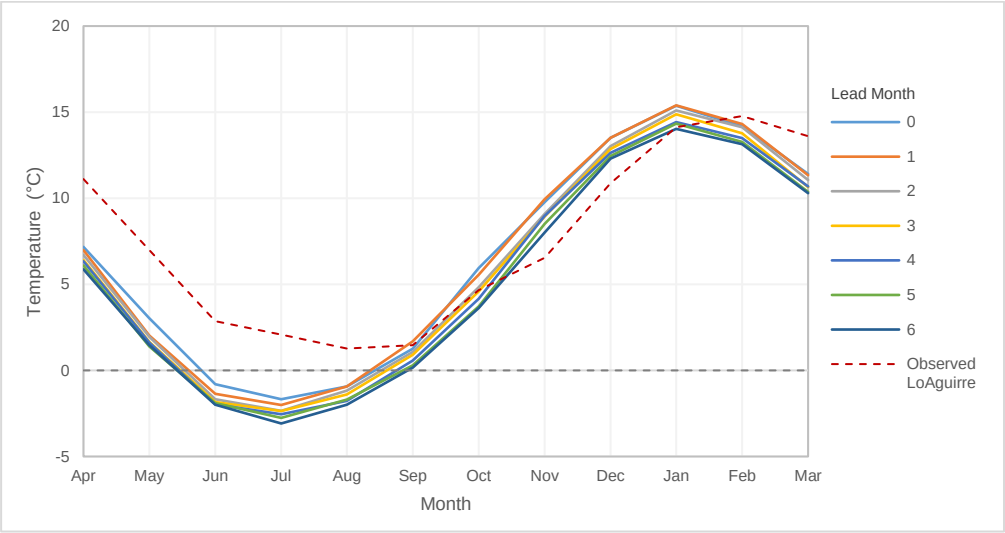

Figure 5-5 | System 4 average monthly temperature per lead month for LoAguirre station location (2000-2009)

Figure 5-5 shows System 4 based forecasts estimate lower average monthly temperatures compared to observed over the period from February to September. Higher average monthly temperatures are forecasted for the period from November to January. The monthly distribution of System 4 based temperatures also appears shifted ahead compared to the observed record, reaching minimum and maximum temperatures approximately one month before observed values. It is also evident *Figure 5-5* that a decrease in average monthly System 4 based temperatures occurs with increasing lead month times.

Elevation zone temperature files used in the calibrated NAM model were based on the established temperature-elevation relationship between the *MauleArmerillo* and *LoAguirre* stations. For forecast simulations, long-term temperature averages for these stations were used in the calculation of elevation zone temperatures. The introduction of System 4 temperature data therefore requires the generation of new elevation zone temperature files based on the established relationship. For each seasonal forecast simulation, System 4 forecast temperature grid data was therefore interpolated to the *MauleArmerillo* and *LoAguirre* stations locations. The known temperature elevations relationship between these locations was then used in the generation of new elevation zone temperature time series file for during the forecast period.

Monthly temperature bias correction factors for *LoAguirre* and *MauleArmerillo* temperature station locations were calculated based on the ratio between the average monthly temperature values for the observed record, and the System 4 interpolated forecast data as a factor of forecast lead month. The calculated monthly temperature additive scaling factors for the *LoAguirre* station are presented in *Figure 5-4.*

.

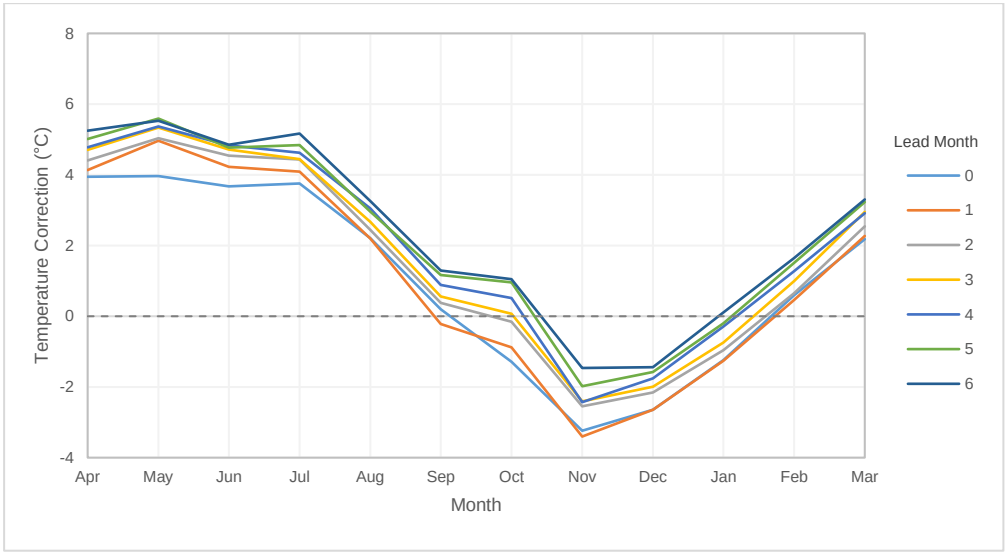

Figure 5-6 | Monthly additive bias correction factors for System 4 temperature data per forecast lead month (LoAguirre station location)

From *Figure 5-6* it can be seen that monthly temperature additive factors are positive for periods of where monthly average System 4 forecast temperatures were lower than observed. Temperature correction factors are also mostly negative during for the snowmelt period from October to January.

Monthly temperature bias correction factors were determined for both of the temperature station locations. These factors were applied to the raw System 4 temperature forecast as collected for each of the two temperature stations. The resulting product is a bias corrected 7-month long time series of forecasted instantaneous temperature data to be used during model simulation.

5.3 Hydrological Models

As mentioned in *Section 4.1*, DHI was contracted by Chilean utility company, Colbún S.A., to establish a real-time modelling system for both short-term and long-term forecasting of inflows to the Colbún Reservoir (DHI, 2011). The implemented modelling system, which is also used in this study, is based on the NAM rainfall-runoff model and the river- and reservoir regulation model, MIKE HYDRO Basin. For this study, the existing real time modelling system developed for Colbún S.A. was

upgraded to the latest version of MIKE OPERATIONS, previously known as MIKE CUSTOMIZED. The seasonal forecast model components for this study are presented in *Table 5-3* and described in this section.

Table 5-3 | Seasonal Forecast Model Components

Rainfall-Runoff Model	NAM
Reservoir- and River Regulation Model	MIKE HYDRO Basin
Real-time Modelling System	MIKE OPERATIONS

5.3.1 Rainfall Runoff Model – NAM

The hydrological model used in this study is the NAM model which is a module of MIKE11 river modelling package. The NAM (Nedbør Afstrømnings Model) was developed at the institute of Hydrodynamics and Hydraulics Engineering at the Technical University of Denmark (DTU) (Nielsen & Hansen, 1973; Madsen, 2000; Butts, et al., 2004; Butts, et al., 2007). NAM is a deterministic, lumped conceptual model designed to simulate catchment runoff with continuous accounting of moisture content in sub-surface zones. Meteorological forcing variables such as precipitation, evaporation and temperature are used to simulate interrelated catchment water storages and resultant streamflows. Observed discharge data can be provided in order to calibrate NAM catchment parameters and validate model output. Calibration of the NAM model parameters for the Upper Maule River Basin is discussed in *Section 5.3.3*.

5.3.2 Basin Configuration Model – MIKE HYDRO Basin

MIKE HYDRO Basin (MHB) is a multipurpose, map-based decision support tool designed for conducting integrated water resources analysis, planning and management of river basins (DHI, 2017; Butts, et al., 2016). MHB used as the basin configuration model for the Colbún S.A. forecasting system. Catchment based runoff generated from the NAM model was fed into the MHB model representing the Upper Maule River Basin drainage configuration of reservoirs, water users and water diversions. A map based representation of the MHB model configuration is shown in *Figure 5-7*. Characteristics of the major reservoirs in the Upper Maule River Basin in presented in *Table 5-4*.

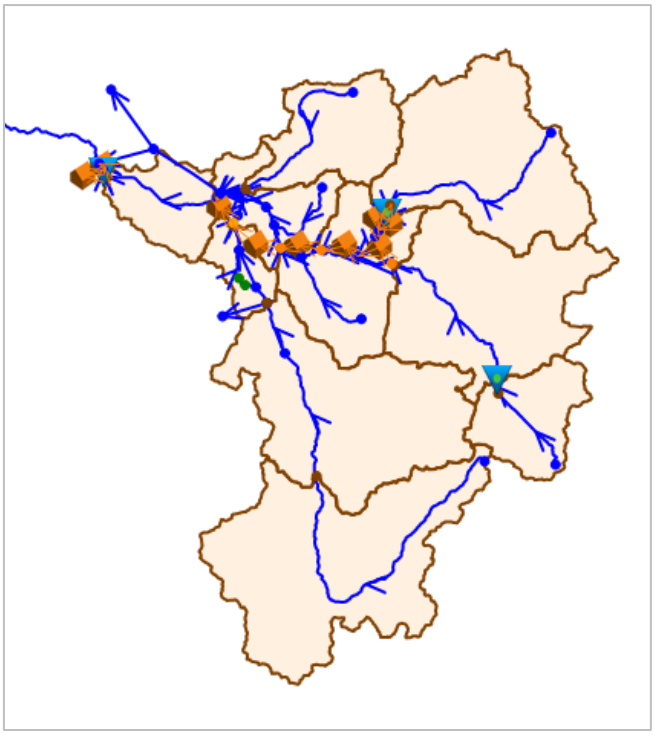

Figure 5-7 | MIKE HYDRO BASIN model configuration for Upper Maule River Basin

Table 5-4 | Characteristics of major reservoirs in Upper Maule River Basin

Reservoir Name	MHB Identifier	Bottom Level	Top of dead storage (DS)	Full supply level (FSL)	Non overspill crest (NOC)	Full Supply Capacity (FSC)
-	R#	masl	masl	masl	masl	million m^3
Embalse Melado	R8	617	625	649	655	137
Embalse Invernada	R10	1270	1278	1318.5	1319	180
Laguna Maule	R15	2152	2153	2180.3	2181	1550
Embalse Colbún	R16	393	397	437	438	1420

At the time of the MHB model configuration and calibration, limited information was available on reservoir regulation in the basin. It was found that attempting to derive such regulation rules from reservoir release records added extra uncertainty in the system, which has limited impact on the accuracy of a hydro-meteorological based forecast system. Therefore, the observed reservoir release records were used in modelled regulation. This approach was justified by the fact that infrastructure based regulation affect less than 20% of seasonal inflow, with the majority of inflow being unregulated or subjected to daily regulation only.

Figure 5-8 presents a schematic chart of Maule River regulation and abstraction upstream of the Colbún Reservoir. The four upstream hydropower facilities are

marked in black, the five off-takes to irrigation schemes are marked in green approximate and streamflow measurement stations are indicated in red.

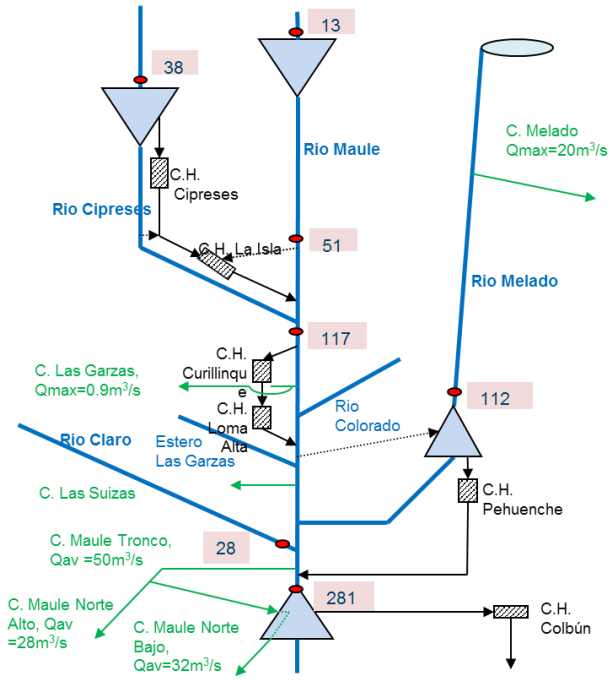

Figure 5-8 | Schematic chart of Maule River regulation and abstraction upstream of the Colbún Reservoir (DHI, 2011)

Although the Colbún Reservoir has a substantial reservoir capacity of around 1400 milllion m^3, reservoir storage can only be fully regulated during average inflow years. Such regulation would also require the full storage capacity of the reservoir, which in turn is not ideal with regards to hydropower turbine efficiency. Seasonal inflow forecasts can therefore provide valuable information to aid planning of hydropower production aspects such as generation periods, energy prices and optimal energy generation mix from available plants.

5.3.3 Model Calibration

Calibration of the seasonal forecast model implemented for Colbún S.A., was based on a calibration period of 1997 to 2009. Criteria for overall calibration performance is the accurate simulation of inflow water balance during and the seasonal distribution of this inflow in the catchment. The latter of these two criteria is particularly relevant in this study, where seasonal forecasts are made and a general bias in the simulation e.g. the snowpack accumulation, will affect the simulation results. A comparison of

the simulated and observed water balance in the form of accumulated Colbún Reservoir inflows is shown in *Figure 5-1*. A comparison of the simulated and observed monthly accumulated inflow to the Colbún Reservoir is shown in *Figure* .

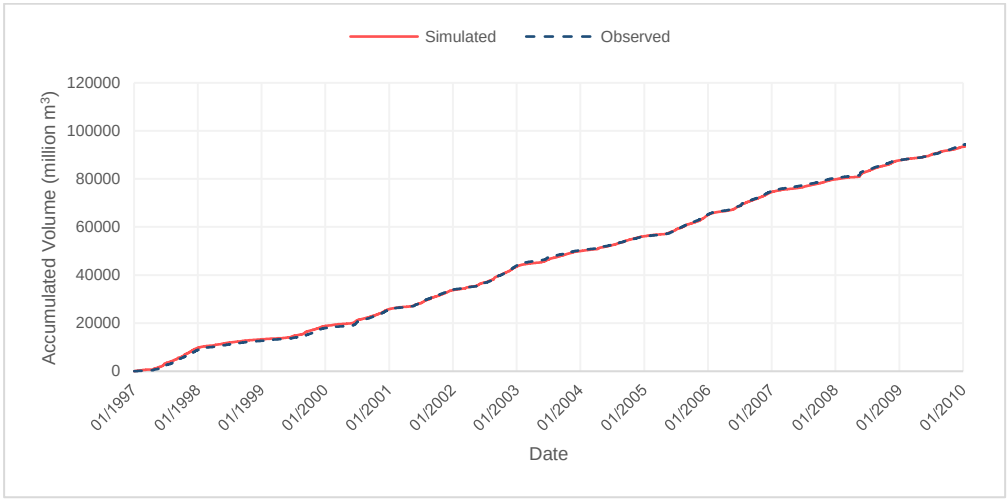

Figure 5-9 | Long term observed- vs simulated accumulated inflow to Colbún Reservoir (1997-2009)

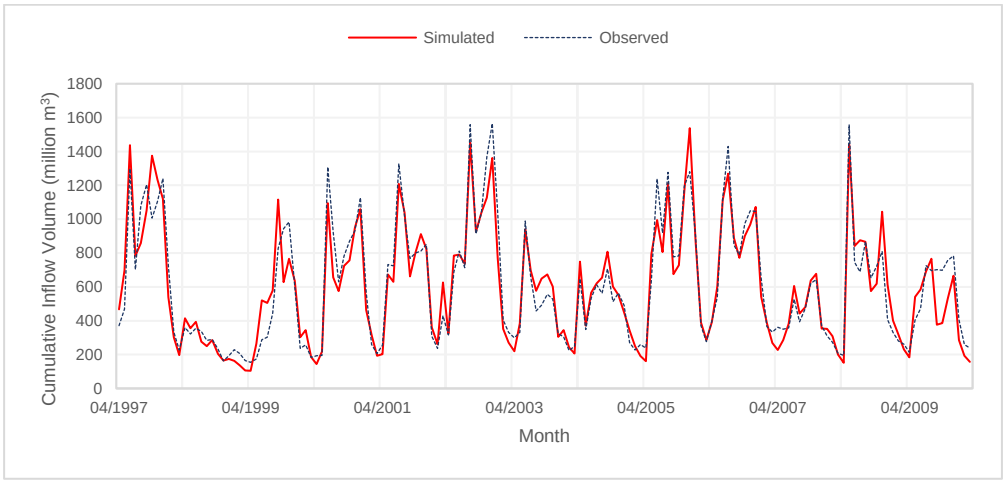

Figure 5-10 | Observed- vs simulated monthly accumulated inflow to Colbún Reservoir (1997-2009)

From *Figure 5-10 and Figure 5-11* it can be seen that a good calibration fit was obtained for Colbún Reservoir inflow in terms inflow water balance during and the seasonal distribution of this inflow. *Figure 5-11* presents a comparison of observed

and simulated monthly mean inflow volumes to the Colbún Reservoir. Calculated percentage volume errors for simulated average monthly inflow volumes are presented in *Table 5-5*.

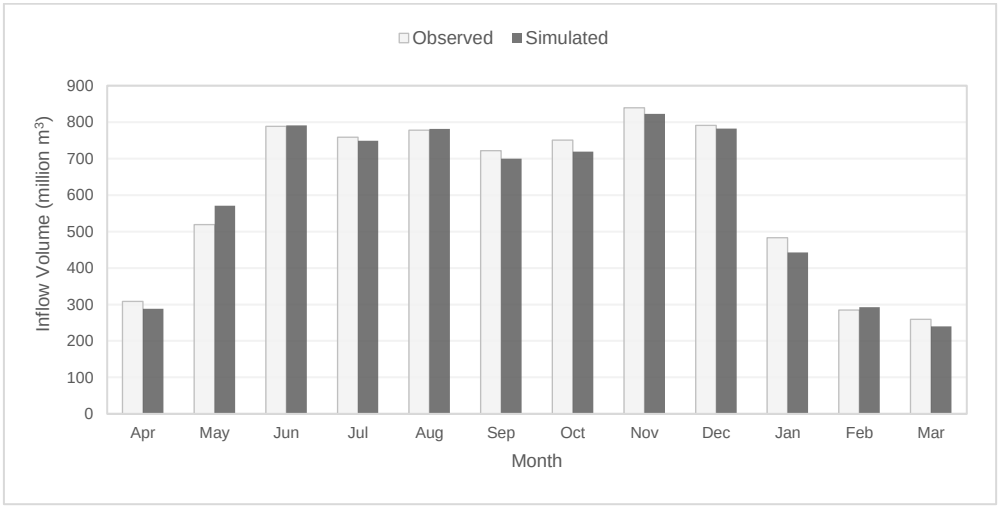

Figure 5-11 | Observed- vs simulated average monthly inflow to Colbún Reservoir (1997-2009)

Table 5-5 | Observed- vs simulated average monthly cumulative inflow to Colbún reservoir (1997-2009)

		Month												
Series	**Unit**	**Apr**	**May**	**Jun**	**Jul**	**Aug**	**Sep**	**Oct**	**Nov**	**Dec**	**Jan**	**Feb**	**Mar**	**Annual**
Observed Inflow	million m^3	308	519	788	759	778	721	751	839	791	483	284	259	7282
Simulated Inflow	million m^3	288	570	791	749	781	700	719	823	782	442	292	240	7179
Volume error	%	-7.1	9.0	0.4	-1.4	0.4	-3.1	-4.4	-2.0	-1.1	-9.3	2.7	-8.0	-1.4

A comparison of observed and simulated total annual accumulated inflow to the Colbún Reservoir is presented in *Figure 5-12*. Initial review of this figure reveals reasonable comparisons between annual accumulated inflow totals of the simulated and observed records for the majority of years. Underestimations of observed inflow can however be seen for above-average precipitation years 2002, 2005 and 2006. Overestimation of inflow however occurs during the below-average precipitation years of 2003 and 2004. The overall performance of the 13-year calibration period was found acceptable, based on the available data at the time and the model's intended use.

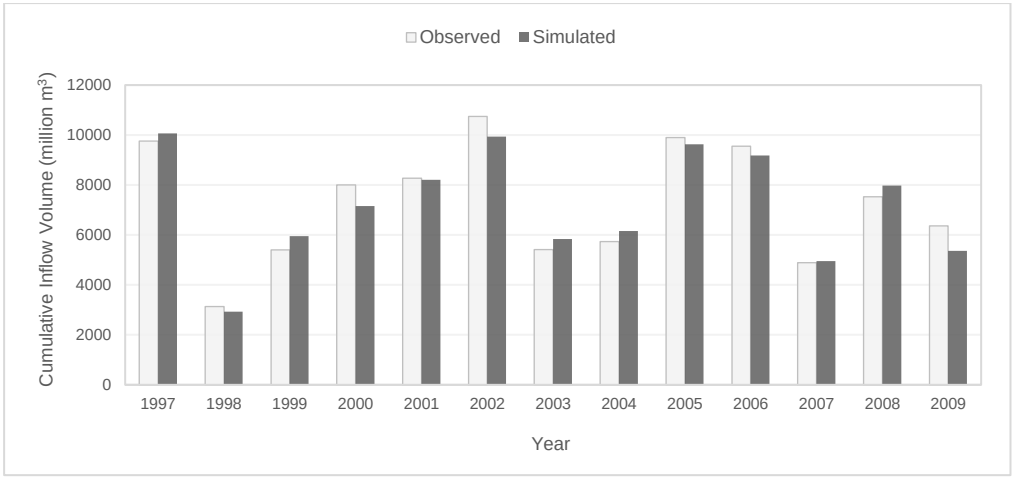

Figure 5-12 | Observed- vs simulated annual accumulated inflow to Colbún Reservoir (hydrological years 1997-2009)

5.3.4 Data Assimilation of streamflow and reservoir levels

The availability of real-time data in hydrological forecasting systems provides the opportunity to update simulated hydraulic states or catchment parameters to improve the accuracy of the forecast. This process is called Data Assimilation (DA) or real-time updating (Sene, 2010). MIKE HYDRO Basin allows for assimilation of model state variables to observed conditions in the basin. Both reservoir levels and streamflows can be assimilated, but only one state variable may be assimilated at a single model calculation node. In some cases however, it is relevant to assimilate both reservoir levels as well as inflow consisting of runoff from the local catchment and inflow from upstream catchment and regulations. In such cases, two calculation nodes were created for the reservoir in question with the aid of an upstream dummy catchment (see *Figure 5-13*). No runoff is generated from the dummy catchment and inflow can be assimilated at the upstream node, while water levels are assimilated at the reservoir node. An example of this set-up for the Colbún Reservoir is illustrated in *Figure 5-13*.

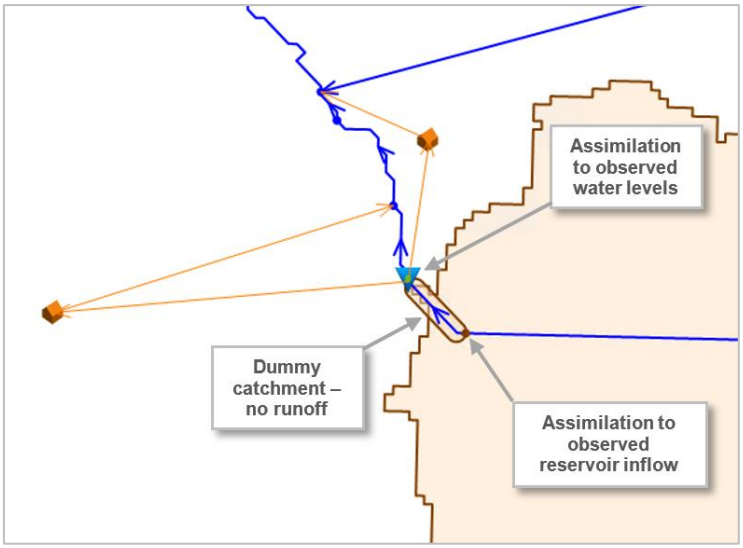

Figure 5-13 | Real and dummy catchments for data assimilation of Colbún Reservoir in MIKE HYDRO Basin

5.4 Support Software Systems

5.4.1 MIKE OPERATIONS

MIKE OPERATIONS, previously known as MIKE CUSTOMIZED, is a software product designed for model-based forecast services and for online operational control of river systems, water collection systems and water distribution systems (DHI, 2016). MIKE OPERATIONS is a product consolidation of software tools developed and applied in DHI projects over the past 6-7 years, providing data management, decision support and operational forecasting services in one parent window.

MIKE Workbench is an advanced desktop client provided alongside MIKE OEPRATIONS. MIKE Workbench is designed for users who apply data analysis and process tools interactively to allow for the configuration of automated workflows, scripts and custom-made data reports (DHI, 2017).

For this study, the existing real time modelling system developed for Colbun S.A. (see Section 4.1) was upgraded to the latest version of MIKE OPERATIONS. The MIKE Workbench platform was used to establish model links between the rainfall-runoff NAM model and reservoir and river regulation model MIKE HYDRO Basin for the study area. Data management and scripting tools inside MIKE Workbench were used for the configuration of automated workflows for multiple seasonal forecast simulations. Seasonal forecast simulations were conducted for 6-month hindcast period until the ToF, followed by a 7-month forecast period. All simulations ran on a 6-hour timestep resulting in a single forecast simulation runtime of approximately 23 minutes.

5.4.2 RStudio

RStudio is an open source integrated development for R, a programming language for statistical computing and graphics. Amongst other features, *RStudio* includes a console and syntax-highlighting editor that supports direct code execution, as well as various tools for plotting (RStudio, 2017). For this study, R was used in the *RStudio* environment for accessing and retrieving dimensional slices of System 4 seasonal forecasts data as well as pre-processing of model input data using custom functions. Some of the main R packages used in this study are listed below:

- loadeR.ECOMS : interface to the ECOMS-UDG
- transformeR : climate data manipulations
- visualizer : visualization tools for forecast verification
- ggplot2 : plotting system of complex multi-layered graphics
- hyfo : hydrological data manipulations

5.5 Model Output

The required seasonal forecast model outputs from the reservoir and river regulation model, MIKE HYDRO Basin, are stored within the MIKE Workbench platform. The model output under analysis is the simulated inflow to Colbún Reservoir for each forecast option. Based on the meteorological forcing variables used in the simulation, streamflow ensembles are produced through ESP or as probabilistic streamflow forecasts.

5.5.1 Extended Streamflow Prediction

The Extended Streamflow Prediction (ESP) was first introduced by the US National Weather Service (NWS) in 1977 and still used in modern streamflow forecasting systems (Twedt, et al., 1977; Najafi, et al., 2012). ESP provides probabilistic streamflow predictions during any user-designated time period for upstream catchments. ESP models typically use calibrated conceptual or physically based hydrological models and long-term historical records of observed meteorological forcing variables, such as precipitation and temperature, to simulate a possible set of streamflow regimes upon the current conditions of the catchment.

In operational settings, the calibrated hydrological model is run up until the ToF to reflect the catchment initial conditions. For the forecast period, the model can be driven by 1) resampled historical meteorological forcing variables or 2) meteorological forecasts to generate a range of possible future streamflows. A core assumption of the ESP approach, is that historical meteorological events are representative of possible future conditions. This provides ESP the basis for considering the uncertainty related to future climate, which could be a significant component of forecast uncertainty during certain seasons (Najafi, et al., 2012).

The ESP based approach can be used for short term- and longer term seasonal forecasts. For seasonal forecasts, the mean value of ensemble streamflow volume is commonly reported as a single best prediction value. In this study, ESP is used to define the range of possible future seasonal inflow volumes to the Colbún Reservoir based on meteorological forcing of resampled precipitation data.

5.5.1.1 ESP-Q

Another method for deriving ensemble streamflow forecast, referred to here as ESP-Q, is based on the use of resampled observed streamflow records under the assumption that historical streamflow events representative of possible future conditions. This simpler approach does not require the use of hydrological model and resampled historical streamflow records are used to determine a possible range of future accumulated streamflow. This approach however does have several limitations as varying catchment conditions over the hindcast and forecast period, such as groundwater and surface water storages, are not taken into account. The ESP-Q was however included in this study for reference, based on the observed inflow record of the Colbún Reservoir.

Figure 5-14 presents an example of an ESP-Q accumulated inflow ensemble for Colbún Reservoir based on 21 years (1991-2011) of resampled observed inflow data. The ESP-Q accumulated inflow ensemble in *Figure 5-14* is based on a ToF of 01 April 2002 and a forecast period of 7 months. ESP-Q ensemble members are based on individual extracted records of observed accumulated inflow to the Colbún Reservoir for the historical period 01 April – 31 October for the years from 1991 to 2011, with available data. The accumulated inflow observed over the forecast period is shown in blue for reference. Tercile based ranges (0.33, 0.66) of predicted future accumulated inflow are determined from ensembles spreads over the forecast period. Thus creating three categories of *below-normal*, *normal* and *above-normal* potential accumulated inflow ranges are created, each containing 7 ensemble members per category as shown in *Figure 5-14.*

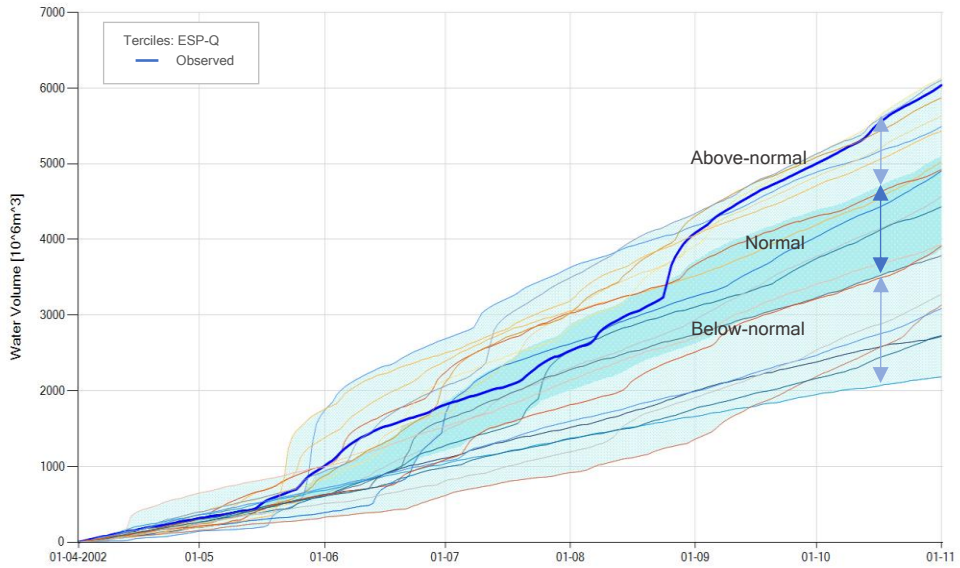

Figure 5-14 | High-rainfall season accumulated inflow forecast: ESP-Q ensemble member and corresponding terciles ToF 2002-04-01

5.5.1.2 ESP-P

The ESP approach based on the use of a calibrated hydrological model and meteorological forcing of resampled historical precipitation data, is referred to as ESP-P. *Figure 5-15* presents an example of an ESP-P accumulated inflow ensemble for Colbún Reservoir based on 21 years (1991-2011). This accumulated streamflow ensemble was produced with the use of the calibrated NAM and MIKE HYDRO Basin hydrological models. From *Figure 5-15* it can be seen that the calibrated hydrological model is run over the 6-month hindcast period up until the ToF (see *Section 2.4*). For the forecast period, the model is driven by the meteorological forcing of resampled historical precipitation data to generate future streamflows.

The ESP-P accumulated inflow ensemble in *Figure 5-15* is based on the same ToF (01 April 2002) and a forecast period of 7 months, as the ESP-Q example in *Figure 5-14*. The observed inflow record is shown in blue and the simulated inflow based on the calibrated model is shown in red. Differences between the simulated and observed records can be attributed to uncertainties in hydrological model prediction skill and uncertainties in IHC. In *Figure 5-15*, ESP-P ensemble members are plotted over ESP-Q based tercile category ranges.

In terms of reservoir management, this study investigates the predicted range of reservoir inflows over the forecast period. The probability of predicting a *below-normal*, *normal* or *above-normal* seasonal inflow range is assigned to the proportion of ensemble members per tercile range. Ensemble members locate above (below) the maximum (minimum) tercile range are considered to be in additional categories during forecast accuracy validation (see *Section 5.6.2*).

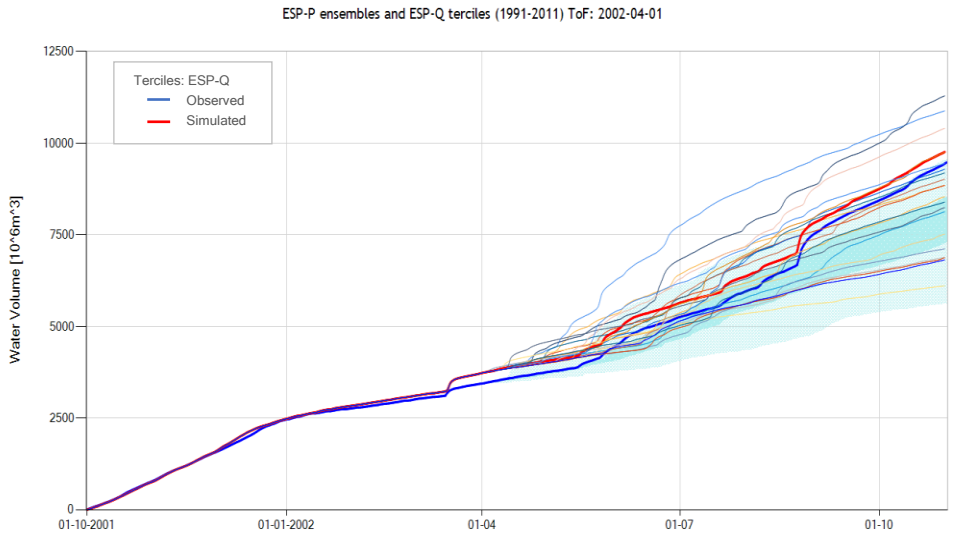

Figure 5-15 | High-rainfall season forecast: ESP-P ensemble and ESP-Q terciles ToF 2002-04-01

5.5.1.3 Probabilistic Streamflow Forecasts

For the forecast period, the ESP based approaches can be driven by resampled historical meteorological forcing variables (ESP-P) or meteorological forecasts to generate a range of possible future streamflow. In the next step of the study, ECMWF-System 4 probabilistic based reforecast datasets were used for meteorological forcing of the hydrological models to produce future streamflow ensembles. *Figure 5-16* presents an example of a future streamflow ensemble produce through the use of a 15 member System 4 seasonal precipitation forecast initialised on 01 April 2002 for a 7-month forecast period. From *Figure 5-16* it can be seen that the calibrated hydrological model is run over the 6-month hindcast period up until the ToF, identical to the ESP-P based approach.

To compare the forecast performance of various System 4 based forecasts options (see *Table 5-2*), System 4 based future accumulated inflow ensembles are plotted on ESP-P based tercile categories of accumulated inflow. Tercile categories are define based on ESP-P ensembles for *below-normal*, *normal* and *above-normal* inflow ranges. The probability of predicting an *above-normal*, *normal*, or *below-normal* seasonal inflow, therefore, is the proportion of the 15 System 4 based inflow ensemble members in each category.

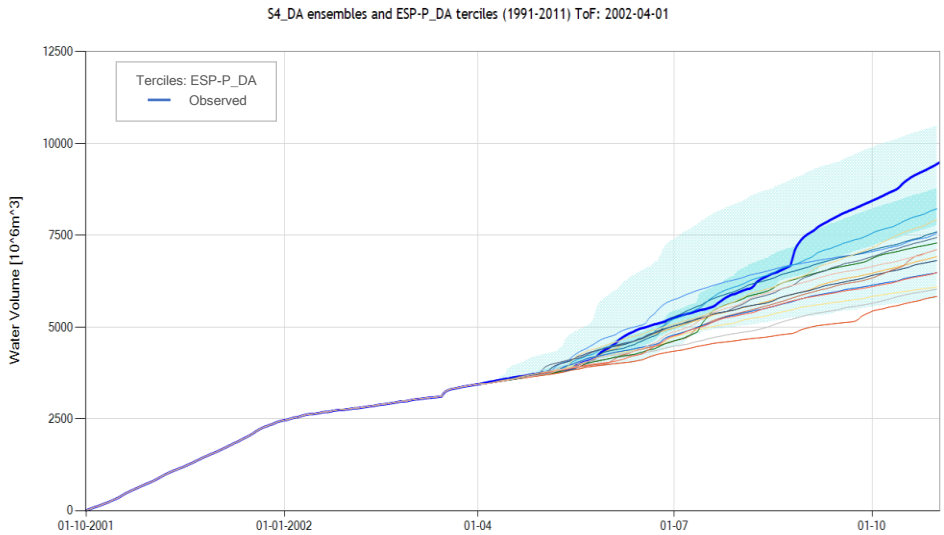

Figure 5-16 | High-rainfall season forecast: S4_DA ensemble and ESP-P_DA terciles ToF 2002-04-01

5.6 Seasonal Forecast Verification

There are several performance aspects of forecast to assess to help identify the strengths and weaknesses of a forecast system. Verification can allow for the identification of areas where effort or resources have improved the forecast. The majority of verification analyses are aimed to assess whether the forecast system has any skill compared to a baseline forecast. Jolli & Stephenson (2012) stated that longer-range forecast are diffucult to verify due to their limited sample sizes for verificaction analysis. Limited sample sizes can also reflect large uncertainty in the quality of results. Thus, it can be difficult to assess the performance of a longer-range seasonal forecast system. Some of the forecast verification aspects addressed in this study are listed below:

Bias: The difference between the mean of the forecasts and the mean of the observations. Can be expressed as a percentage of the mean observation.

Accuracy: The correspondence between the forecast and the reality which is recorded as observed realizations.

Skill: A measure of the relative improvement of the forecast over a reference or 'low-skill' baseline forecast. Typical used reference forecasts include climatology or output from an earlier version of the forecasting system.

The seasonal forecast skill assessment measures used in the study are discussed in the following sections.

5.6.1 Seasonal Forecast Model Bias

Seasonal forecast model bias for all forecast options (see *Section 5.1.2*) was calculated as the difference of the forecasted mean accumulated inflow volume to the Colbún Reservoir and the observed inflow volume. For ESP-Q and ESP-P ensembles, the forecast mean was based on the mean value of the 21 inflow ensemble members. System 4 based seasonal forecast model bias was calculated based on the mean value for the 15 probabilistic based inflow ensemble members. Bias values were calculated at the end of each lead month and expressed percentage volume error of the observed value.

5.6.2 Ranked Probability Score (RPS)

The Ranked Probability Score (RPS) measures the accuracy of discrete probabilistic based forecasts issued for multi-categorical events in matching observed outcomes. Both the location and spread of the forecast distribution taken into account in the evaluation of how close the distribution is to the observed value (Wilks, 2005). The formula for RPS calculation is given by *Equation 3* and *Equation 4*. For each event, the RPS^n is calculated after accumulating the observation and forecasts vectors. The overall RPS, therefore, is the mean value of the RPS^n.

$$RPS^n = \frac{1}{K-1}\sum_{k=1}^{K}(CDFF_{fc,k}^n - CDFF_{obs,k}^n)^2 \quad (3)$$

$$RPS = \frac{1}{N}\sum_{n=1}^{N} RPS^n \quad (4)$$

where

K denotes the total number of categories (k= 1, 2,…, K)

N denotes the total number of forecast observation pairs (n= 1, 2,…, N)

$CDF_{fc,k}^n$ is the cumulative forecast probability for each category and forecast-observation pair

$CDF_{obs,k}^n$ is the cumulative observation vector for each category and forecast-observation pair

A RPS value of zero would represent a perfect forecast and positive values indicate a less than perfect forecast with a maximum value of 1. For this study, a total of five categories were defined for the calculation of RPS scores for probabilistic based forecast ensembles. Three of the five categories were defined by the ESP-P terciles ranges based on climatology; *below-normal*, *normal* and *above-normal*. Two additional categories were created to include forecast ensemble members located outside the range of established ESP-P terciles; *below ESP-P min* and *above ESP-P max*.

Table 5-6 presents example inputs for RPS^n calculation for a System 4 precipitation based (S4_DA) high-rainfall season inflow forecast as shown in *Figure 5-17*. RPS^n values are calculated for each of the System 4 based forecast options for the high-rainfall and low-rainfall seasonal periods separately. It should be noted that RPS calculations are based on time slicing of forecast and observed time series at the end of each forecast lead moth period, and are thus not representative of an average RPS score over the entire lead month.

Note: RPS scores were calculated per forecast option with consideration if DA was included during the hindcast period. RPS for forecast options without DA were based on tercile categories from forecast option 2, 'ESP-P'. RPS for forecast options including DA were based on tercile categories from forecast option 3, 'ESP-P_DA' which included DA in the ESP-P based approach.

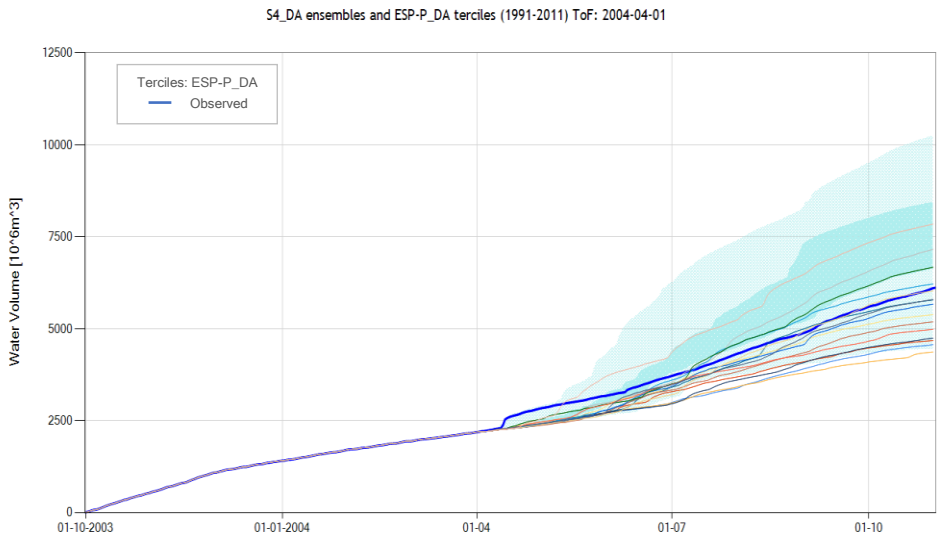

Figure 5-17 | High-rainfall season forecast: S4_DA ensemble and ESP-P_DA terciles ToF 2004-04-01

Table 5-6 | Example of RPS^n calculation inputs S4_DA ensemble forecast ToF 2004-04-01

Cumulative forecast probability per category							
Category	at end of Lead Month						
	0	1	2	3	4	5	6
Above ESP-Q max	100.0%	100.0%	100.0%	100.0%	100.0%	100.0%	100.0%
Above Normal	100.0%	100.0%	100.0%	100.0%	100.0%	100.0%	100.0%
Normal	86.7%	93.3%	100.0%	100.0%	100.0%	100.0%	100.0%
Below Normal	13.3%	86.7%	93.3%	73.3%	73.3%	80.0%	80.0%
Below ESP-Q min	0.0%	0.0%	20.0%	26.7%	13.3%	13.3%	6.7%
Cumulative observation vector							
Category	at end of Lead Month						
	0	1	2	3	4	5	6
Above ESP-Q max	1	1	1	1	1	1	1
Above Normal	1	1	1	1	1	1	1
Normal	0	1	1	1	1	1	1
Below Normal	0	0	1	1	1	1	1
Below ESP-Q min	0	0	0	0	0	0	0
RPS^n	0.19	0.19	0.01	0.04	0.02	0.01	0.01

The RPS^n at the end of lead month 0 for the above example would be calculated as follows:

$$RPS^n = \frac{1}{5-1} \times ((0-0)^2 + (0.133-0)^2 + (0.867-0)^2 + (1-1)^2 + (1-1)^2) = 0.19$$

5.6.3 Ranked Probability Skill Score (RPSS)

The Ranked Probability Skill Score (RPSS) measures the RPS improvement of forecast to a reference forecast (RPS_{ref}) (Weigel, et al., 2007). The RPSS is calculated as follows:

$$RPSS = 1 - \frac{RPS}{RPS_{ref}} \quad (5)$$

The RPSS relates RPS and RPS_{ref} in such a sway that positive RPSS values indicate forecast benefit with respect to the reference forecast. A RPSS value of zero would indicate identical score for the forecast RPS and RPS_{ref}. In this study, the seasonal forecast option based on raw System 4 precipitation forecast ensemble (forecast option 4, 'S4') was used as the RPS_{ref} reference forecast. This would allow for the assessment on forecast benefit for System 4 based forecast options.

6 Results and Discussion

This chapter presents seasonal forecast model results in the form of time series plots as well as discussion around the visual inspection of results. Due to the large volume of forecast model output data, result plots for selected forecast options and study years are presented and discussed. Additional seasonal forecast model output plots can be found in *Appendix B*.

6.1 ESP-Q and ESP-P

Figure 6-1 through *Figure 6-7* present the results of the ESP-Q and ESP-P (see 5.5.1) forecast simulations for the selected study years. Accumulated inflow volume time series to the Colbún reservoir are plotted for all ESP-P ensemble members. These are compared to ESP-Q terciles for the 7-month forecast period, which provides a historical reference of observed accumulated inflow over the seasonal period. The observed inflow time series as well as the rainfall-runoff based simulated accumulated inflow time series, are presented over the hindcast and forecast periods. Seasonal inflow forecast results are displayed in chronological order according to the ToF, with high-rainfall season (April-October) forecasts preceding low-rainfall season (October-April) forecasts for each study year. Comparisons of observed and simulated total accumulated seasonal inflow volumes to the Colbún at ToF are presented in *Table 6-1* and *Table 6-2*. Simulated seasonal accumulated inflows are based on the use of historical precipitation time series of the corresponding years.

Table 6-1 | High-rainfall season (Apr-Oct): Total accumulated Colbún Reservoir inflow at ToF (million m^3)

	01 April 2002	01 April 2003	01 April 2004	01 April 2005
Observed	3439	5741	2186	2324
Simulated	3728	4835	2318	2316

Table 6-2 | Low-rainfall season (Oct-Apr): Total accumulated Colbún Reservoir inflow at ToF (million m^3)

	01 October 2002	01 October 2003	01 October 2004
Observed	5001	3229	3412
Simulated	5025	3485	3766

6.1.1 2002: Above-average precipitation year

The results of forecasts for the high-rainfall season and the low-rainfall season for 2002 are presented in *Figure 6-1* and Figure 6-2 respectively.

6.1.1.1 High-rainfall season (Apr-Oct) ToF: 2002-04-01

Seasonal inflow forecast conducted at the start onset of the high-rainfall season will provided reservoir managers with predictions of reservoir inflow, allowing for water

allocation and power generation planning over long lead times. From *Figure 6-1* it can be seen that the observed inflow during the forecast period falls within above-normal flow category based on the ESP-Q terciles. The simulated flow appears to have a good fit to the observed record until approximately one month before the ToF, when an overestimation of inflow occurs. This deviation from the observed record remains until the ToF, creating an overestimation of total accumulated inflow at the start of the forecast period.

The majority of the ESP-P ensemble members also fall within or above the *above-normal* ESP-Q tercile, which agrees well with the observed inflow for this year. As the ESP-P ensemble members are based on historical precipitation data, ensemble members falling outside the ESP-Q terciles indicate an accumulation of inflow over the forecast time period that has not historically been experienced. These ensemble members are associated with the high rainfall years of such as 1991, 1997 and 2005. The reason that these high rainfall year ensembles fall outside the historically based ESP-Q terciles, is that these high rainfall years were typically preceded by drier years of low precipitation and runoff (see *Figure 4-8*). Indicating an increased percentage reduction in runoff due to initial drier catchment conditions, as discussed in *Section 4.6.3.*

The 2002 hydrological year was preceded by two above average rainfall years (*see Figure 4-8*). The simulated total accumulated inflow volume to the Colbún reservoir over the hindcast period is an above-average value of 3728 million m^3 (see *Table 6-1)*, resulting in increased surface water and groundwater storage levels, limiting storage capacity and regulation of inflow. The meteorological forcing of resampled historical precipitation series thus results in increased predicted runoff compared to historical years.

The ESP-P ensemble spread does create a wider range of possible flow accumulation volumes at later lead month times compared to the ESP-Q terciles. Due to the large spread of both the ESP-Q and ESP-P ensemble members, accurate estimation of accumulated flow at later lead months would be challenging. If the average accumulated flow value over all ensemble members were used as a forecast estimate, the higher ESP-P ensemble would provide a result closer to the observed record compared to ESP-Q.

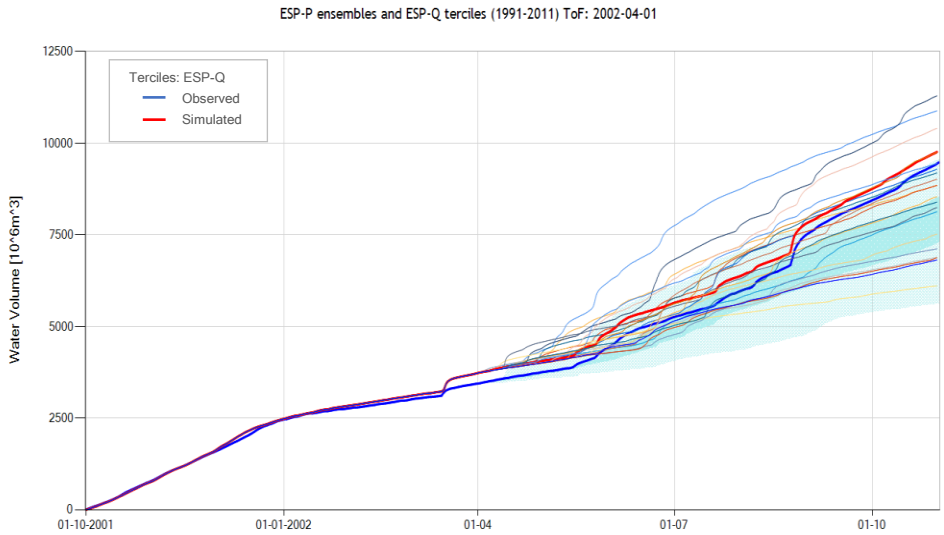

Figure 6-1 | High-rainfall season forecast: ESP-P ensemble and ESP-Q terciles ToF 2002-04-01

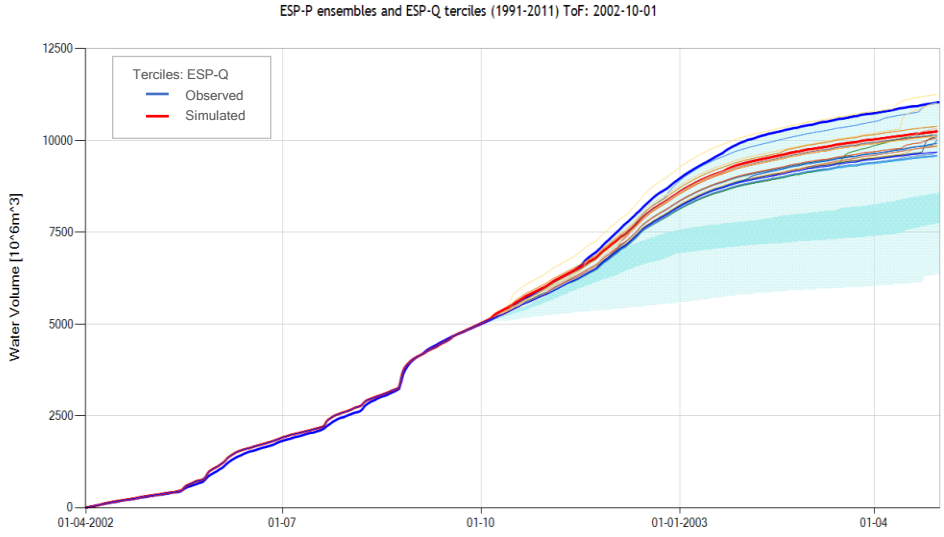

Figure 6-2 | Low-rainfall season forecast: ESP-P ensemble and ESP-Q terciles ToF 2002-10-01

6.1.1.2 Low-rainfall season (Oct-Apr) ToF: 2002-10-01

Seasonal inflow forecast conducted at the start onset of the low-rainfall season will provided reservoir managers with temporal and quantitative information about predominantly snowmelt-based inflow, allowing for efficient planning and water use over longer lead times. From *Figure 6-2* it can be seen that simulated inflow shows good performance over the hindcast period and simulated and observed values are almost identical at ToF, thus reducing the potential accumulated volume error at the start of the forecast period. The observed record over the forecast period indicates that exceptionally high inflow was experienced when compared to the ESP-Q terciles. The observed accumulated inflow is close to the upper limit of the ESP-Q terciles, and is the largest historical inflow volume for this 7-month period.

Figure 6-2 shows a wide range for the ESP-Q terciles. The *normal* tercile range also appears relatively narrow compared to its adjacent terciles, indicating that the majority of inflow time series are closely group together with a fewer number of uncommon high or low inflow events (see *Figure 4-3*) .

As shown in *Figure 4-3*, inflow to the Colbún Reservoir during the low-rainfall season is largely dependent on snowmelt, as precipitation is limited during this seasonal period. As discussed in *Section 4.6.3*, runoff during the low-rainfall season is greatly dependent on the total amount of precipitation during the preceding season. The resultant ESP-Q terciles during the low-rainfall season are therefore compromised of a wide range of historical inflow time series.

The ESP-P ensemble members for this season form a narrower grouping over the entire forecast period. This is due to the limited amount and variability of historical rainfall over the seasonal period from November to March (see *Figure 4-1*). The narrow range of ESP-P ensemble members provide significantly improved forecast estimate of accumulated flow volumes compared to ESP-Q. The ESP-P however still underestimates the accumulated flow at later lead months, as the majority of input precipitation time series are lower than the observed record. A single ESP-P ensemble member can be seen above the ESP-Q tercile range, corresponding to the 1997 high rainfall year experienced during the very strong El Niño phase.

These results clearly show that forecasts for the low-rainfall season are more strongly dependent on the initial conditions than on the precipitation forecasts. The initial conditions are accurately represented in our inflow forecasts by using a well-calibrated hydrological model and a long hindcast period prior to the ToF to incorporate the high rainfall season. Therefore using hydrological models to provide seasonal forecasts during this low-rainfall season appears to provide accurate and reliable inflow forecasts for lead times of many months in this case.

As discussed in the previous section, above-average precipitation was experienced in the 2002 hydrological year. Simulated total accumulated inflow at ToF is an above-average value of 5025 million m^3 (see *Table 6-2),* thus limiting the catchment water storage capacity and increasing the runoff percentage.

6.1.2 2003: Below-average precipitation year

The results of forecasts for the high-rainfall season and the low-rainfall season for 2003 are presented in *Figure 6-3* and *Figure 6-4* respectively.

6.1.2.1 High-rainfall season (Apr-Oct) ToF: 2003-04-01

Figure 6-3 shows a clear divergence of the simulated and observed inflow records, with a large underestimation of simulated inflow volumes during the hindcast period. This underestimation of simulated inflow could be a result of multiple contributing factors such as poorer performance by the calibrated model, as well as unaccounted reservoir regulation over this time period. The observed inflows over the forecast period corresponds to a *normal* inflow for the initial months, after which accumulated flow decreases to the *below-normal* range. The simulated total accumulated inflow at ToF is an above-average value of 4835 million m^3, compared to the previous year's value of 3728 million m^3 (see *Table 6-1)*, resulting in above-average catchment water storage levels due to increased snowmelt based runoff.

Although the simulated underestimates the accumulated inflow at ToF, the majority of ESP-P ensemble members overestimate the accumulated flow value for multiple lead months. Similar to the 2002 high-rainfall season (see *Figure 6-1*), the meteorological forcing of resampled historical precipitation series and limited available storage capacity, results increased predicted inflow compared to historical years. As 2003 experienced below-average precipitation, the majority of ESP-P ensembles overestimate the resultant inflow compared to the observed.

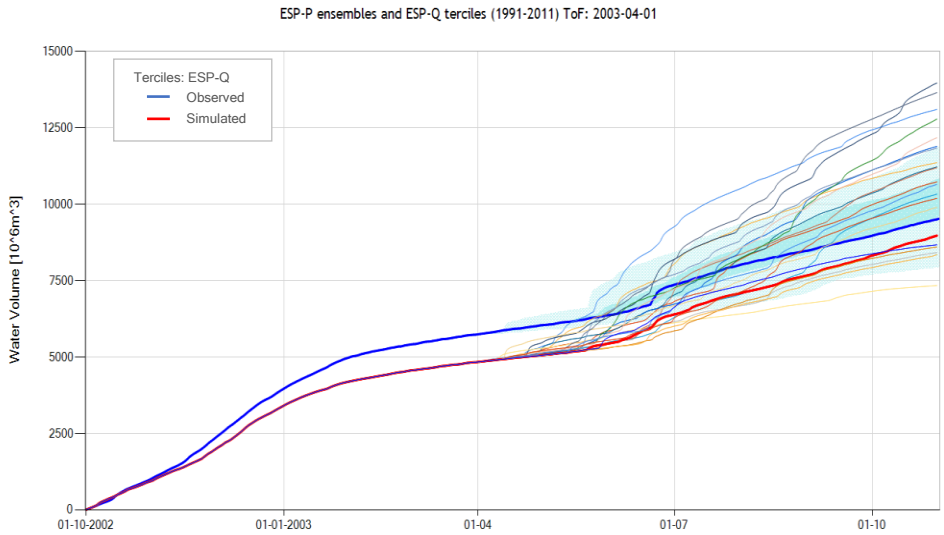

Figure 6-3 | High-rainfall season forecast: ESP-P ensemble and ESP-Q terciles ToF 2003-04-01

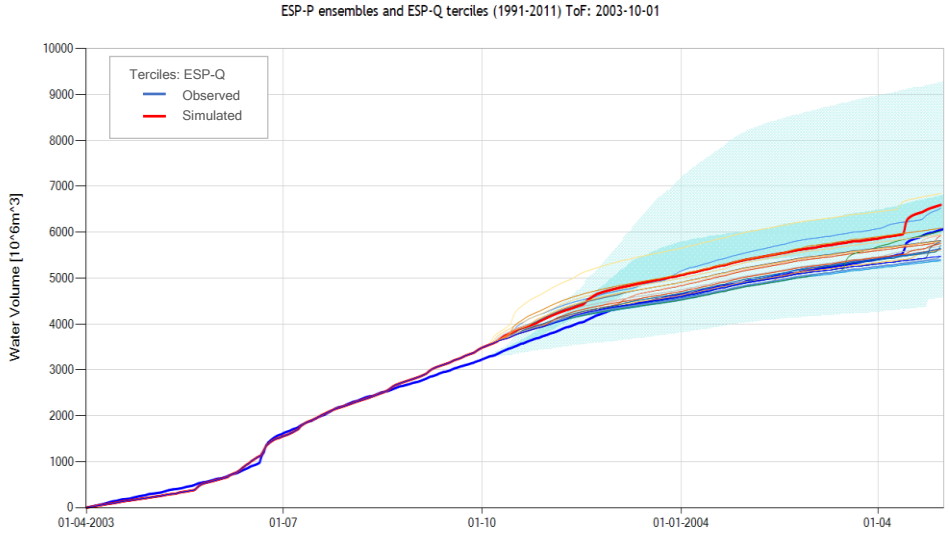

Figure 6-4 | Low-rainfall season forecast: ESP-P ensemble and ESP-Q terciles ToF 2003-10-01

6.1.2.2 Low-rainfall season (Oct-Apr) ToF: 2003-10-01

Figure 6-4 shows a reasonably good correlation between the observed and simulated inflow records for the hindcast period. The simulated record however shows an increasing overestimation of accumulated inflow approximately 1.5 months before the ToF. This earlier onset of simulated, predominantly snowmelt-based inflow could be a result of the above-average temperatures measured in the spring 2003 (see *Figure 5-2*). Constructed temperature-elevation zones over this period might have overestimated the overall catchment temperature increase, particularly at higher altitudes, which would result in increased snowmelt-based inflow. The simulated total accumulated inflow volume at the ToF is a below-average value 3485 million m^3, due to the below-average precipitation experienced in the preceding high season.

The observed inflows over the forecast period corresponds to *below-normal* inflow for the entire forecast period. Similar to the 2002 low-rainfall season, ESP-P ensemble members form a narrower grouping over the entire forecast period. Despite overestimation of accumulated inflow the ToF, the majority of the ESP-P ensemble members fall within close proximity to the observed record for the majority of the forecast period.

The simulated record, indicated in red, can however be seen to be positioned in the upper range of the ESP-P range. This result foreseen as the 2002 hydrological year received below average rainfall and was expected to fall below the majority of ensemble members. Further inspection of the precipitation records indicated that above-average precipitation and monthly temperatures were experienced during the months of October and November 2002. Thus providing some explanation behind the increased inflow over this time period.

6.1.3 2004: Below-average precipitation year

The results of forecasts for the high-rainfall season and the low-rainfall season for 2004 are presented in *Figure 6-5* and *Figure 6-6* respectively.

6.1.3.1 High-rainfall season (Apr-Oct) ToF: 2004-04-01

Figure 6-5 shows a slight overestimation of simulated inflow record compared to observed record for the hindcast period. This overestimation increases throughout the forecast period, the effect of a less optimal calibration. The simulated total accumulated inflow volume ToF is a below-average value of 2318 million m^3. The reduction is a result of the preceding below-average precipitation year. The observed record corresponds to *normal* inflow for the initial months, after which accumulated flow decrease to the lower edge of the *normal* range.

The ESP-P ensemble spread appears similar in range compared to the high-rainfall seasons of the previous study years. A large number of ESP-P ensembles do however fall above the ESP-Q tercile range, although the total accumulated inflow at ToF is below-average. Part of this could be attributed to the overestimation of simulated inflow over the hindcast period, resulting in an accumulated volume error at ToF and overestimation of accumulated inflow over the forecast period. However, the wide spread seems to reflect the large variability in historical rainfall for this period

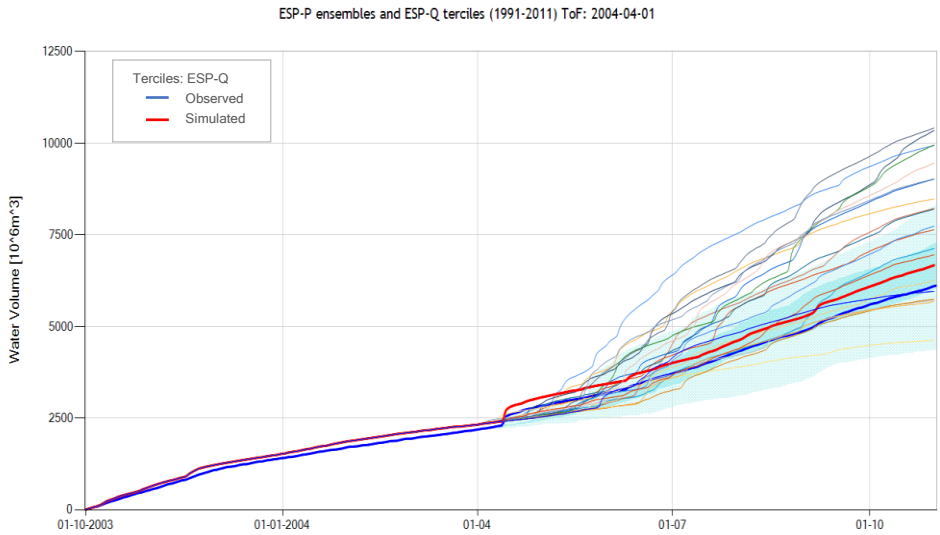

Figure 6-5 | High-rainfall season forecast: ESP-P ensemble and ESP-Q terciles ToF 2004-04-01

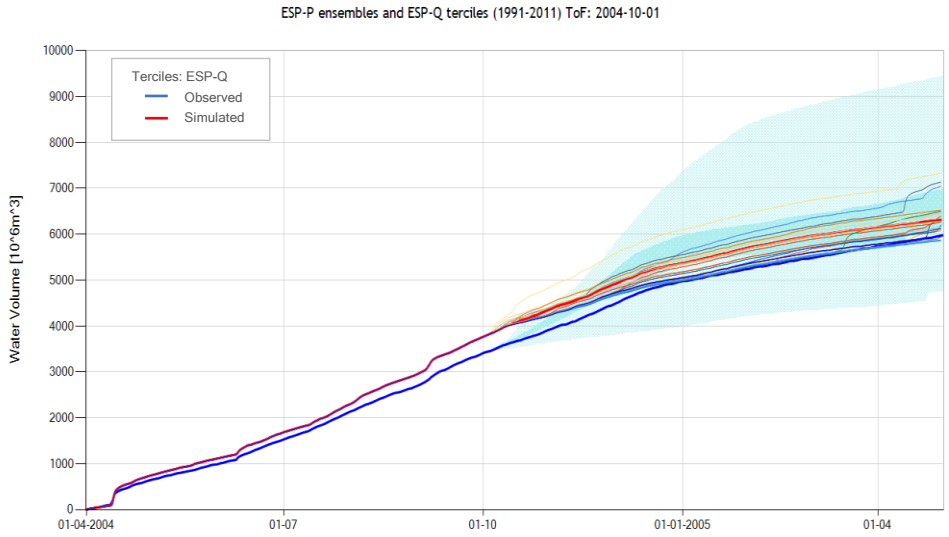

Figure 6-6 | Low-rainfall season forecast: ESP-P ensemble and ESP-Q terciles ToF 2004-10-01

6.1.3.2 Low-rainfall season (Oct-Apr) ToF: 2004-10-01

Figure 6-6 shows an increasing overestimation of the simulated inflow record compared to observed record, through the hindcast- as well as the forecast period. The simulated total accumulated inflow volume at the ToF is a below-average value of 3766 million m^3. The observed inflow over the forecast period corresponds to below-normal for the entire forecast period.

Similar to the previously assessed low-rainfall seasons, the ESP-P ensemble members form a narrower grouping over the entire forecast period due to limited variations in historical precipitation totals over this period. The majority of the ESP-P ensemble members fall above the observed record for the majority of the forecast period which can be attributed to the overestimation of accumulated inflow at ToF. It is expected that by correcting the overestimation at ToF this grouping would shift downwards, providing a more accurate estimation of accumulated inflow over the forecast period. This could be achieved by improving the model calibration or incorporation of Data Assimilation (DA) prior to ToF.

6.1.4 2005: Above-average precipitation year

The results of forecasts for the high-rainfall season for 2005 are presented *Figure 6-7*.

6.1.4.1 High-rainfall season (Apr-Oct) ToF: 2005-04-01

Figure 6-7 shows good correlation of the simulated and observed accumulated inflow record for the hindcast period. Increasing underestimation however occurs throughout the forecast period. The simulated total accumulated inflow volume at the October ToF is a below-average value of 2316 million m^3, due to the two consecutive below-average precipitation preceding years. The observed record over the forecast period corresponds to *above-normal* inflow based on the ESP-Q terciles.

The ESP-P ensemble spread appears similar in range compared to the high-rainfall seasons of the previous study years. Due to the large spread of both the ESP-Q and ESP-P ensemble members, accurate estimation of accumulated flow at later lead months would be challenging. If the average accumulated inflow value over all ensemble members would be used as a forecast estimate, both ESP-P and ESP-Q approaches would provide similar underestimated values compared to the observed record.

From the analysis of high-rainfall season forecasts for all of the selected study years, it can be seen that due to the greater historical precipitation variability over this season, initial hydrological conditions do not have such a strong impact on seasonal forecast performance compared to the low-rainfall season. The ESP-P approach therefore results in a wide ensemble range of predicted inflow volumes. In extreme precipitation years such as 2005, the ESP-P therefore cannot provide an indication of above-average precipitation periods in advance. This suggest that if climate model based seasonal forecast were able to capture extreme inflow years, it would be very useful for reservoir operation.

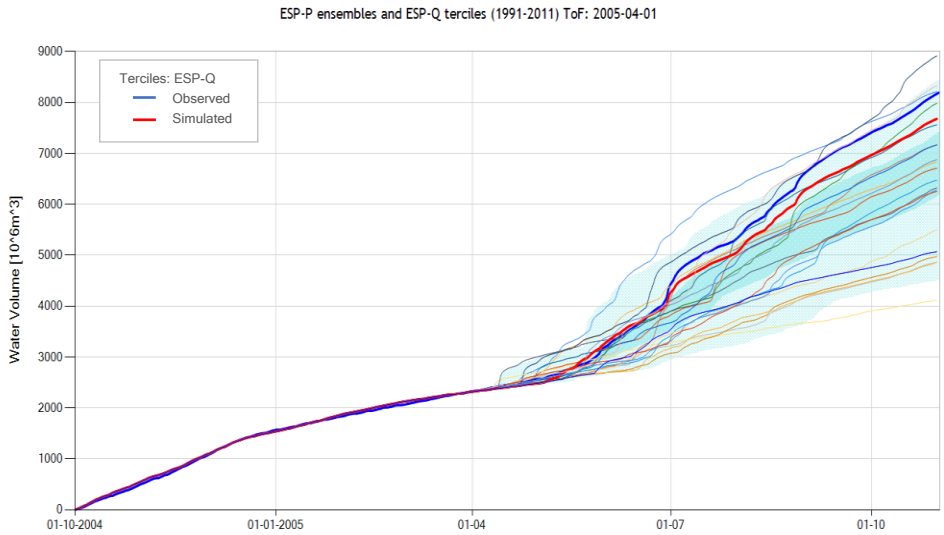

Figure 6-7 | High-rainfall season forecast: ESP-P ensemble and ESP-Q terciles ToF 2005-04-01

6.2 Performance of Data Assimilation

The availability real-time observed data in hydrological forecasting systems allows for updating simulated hydrologic states or catchment parameters to improve the accuracy of the forecast. In this study, DA was introduced to assimilate both reservoir levels and streamflows to observed values over the hindcast period (see *Section 5.3.4*). The performance of ESP-P based ensemble forecasts with DA inclusion during the 6-month hindcast period is discussed in the following section. A limited number of result plots are presented as reference to discussion points and additional plots can be found in *Appendix B.* A numerical performance comparison between different simulations methods per ToF is presented in *Appendix C.*

6.2.1 2003: Below-average precipitation year

The results of forecasts for the high-rainfall season and the low-rainfall season for 2003 are presented in *Figure 6-8* and *Figure 6-9* respectively.

6.2.1.1 High-rainfall season (Apr-Oct) ToF: 2003-04-01

From *Figure 6-8,* the impact of DA inclusion for ESP-P ensemble forecast can be seen during the hindcast period. With the updating of reservoir levels and discharge, the percentage volume error between simulated and observed records during the hindcast period is effectively reduced to zero. This results in equal amounts of total accumulated inflow volumes at ToF for both series, providing a closer representation of observed conditions at the start of the forecast period. *Figure 6-8* can be compared to *Figure 6-3*, which present the results of the ESP-P forecast with no DA applied

over the same simulation period. Comparison of these figures reveal that the inclusion of DA provides a more accurate performance over the forecast period. The majority of ESP-P ensembles members however still appear outside of the *above-normal* ESP-Q tercile range. This can be attributed to the large accumulated inflow volume at the ToF, as a result of the 2002 above-average precipitation year.

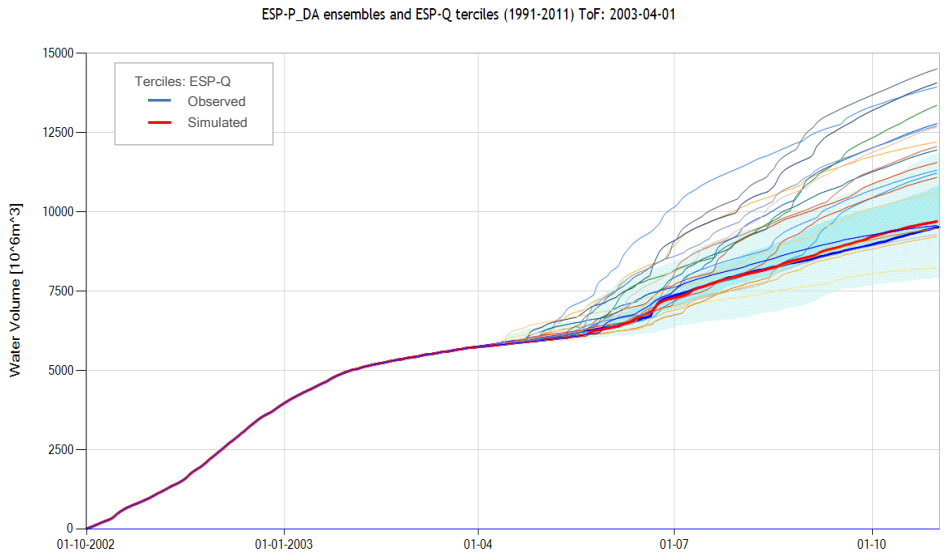

Figure 6-8 | High-rainfall season forecast: ESP-P ensemble including DA and ESP-Q terciles ToF 2003-04-01

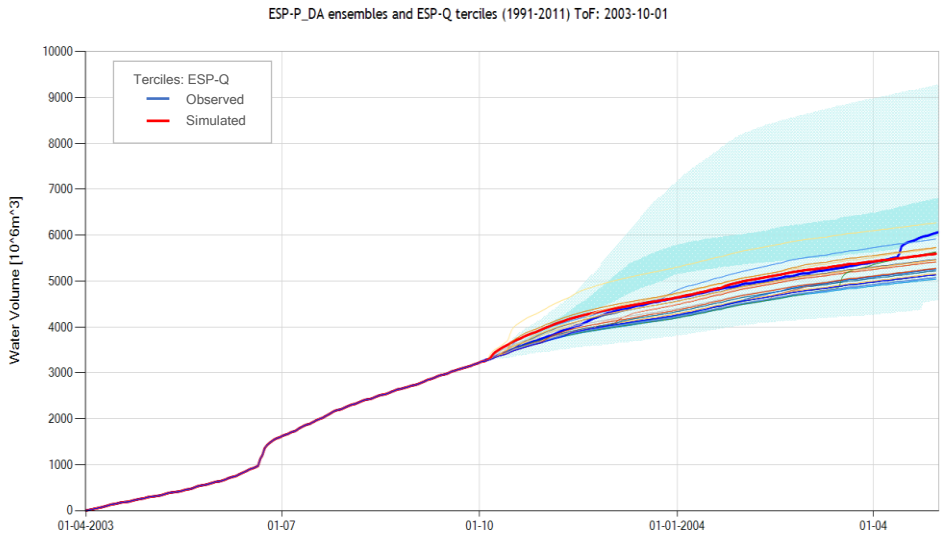

Figure 6-9 | Low-rainfall season forecast: ESP-P ensemble including DA and ESP-Q terciles ToF 2003-10-01

6.2.1.2 Low-rainfall season (Oct-Apr) ToF: 2003-10-01

Figure 6-9 indicates the effects of DA inclusion for the ESP-P ensemble forecast during the low-rainfall season in 2003. This figure can be compared to *Figure 6-4*, which present the results of the ESP-P forecast with no DA applied over the same simulation period. Based on this comparison, it can be seen that the inclusion of DA primarily reduced the accumulated volume error for the over the 1.5 month period leading up to the ToF. The resultant performance of the ESP-P ensemble over forecast period is improved, providing more accurate estimates of accumulated inflow for the majority of forecast lead months.

6.2.2 General remarks on DA

For simulation periods where a good match between simulated and observed records are been obtained, inclusion of DA provides limited forecast improvement over the hindcast and forecast period. DA is used in both short-term and seasonal forecasting to improve the match between the observed and simulated states at the ToF which in turn will improve forecast accuracy. Even for well-calibrated models deviations can occur because of errors in the raingauge measurements or poor representativeness of the network of the storms and spatial patterns. Therefore, it is always recommended to use DA methods in operational forecasting.

During the low rainfall season when the forecasts depend strongly on the initial conditions then using DA is expected to improve forecast accuracy. In these

simulations the river flows and reservoir storages were updated, but the snow storage is not. Adjusting the flows in the model can compensate for any deviations in the water storage in the catchment (soil moisture or snow water content). During the high-rainfall season obtaining the correct initial conditions is still important, but due to the large variability in the historical rainfall DA does not significantly improve (reduce) the range of the ESP-P forecast ensemble.

Although DA provides a more accurate representation of total accumulated inflow volume at ToF, simulation model biases can however still be included in the forecast period. DA should therefore not be included to compensate for poor calibration performance, as this could lead to simulation bias in the forecast period.

6.3 System 4 precipitation forecasts

Figure 6-10 through *Figure 6-13* present the results of the forecast simulations directly using System 4 forecasts of precipitation for the 7-month forecast period. As System 4 based forecast are to be compared to ESP-P based simulation results, System 4 ensemble members are plotted on ESP-P based terciles for the forecast period. To ensure correct visual comparison of simulation results, both System 4 and ESP-P result time series were selected from simulation runs, which include DA. Thus providing equal accumulated inflow volumes at ToF, limiting the influence of accumulated volume errors in the hindcast period.

The actual observed accumulated inflow time series is presented for each simulation period. Results are displayed in chronological order according to the ToF, with high-rainfall season (Apr-Oct) forecasts preceding low-rainfall season (Oct-Apr) forecasts. Due to the large amount of output data, forecast model output plots are only presented for the 2002 and 2003 study years. Additional study year forecast results plots can be found in *Appendix B.*

6.3.1 2002: Above-average precipitation year

The results of forecasts for the high-rainfall season and the low-rainfall season for 2002 are presented in *Figure 6-10* and *Figure 6-11* respectively.

6.3.1.1 High-rainfall season (Apr-Oct) ToF: 2002-04-01

From *Figure 6-10* it can be seen that the majority of System 4 ensemble members are positioned in the *below-normal* ESP-P based tercile throughout the forecast period. The observed inflow record for the above-average precipitation (El Niño) year however indicates *normal* inflow for the initial forecast months followed by *above-normal* inflow. The underestimation of inflow by the System 4 based forecast can be attributed to the general underestimation of forecast precipitation (see *Section 5.2.2).*

The System 4 based forecast ensemble forms a narrower spread throughout the forecast period compared to the ESP-P based terciles. This is due to use of varied initial conditions and the use of stochastic physics during System 4 ensemble

generation (see *Section 5.1.3*) compared to the use of historical varied time series during ESP-P ensemble creation.

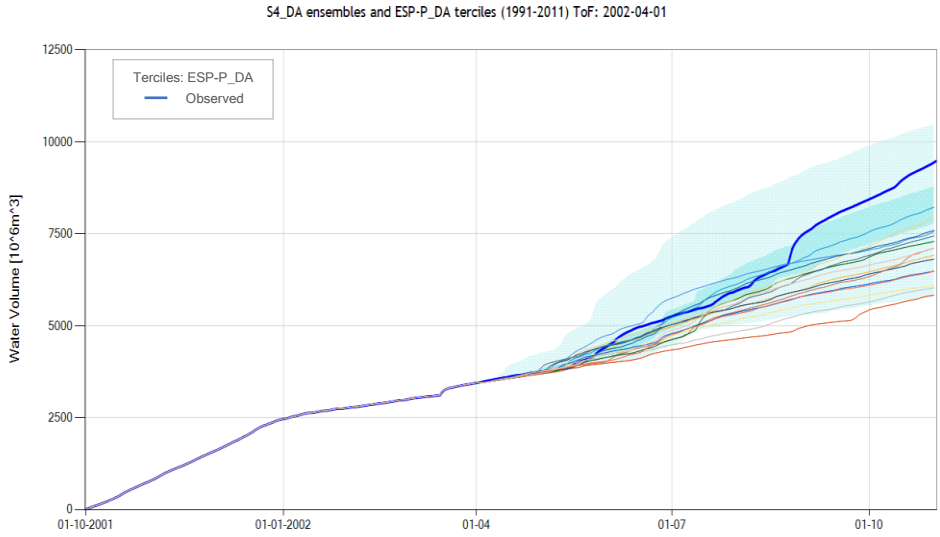

Figure 6-10 | High-rainfall season forecast: S4_DA ensemble and ESP-P_DA terciles ToF 2002-04-01

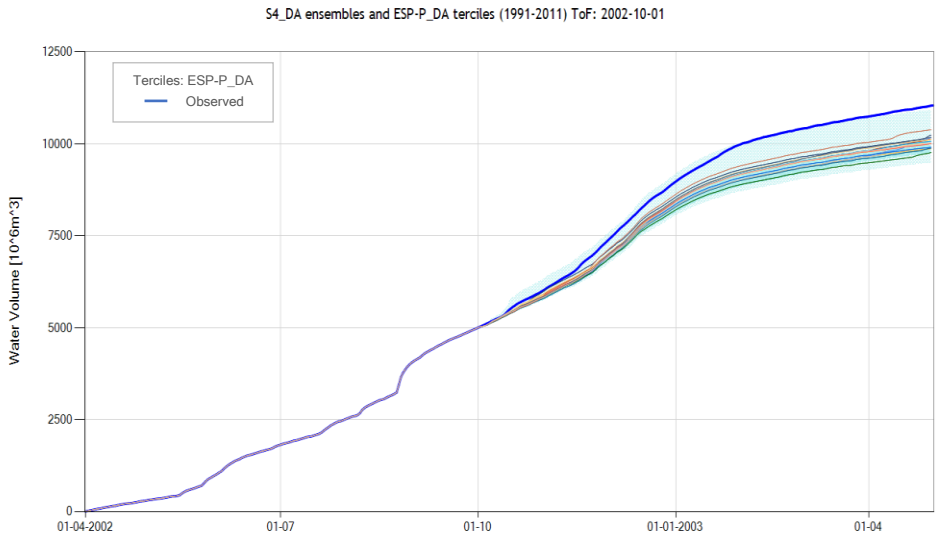

Figure 6-11 | Low-rainfall season forecast: S4_DA ensemble and ESP-P_DA terciles ToF 2002-10-01

6.3.1.2 Low-rainfall season (Oct-Apr) ToF: 2002-10-01

System 4 based ensemble members in *Figure 6-11* appear in a narrower grouping throughout the forecast period compared to an ESP-P based terciles, similar to the results of preceding high-rainfall season. The majority of these members are located in the *normal* ESP-P based tercile. As the observed time series indicated *above-normal* inflow over the entire forecast period, there is also an underestimation of precipitation during this low-rainfall season. The introduction of bias corrected System 4 precipitation data could therefore be expected to provide some improvement in forecast accuracy.

6.3.2 2003: Below-average precipitation year

The results of forecasts for the high-rainfall season and the low-rainfall season for 2003 are presented in *Figure 6-12* and *Figure 6-13* respectively.

6.3.2.1 High-rainfall season (Apr-Oct) ToF: 2003-04-01

Figure 6-12 shows a greatly improved performance by the System 4 based forecast compared to the observed inflows. The System 4 ensemble provides a much narrower spread over the forecast period for this below-average precipitation year. The wider ESP-P tercile spread is created as a result of the natural annual variability of precipitation during the high-rainfall season (see *Figure 4-1*).

The System 4 based inflow forecast appear to be able to better represent inflows during a below-average precipitation year, but this may just be a result of the climate model biases. The application of bias correction scaling factors based long-term averages can therefore be expected to increase the forecasted precipitation amounts, resulting in higher forecasted inflows than observed.

6.3.2.2 Low-rainfall season (Oct-Apr) ToF: 2003-10-01

Figure 6-13 indicates a slight underestimation of forecasted inflow for the System 4 based ensemble. The narrow width of the forecasted inflow range is found comparable to the previous low-rainfall season. Bias correction of forecasted precipitation data could potentially increase the forested inflow amount based on the general underestimation of System 4 precipitation data.

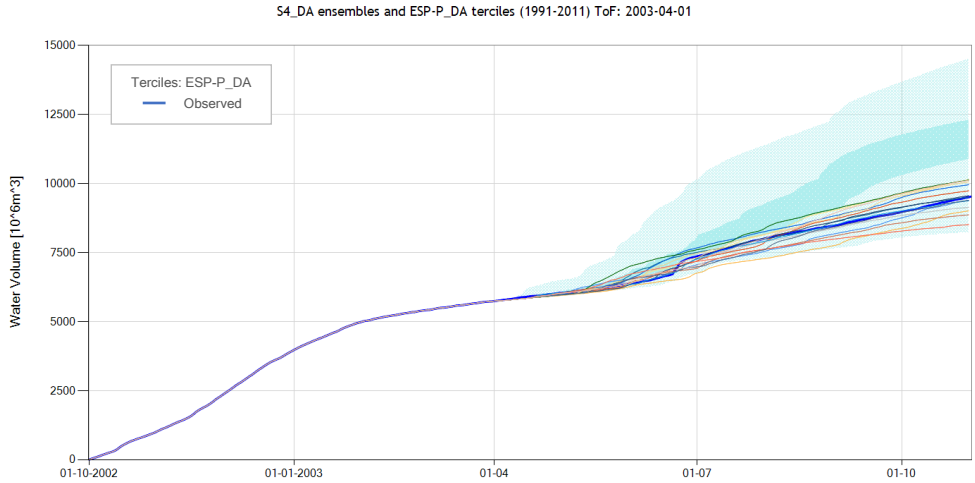

Figure 6-12 | High-rainfall season forecast: S4_DA ensemble and ESP-P_DA terciles ToF 2003-04-01

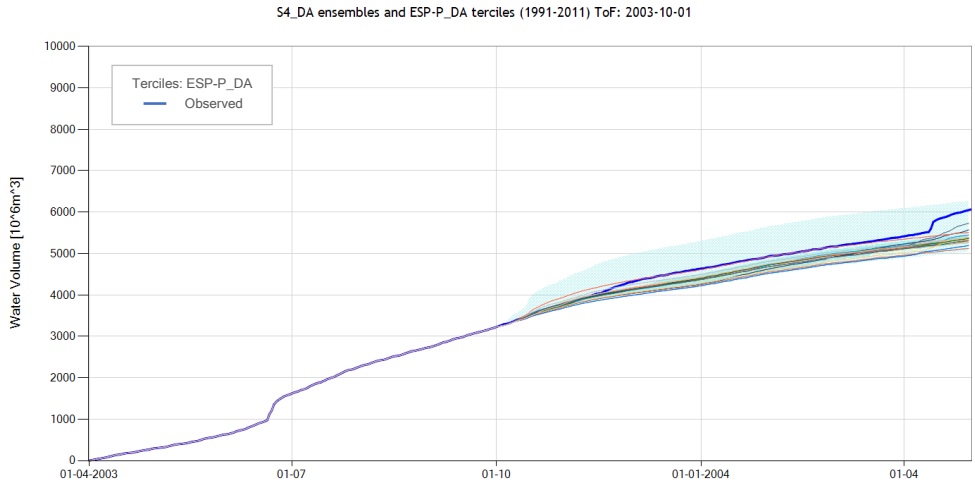

Figure 6-13 | Low-rainfall season forecast: S4_DA ensemble and ESP-P_DA terciles ToF 2003-10-01

6.3.3 General remarks on System 4 precipitation forecasts

Seasonal inflow forecasts based directly on System 4 precipitation forecast generally underestimated future accumulated inflow over the high-rainfall season due to underestimation of precipitation over this period. This underestimation of precipitation could be attributed to the coarse resolution of System 4 variable datasets compared to the size of the study area and model biases from the process descriptions. Bias correction of raw System 4 precipitation forecast could therefore provide closer precipitation estimates to observed values. Seasonal forecasts in the low-rainfall achieved relative good accuracy of predicted future inflows, which could be attributed to low precipitation estimates and the limited impact of precipitation estimates compared to the initial hydrological conditions. Underestimation of accumulated inflow was however apparent in periods of above-average precipitation. System 4 based seasonal forecasts also result in a narrower inflow ensemble spreads compared to ESP-P, due to the use of varied initial conditions and the use of stochastic physics during System 4 ensemble initialization (see *Section 5.1.3*).

6.4 Performance of downscaling precipitation forecasts

6.4.1 2002: Above-average precipitation year

The results of forecasts for the high-rainfall season and the low-rainfall season for 2002 are presented in *Figure 6-14* and *Figure 6-15* respectively.

6.4.1.1 High-rainfall season (Apr-Oct) ToF: 2002-04-01

Figure 6-14 shows an increase in average predicted inflow with the use bias corrected System 4 precipitation data, compared to use of raw precipitation forecast (see *Figure 6-10*). With the majority of monthly precipitation scaling factors values larger than 1.0 (see *Figure 5-4*), use of bias corrected precipitation data results in a wider ensemble spread compared to raw System 4 precipitation forecasts, due to higher forecasted inflows. If the mean value of ensemble inflow is to be reported as a single best prediction value, the bias corrected System 4 inflow ensemble would provide a more accurate estimate of the observed value compared to the raw System 4 results.

6.4.1.2 Low-rainfall season (Oct-Apr) ToF: 2002-10-01

Similar to the preceding high-rainfall season, *Figure 6-15* shows the improved forecast accuracy over the raw System 4 based forecast with introduction bias corrected precipitation data. The improvement is especially evident during the first three months of the forecast period and can be compared to the raw System 4 precipitation based inflow forecast (see *Figure 6-11).* During the majority of the forecast period however, accumulated inflow is still underestimated compared to the observed record. This underestimation could be partly attributed use of long-term average based precipitation scaling factors, reducing the potential to successfully reproduce extreme events such as the record high accumulated inflow experienced during the 2002 hydrological year. The predominant source to forecast inaccuracy however is the inaccurate forecast of total seasonal precipitation by System 4, as scaling only adjusts the average of the precipitation time series.

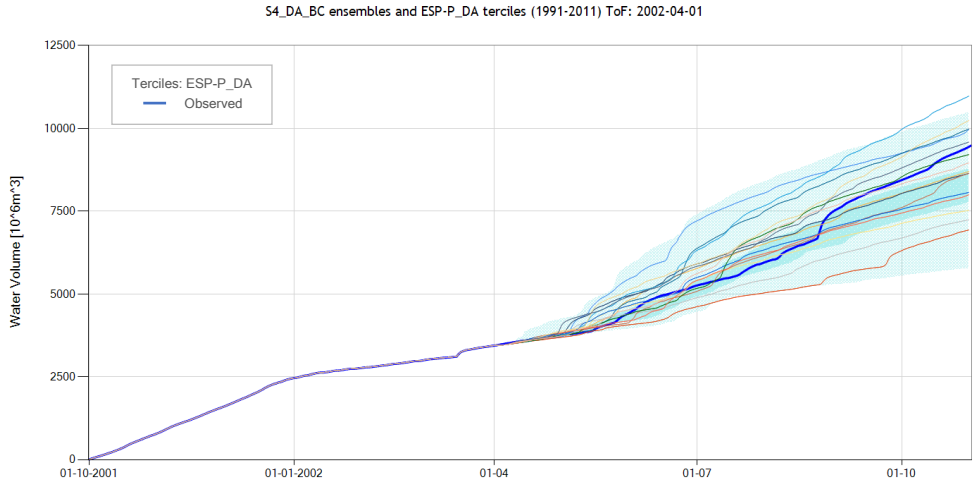

Figure 6-14 | High-rainfall season forecast: S4_DA_BC ensemble and ESP-P_DA terciles ToF 2002-04-01

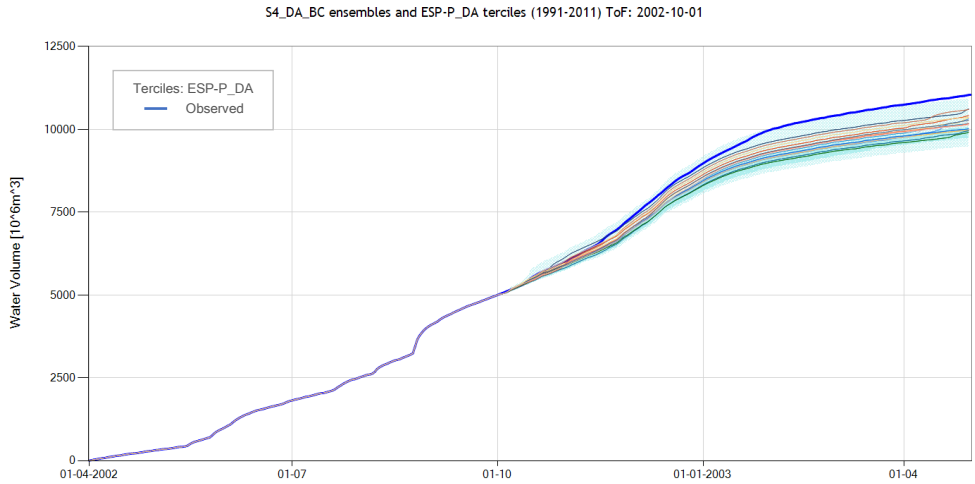

Figure 6-15 | Low-rainfall season forecast: S4_DA_BC ensemble and ESP-P_DA terciles ToF 2002-10-01

6.4.2 2003: Below-average precipitation year

The results of forecasts for the high-rainfall season and the low-rainfall season for 2003 are presented in *Figure 6-16* and *Figure 6-17* respectively.

6.4.2.1 High-rainfall season (Apr-Oct) ToF: 2003-04-01

From *Figure 6-16* it can be seen that the use of bias corrected System 4 precipitation data, increases the forecasted inflow volume significantly compared to the raw System 4 based forecast, resulting in reduced forecast accuracy (see *Figure 6-12*). The overestimation can be partly attributed to the use of long-term average based precipitation scaling factors, as below-average precipitation was experienced during the 2003 hydrological year.

6.4.2.2 Low-rainfall season (Oct-Apr) ToF: 2003-10-01

Figure 6-17 shows improved performance of the System 4 based forecast with the use bias corrected precipitation data (see *Figure 6-13*). A slight underestimation of accumulated inflow volume however still exists during the majority of the forecast period. Due to the below-average precipitation experienced during seasonal period, bias correction of precipitation data could still result in an underestimation of total seasonal precipitation.

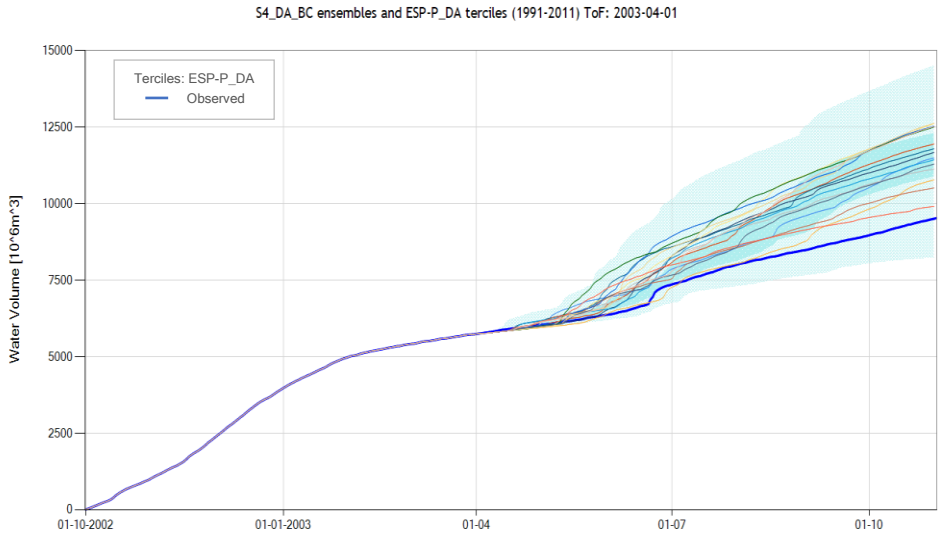

Figure 6-16 | Low-rainfall season forecast: S4_DA_BC ensemble and ESP-P_DA terciles ToF 2003-04-01

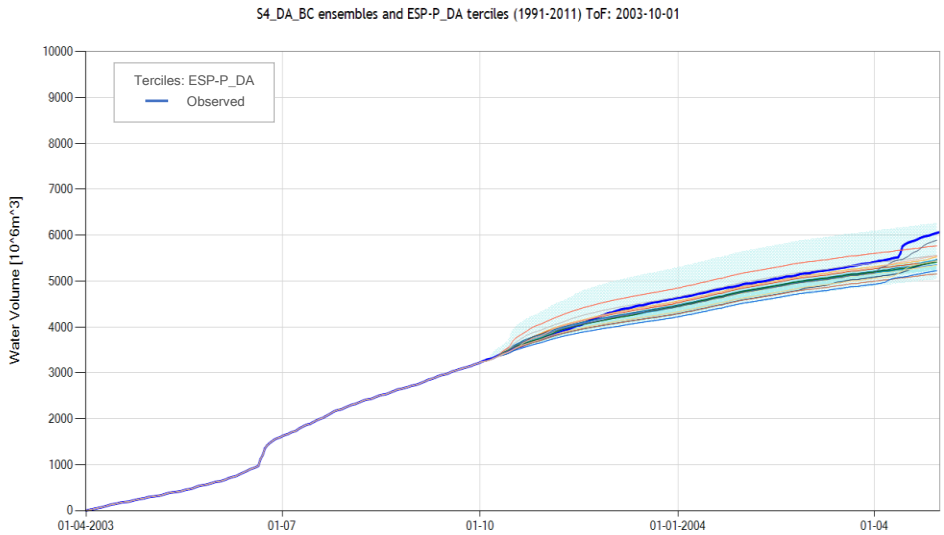

Figure 6-17 | Low-rainfall season forecast: S4_DA_BC ensemble and ESP-P_DA terciles ToF 2003-10-01

6.4.3 General remarks on bias correction of precipitation forecasts

Bias correction of System 4 precipitation forecasts generally provided increased forecast accuracy, compared to raw System 4 precipitation data, for high-rainfall seasons with above-average precipitation. Accumulated reservoir inflow was underestimated for the raw System 4 based forecast (S4) for the 2002 moderate El Niño year, but was improved with the use of bias corrected precipitation data. Forecasted inflow ensemble ranges were found to be wider in inflow range compared to System 4 precipitation based forecasts, due to increased variability in precipitation time series with the introduction scaling factors over 1.0 values. During seasonal periods of below-average precipitation, bias correction of System 4 leads to the overestimation of precipitation and resultant seasonal inflow. The predominant source to forecast inaccuracy however is the inaccurate forecast of total seasonal precipitation by System 4, as bias correction scaling only adjusts the average of the precipitation time series.

6.5 Introduction of temperature forecasts

Snow melt processes are important in the Upper Maule catchment. To assess the impact of forecasted temperature data, forecasted inflow ensembles based on System 4 temperature data are plotted on the minimum-maximum ensemble spread of the raw System 4 based forecast option including DA (S4_DA.) In comparison, the S4_DA forecast scenario uses historical observed temperature averages over the forecast period. The potential benefit of using temperature forecasts over historical average

values, is the prediction of abnormal temperatures related to ocean–atmosphere teleconnections which could have significant hydrological impacts such as increased snowmelt. No bias correction was applied to precipitation forecasts used in the simulations.

6.5.1 2002: Above-average precipitation year

The results of forecasts for the high-rainfall season and the low-rainfall season for 2002 are presented in *Figure 6-18* and *Figure 6-19* respectively.

6.5.1.1 High-rainfall season (Apr-Oct) ToF: 2002-04-01

From *Figure 6-18* it can be seen that the introduction of System 4 temperature data has resulted in the reduction of the mean forecasted inflow volume compared to the S4_DA forecast spread. As discussed in *Section 5.2.3*, average monthly System 4 based temperatures were found to be lower than observed values for the months from February to September. Outside this period, October to January, average monthly System 4 based temperatures were found to be higher than observed values.

The reduction of forecasted inflow volume is likely to be caused by the biased (lower) temperature estimates from System 4. The lower average monthly temperatures during the high-rainfall season likely resulted in greater snow accumulation and reduced runoff at lower altitudes over the austral winter period. This theory would however required further investigation for other years.

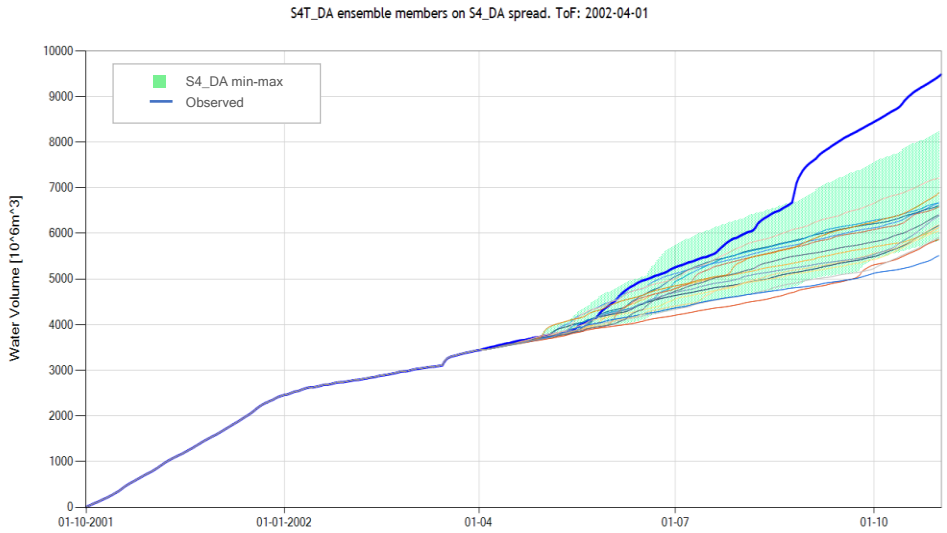

Figure 6-18 | High-rainfall season forecast: S4T_DA ensemble and S4_DA min-max spread. ToF 2002-04-01

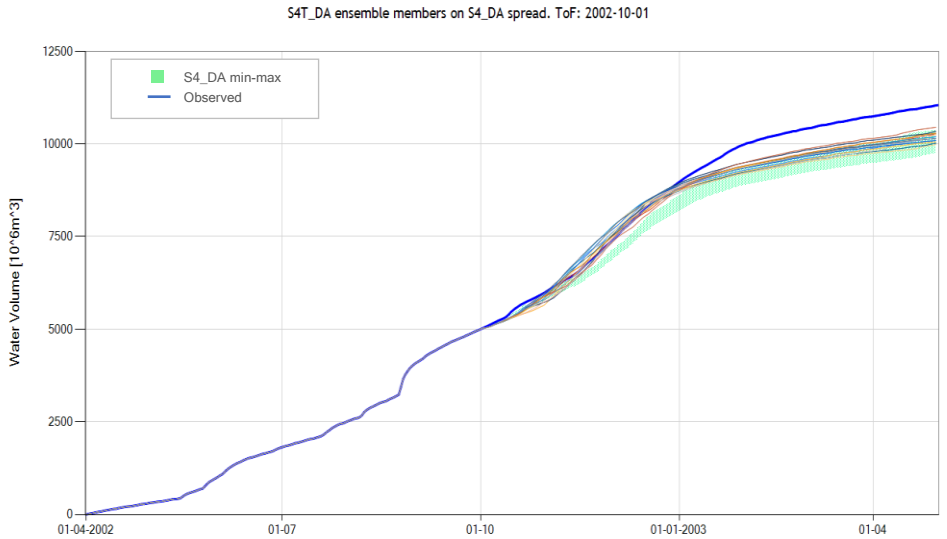

Figure 6-19 | Low-rainfall season forecast: S4T_DA ensemble and S4_DA min-max spread. ToF 2002-10-01

6.5.1.2 Low-rainfall season (Oct-Apr) ToF: 2002-10-01

Figure 6-19 shows that an improved forecast accuracy was obtained with the introduction of System 4 temperature data compared to the S4_DA forecast spread. Underestimation of accumulated inflow in the latter months of the forecast period is reduced, but still remains lower than the observed record.

Average monthly System 4 based temperatures were found to be higher than observed values for the months of October through January (see *Section 5.2.3)*. Increased temperatures during these months would result in increased snowmelt based runoff, resulting in increased accumulated inflow during the initial forecast lead months, compared to raw System 4 temperature forecasts (see *Figure 6-19*).

6.5.2 Performance of downscaling temperature forecasts

To assess the impact bias correction temperature data, forecasted inflow ensembles based on System 4 temperature data are plotted on the minimum-maximum ensemble spread of the S4_DA forecast option. No precipitation bias correction was applied to System 4 precipitation forecasts.

6.5.3 2002: Above-average precipitation year

The results of forecasts for the high-rainfall season and the low-rainfall season for 2002 are presented in in *Figure 6-20* and *Figure 6-21* respectively.

6.5.3.1 High-rainfall season (Apr-Oct) ToF: 2002-04-01

From *Figure 6-20* it can be seen that the introduction of bias corrected System 4 temperature data resulted in a more varied forecast ensemble spread of increased accumulated inflow. Bias correction resulted in the increase of temperatures for the period between April and October, thus increasing snowmelt based runoff. The resultant bias correct based ensemble however still underestimates the observed inflow.

6.5.3.2 Low-rainfall season (Oct-Apr) ToF: 2002-10-01

Figure 6-21 indicates that the introduction of bias corrected System 4 temperature data resulted in a significant decreases in the forecasted inflow volume. Review of observed temperatures records over this seasonal period reveals below-average monthly temperatures were experienced for the period between October and November 2002. As bias correction scaling values are based on long-term monthly temperature averages, above-average forecasted System 4 temperatures over this time period were reduced further by the bias correction process. The effect of these reduced temperatures can be seen by the delayed snowmelt period and associated runoff.

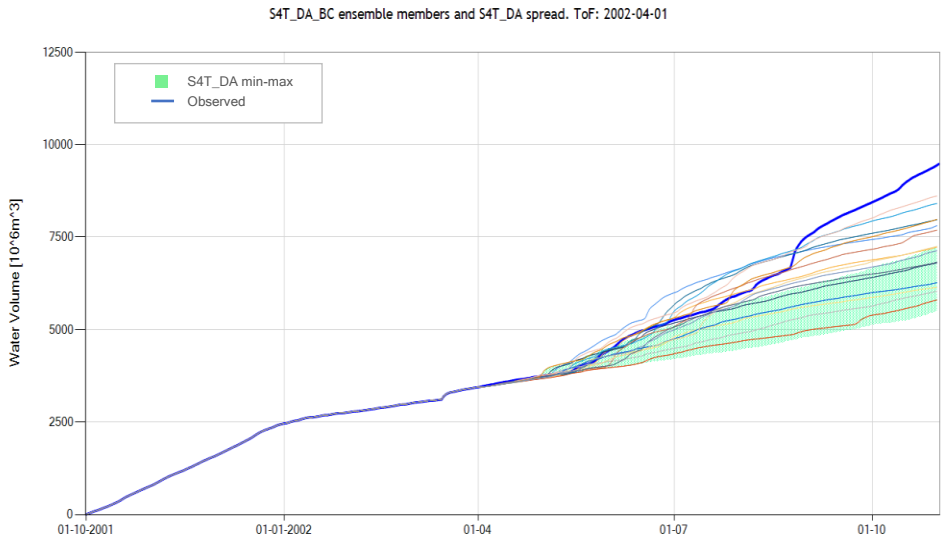

Figure 6-20 | High-rainfall season forecast: S4T_DA_BC ensemble and S4T_DA min-max spread. ToF 2002-04-01

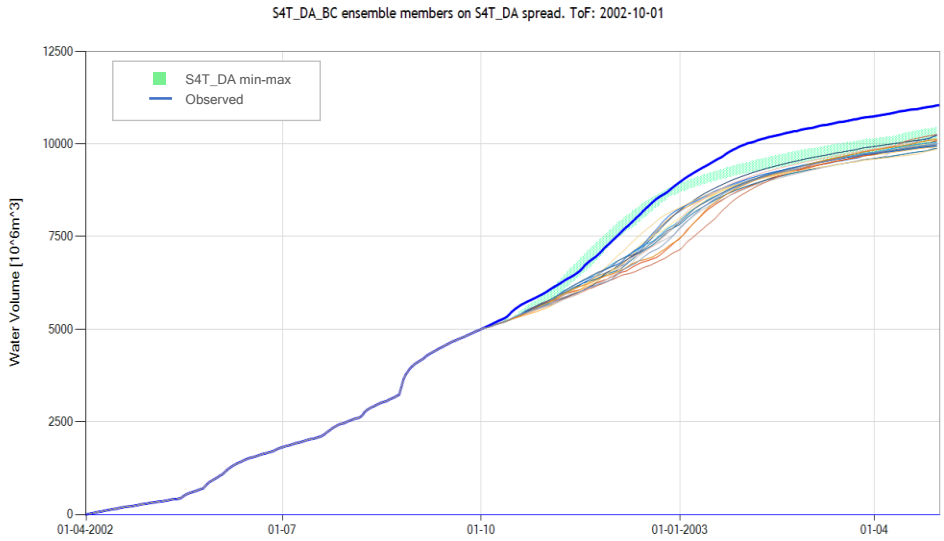

Figure 6-21 | Low-rainfall season forecast: S4T_DA_BC ensemble and S4T_DA min-max spread. ToF 2002-10-01

6.5.4 General remarks on temperature forecasts

The use of forecasted temperature data over historical temperature averages can potentially provide increased forecast accuracy over periods of above- or below-average temperatures. This could provide valuable information to reservoir managers, especially during the low-rainfall season where inflow is predominantly snowmelt based.

Introduction of System 4 temperature forecast causes shifts in forecasted inflow ensembles predominantly due to differences between System 4 temperature forecast and historical observed averages. Average monthly System 4 forecasted temperature values were found to be lower compared to observed averages for the period from February to September and higher for the period from November to January. Bias correction scaling factors based on long-term temperature averages aim to reduce this difference, but bias correction value during periods of above- or below average temperatures is limited.

6.6 Performance of downscaling temperature and precipitation data

6.6.1 2002: Above-average precipitation year

The results of forecasts for the high-rainfall season and the low-rainfall season for 2002 are presented in *Figure 6-22 and Figure 6-23* respectively.

6.6.1.1 High-rainfall season (Apr-Oct) ToF: 2002-04-01

From *Figure 6-22* it can be seen that the inclusion of System 4 bias corrected precipitation data provides increased forecast accuracy compared to the use of uncorrected precipitation data (see *Figure 6-20*). During the initial months of the forecast period, the majority of the forecast ensemble members do however overestimate inflow volume compared to the observed record.

6.6.1.2 Low-rainfall season (Oct-Apr) ToF: 2002-10-01

From *Figure 6-23* it can be seen that the inclusion of System 4 bias corrected precipitation data increases forecasted inflow during the initial parts of the forecast period (see *Figure 6-21*). This increase in precipitation values however does not offset the effect of the temperature reduction as discussed in the previous section. There is thus a large underestimation of snowmelt based inflow over the initial forecast period due to the delay of the snowmelt period.

6.6.2 2005: Above-average precipitation year

The results of the high-rainfall season forecasts for the 2005 study year is presented in *Figure 6-24* . An ensemble spread comparison of forecast options S4_DA, S4_DA_BC and S4TP _DA_BC, is presented in *Figure 6-25.*

6.6.2.1 High-rainfall season (Apr-Oct) ToF: 2005-04-01

From *Figure 6-24* it can be seen that the introduction of bias corrected S4 forecasts of both precipitation and temperature data provides a improvement to the seasonal forecast performance in this above-average rainfall year. The majority of ensemble members indicate a *normal* to *above-normal* seasonal inflow period, which corresponds well to the observed record. The result shows the potential advantage of a using probabilistic based forecast approach over ESP-P based methods during periods of *above-normal* inflow.

Figure 6-25 shows the stepwise improvement of forecast option performance with the introduction of bias corrected precipitation and temperature data. It can be seen that with the introduction of bias corrected data, variability between ensemble members increases resulting in larger ensemble spreads over the forecast period.

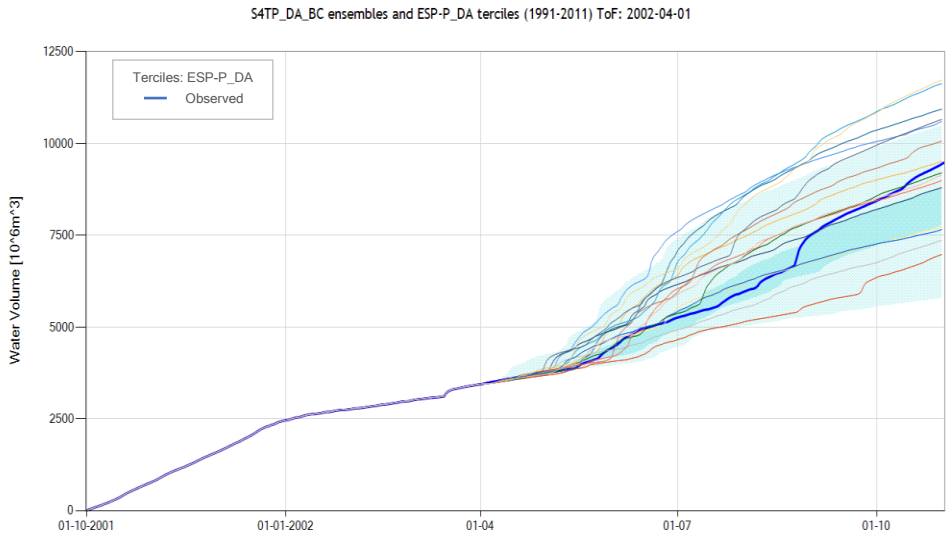

Figure 6-22 | High-rainfall season forecast: S4TP_DA_BC ensemble and ESP-P_DA terciles ToF 2002-04-01

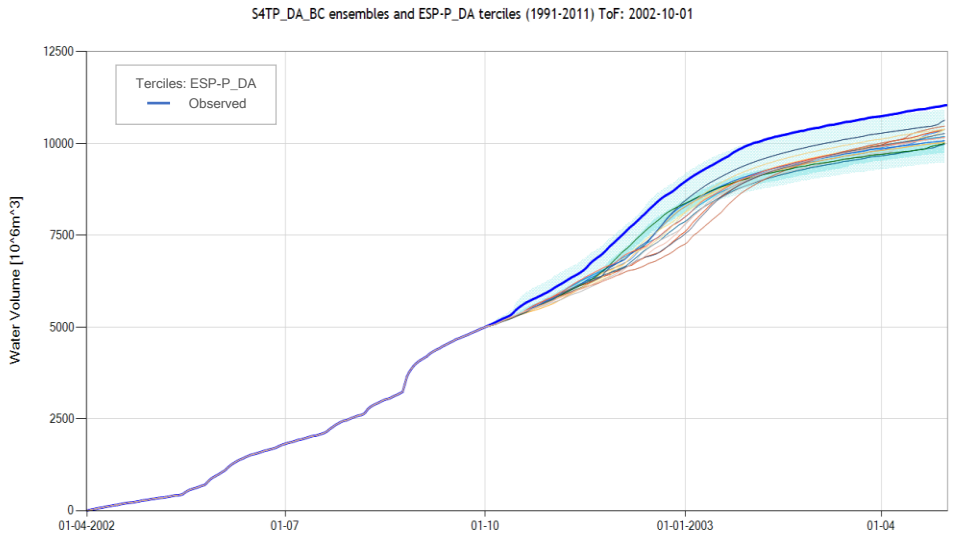

Figure 6-23 | Low-rainfall season forecast: S4_DA_BC ensemble and ESP-P_DA terciles ToF 2003-10-01

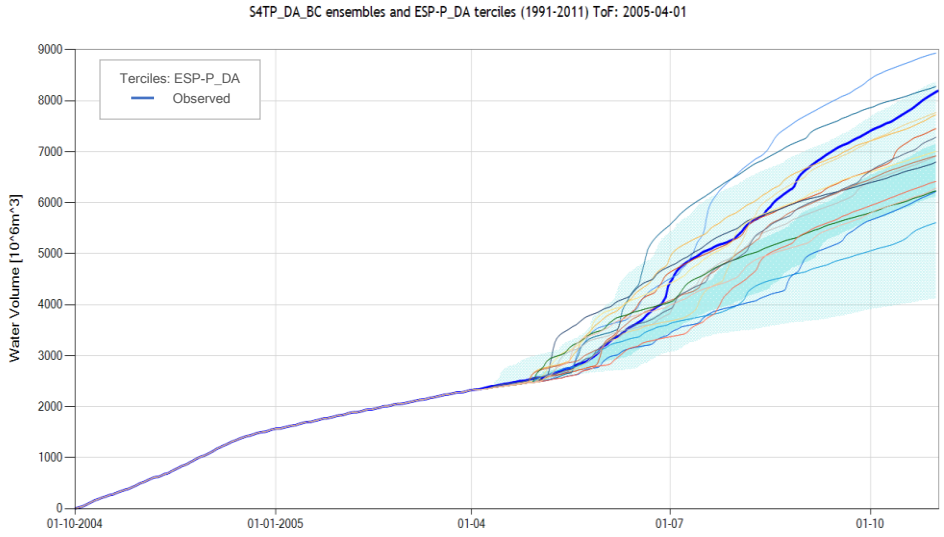

Figure 6-24 | High-rainfall season forecast: S4TP_DA_BC ensemble and ESP-P_DA terciles ToF 2005-04-01

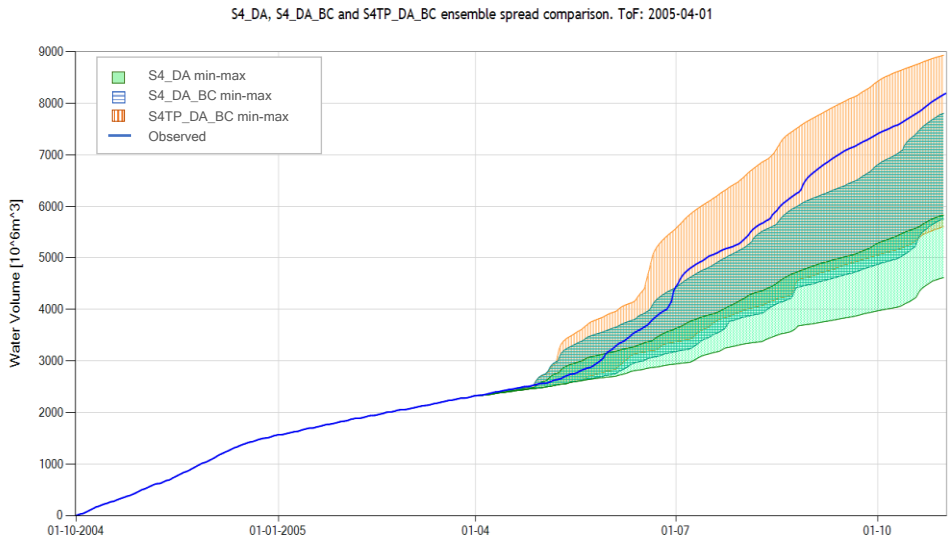

Figure 6-25 | High-rainfall season forecast ensemble spread comparison of raw System 4 precipitation (S4_DA), bias corrected precipitation (S4_DA_BC) and bias corrected precipitation and temperature data (S4TP_DA_BC). ToF 2005-04-01

6.6.3 General remarks on bias correction of temperature and precipitation forecasts

In comparison with System 4 bias corrected precipitation inflow forecasts, we find that bias-corrected precipitation and temperature forecasts improves mean seasonal inflow estimates during the high-rainfall season. During periods of below-average precipitation, seasonal inflow volumes are still however overestimated due to the limited influence of bias corrected temperature data over this period. During the low-rainfall season, inclusion of temperature forecasts reduces the accuracy of mean seasonal inflow estimates during initial lead months and results in comparable performance over latter lead months, when compared to System 4 bias corrected precipitation inflow forecasts.

7 Seasonal Forecast Verification of climate model-based forecasts

7.1 Seasonal Forecast Model Bias

The bias of each seasonal forecast model was calculated as the difference in the accumulated inflow mean of the forecast ensemble members and the observed inflow. Bias values are expressed as a percentage of the observed value. *Table 7-1* and *Table 7-2* presents a summary of calculated forecast model bias at the end of forecast lead month 2 and lead month 6, for each selected forecast options and study years. Positive bias values indicate an overestimation of forecasted accumulated inflow, while a negative bias indicates an underestimation. Mean ensemble inflow values for the ESP-P and ESP-Q based approaches are calculated from the respective 21 member ensembles, which includes inflow ensemble based on the observed data of the simulation year. Additional tabulated results presenting calculated forecast bias per lead month can be found in *Appendix C*.

Table 7-1 | Seasonal forecast model bias at end of lead month 2

		Percentage volume error of accumualted inflow at end of Lead month 2 (based on forecast ensemble member average)						
Forecast Option		High-rainfall season: ToF 01 Apr				Low-rainfall season: ToF 01 Oct		
No.	Name	2002	2003	2004	2005	2002	2003	2004
1	ESP-Q	-3.9%	0.0%	2.2%	-10.0%	-19.2%	17.4%	13.1%
2	ESP-P	7.7%	-5.3%	18.0%	-12.5%	-5.8%	3.4%	5.6%
3	ESP-P_DA	1.6%	6.9%	13.9%	-12.4%	-6.7%	-3.9%	-2.4%
4	S4	-0.5%	-13.8%	-4.3%	-24.4%	-5.3%	1.7%	2.9%
5	S4_DA	-6.6%	-1.6%	-8.5%	-24.3%	-6.2%	-5.6%	-5.0%
6	S4_DA_BC	7.8%	10.5%	8.6%	-11.6%	-4.8%	-3.6%	-4.1%
7	S4T	-5.3%	-19.4%	-11.5%	-27.1%	-4.1%	-2.3%	-0.1%
8	S4T_DA	-10.5%	-7.1%	-15.1%	-26.1%	-1.5%	-5.1%	-3.6%
9	S4T_DA_BC	-2.8%	-1.3%	-8.2%	-20.3%	-12.1%	-8.1%	-7.5%
10	S4TP_DA_BC	14.8%	10.8%	8.7%	-4.3%	-10.8%	-6.1%	-6.5%

Table 7-2 | Seasonal forecast model bias at end of 7-month forecast period (lead month 6)

		Percentage volume error of accumualted inflow at end of Lead month 6 (based on forecast ensemble member average)						
Forecast Option		High-rainfall season: ToF 01 Apr				Low-rainfall season: ToF 01 Oct		
No.	Name	2002	2003	2004	2005	2002	2003	2004
1	ESP-Q	-16.8%	6.9%	8.3%	-17.5%	-24.3%	9.0%	13.3%
2	ESP-P	-8.5%	12.9%	27.4%	-19.5%	-7.9%	-3.1%	6.3%
3	ESP-P_DA	-13.0%	21.0%	23.5%	-20.6%	-9.8%	-10.6%	-2.3%
4	S4	-22.6%	-9.2%	-4.6%	-36.4%	-8.1%	-5.5%	2.7%
5	S4_DA	-25.9%	0.2%	-7.0%	-36.3%	-8.9%	-11.1%	-4.0%
6	S4_DA_BC	-6.3%	22.6%	24.6%	-17.3%	-7.3%	-9.5%	-3.3%
7	S4T	-29.9%	-19.4%	-18.6%	-43.2%	-9.7%	-9.2%	-1.1%
8	S4T_DA	-32.7%	-9.9%	-20.7%	-42.7%	-7.6%	-11.4%	-4.1%
9	S4T_DA_BC	-23.8%	-2.7%	-10.6%	-35.5%	-8.9%	-12.5%	-5.4%
10	S4TP_DA_BC	-0.4%	17.7%	18.7%	-13.7%	-7.1%	-10.5%	-4.3%

7.1.1 High-rainfall season (Apr – Oct)

When studying high-rainfall season bias values presented in *Table 7-2*, different trends can be observed between the above-average precipitation years (2002, 2005) and below-average precipitation years (2003, 2004). The majority of simulated forecast options underestimate accumulated inflow during above-average precipitation years. This is due to the underestimation of System 4 based precipitation data compared to observed values. Bias correction of forecasted temperature and precipitation results in increased flow prediction and a decrease in the percentage volume error.

During below-average precipitation years, bias correction of System 4 based precipitation data results in the overestimation of inflow. This is due to the application of multiplicative scaling factors that are based on long-term precipitation averages. As the 2003 and 2004 hydrological years experienced below-average rainfall, scaling factors applied to forecasted precipitation data likely resulted in the overestimation of seasonal precipitation. For the below-average precipitation years, the use of bias corrected System 4 temperature data (S4T_DA) provided improved performance in terms of forecast model bias and net accumulated flow per lead month (see *Appendix C*).

7.1.2 Low-rainfall season (Oct– Apr)

Overall forecast model bias for the low-rainfall season can be seen to be much lower compared to the high rainfall-season. This is due to the increased predictability of seasonal inflow over this period, which is highly dependent on the preceding season's total precipitation (see *Section 4.6.3*). Successful simulation of the snowmelt period can therefore provide accurate estimates of seasonal inflow over the low-rainfall season.

From *Table 7-2* it can be seen that the majority of forecast options result in a negative forecast model bias under 10%. The introduction of bias corrected System 4 precipitation data (S4_DA_BC) results in a small improvement of forecast model bias for all study years. The introduction of bias corrected System 4 temperature data (S4T_DA_BC) however appears to results in lower total forecasted inflow.

The majority of forecast options do however provide estimations of total accumulated inflow over a 7-month forecast period within 10% of observed values. Values in *Table 7-2* are based on average forecasted inflow at the end of the forecast period (lead month 6). Model bias values calculated per forecast lead month can also be viewed in *Appendix C* to assess model bias development with increasing forecast lead month.

7.2 Ranked Probability Score (RPS)

The Ranked Probability Score (RPS) measures the accuracy of discrete probabilistic based forecasts issued for multi-categorical events in matching observed outcomes (see *Section 5.6.2*). A RPS value of zero would represent a perfect forecast and positive values indicate a less than perfect forecast with a maximum value of 1. In the following section, RPS results are presented and discussed based on the selected seasonal forecast periods in this study, i.e. high-rainfall season and low-rainfall season.

7.2.1 High-rainfall season

The RPS results for the high-rainfall season are presented in *Table 7-3.* Colour shading has been added to aid visual presentation of results, with green shading indicating a perfect RPS score equal by 0, and red shading for a maximum value of 1.

Table 7-3 | High-rainfall season RPS per forecast option (2002-2005)

Forecast Option		RPS at end of Lead month						
No.	Name	0	1	2	3	4	5	6
4	S4	0.29	0.21	0.21	0.16	0.23	0.18	0.24
5	S4_DA	0.08	0.14	0.12	0.15	0.17	0.25	0.24
6	S4_DA_BC	0.05	0.14	0.17	0.16	0.15	0.14	0.13
7	S4T	0.32	0.24	0.30	0.27	0.32	0.25	0.26
8	S4T_DA	0.52	0.14	0.18	0.26	0.26	0.30	0.25
9	S4T_DA_BC	0.10	0.11	0.10	0.11	0.12	0.21	0.21
10	S4TP_DA_BC	0.05	0.12	0.15	0.16	0.14	0.09	0.10

Table 7-3 indicates high forecast accuracy over initial lead months for the majority of forecast options. Higher forecast accuracy is obtained with the introduction of bias corrected precipitation data (forecast options 6 and 10). The inclusion of DA also provides increased forecast accuracy, which is especially evident during initial lead months. Interdiction of temperature forecast data however does not increase forecast accuracy and bias correction is required to improve forecast performance.

Due to high interannual variation of forecasted reservoir inflow, RPS^n results per forecast option were evaluated individually for selected study years. *Table 7-4 and Table 7-5* present RPS^n results for the S4_DA and S4TP_DA_BC forecast options. Additional high-rainfall season RPS^n result tables for each forecast option can be found in *Appendix D*.

Table 7-4 | High-rainfall season - RPS^n results for S4_DA forecast option

High-rainfall season		RPS^n at end of Lead month						
SoS	ToF	0	1	2	3	4	5	6
2001-10-01	2002-04-01	0.02	0.03	0.07	0.12	0.16	0.47	0.44
2002-10-01	2003-04-01	0.02	0.07	0.02	0.02	0.00	0.00	0.00
2003-10-01	2004-04-01	0.19	0.19	0.01	0.04	0.02	0.01	0.01
2004-10-01	2005-04-01	0.09	0.29	0.39	0.44	0.50	0.50	0.50
RPS		0.08	0.14	0.12	0.15	0.17	0.25	0.24

From the results in *Table 7-4* it can be seen that S4_DA ensemble forecast achieved significantly lower RPS^n values for the 2003 and 2004 below-average precipitation years. Above-average precipitation years (2002, 2005) did not achieved such success with decreasing accuracy over the forecast period. This is largely due to the underestimation of System 4 precipitation compared to observed values (see *Section 5.2.2*).

Table 7-5 | High-rainfall season - RPS^n results for S4TP_DA_BC forecast option

High-rainfall season		RPS^n at end of Lead month						
SoS	ToF	0	1	2	3	4	5	6
2001-10-01	2002-04-01	0.01	0.12	0.14	0.15	0.13	0.06	0.07
2002-10-01	2003-04-01	0.04	0.29	0.28	0.27	0.23	0.11	0.13
2003-10-01	2004-04-01	0.11	0.07	0.14	0.15	0.15	0.10	0.10
2004-10-01	2005-04-01	0.05	0.01	0.06	0.08	0.05	0.08	0.09
RPS		0.05	0.12	0.15	0.16	0.14	0.09	0.10

Table 7-5 indicates that the introduction of bias corrected System 4 precipitation and temperature data greatly increases the forecast accuracy for the above-average precipitation years of 2002 and 2005. The accuracy of below-average precipitation years 2003 and 2004 is however reduced. This is due to the overcorrection of forecasted precipitation data over the below-average precipitation period

Table 7-6 has been constructed to assess forecast option RPS values based on the 2002 and 2005 above-average precipitation years. From these results, it is clear that the introduction of bias corrected System 4 precipitation data greatly increases the forecast accuracy over these above-average precipitation years. The introduction of

bias corrected temperature data alone has a smaller positive effect on seasonal forecast accuracy as inflow is predominantly generated though precipitation.

Table 7-6 | High-rainfall season RPS per forecast option (2002, 2005)

Forecast Option		RPS at end of Lead month						
No.	Name	0	1	2	3	4	5	6
4	S4	0.23	0.20	0.23	0.24	0.33	0.36	0.47
5	S4_DA	0.05	0.16	0.23	0.28	0.33	0.48	0.47
6	S4_DA_BC	0.02	0.09	0.12	0.11	0.11	0.14	0.11
7	S4T	0.18	0.16	0.31	0.28	0.42	0.41	0.50
8	S4T_DA	0.45	0.16	0.30	0.39	0.42	0.53	0.50
9	S4T_DA_BC	0.09	0.10	0.18	0.19	0.24	0.42	0.41
10	S4TP_DA_BC	0.03	0.06	0.10	0.11	0.09	0.07	0.08

7.2.2 Low-rainfall season

RPS results for the low-rainfall season are presented in *Table 7-7*.

Table 7-7 | Low-rainfall season - RPS per forecast option (2002-2004)

Forecast Option		RPS at end of Lead month						
No.	Name	0	1	2	3	4	5	6
4	S4	0.36	0.18	0.16	0.07	0.13	0.08	0.15
5	S4_DA	0.08	0.10	0.03	0.06	0.06	0.16	0.15
6	S4_DA_BC	0.05	0.16	0.18	0.16	0.14	0.12	0.13
7	S4T	0.31	0.23	0.26	0.19	0.25	0.16	0.18
8	S4T_DA	0.42	0.10	0.09	0.19	0.16	0.23	0.17
9	S4T_DA_BC	0.10	0.09	0.03	0.04	0.04	0.13	0.12
10	S4TP_DA_BC	0.05	0.16	0.19	0.19	0.17	0.09	0.10

Table 7-7 indicates that the reduced variability of inflow over the low-rainfall seasons, lead to increased overall forecast accuracy when compared to high-rainfall results. Forecast accuracy was however reduced with the introduction of bias corrected precipitation data (S4_DA_BC; S4T_DA_BC), related to the inaccurate estimation of precipitation. Increased forecast accuracy was obtained with the use of bias corrected temperature data, due to the important role temperature plays in runoff generation during this season.

Table 7-8 and *Table 7-9* present RPS^n results for the S4_DA and S4TP_DA_BC forecast options. Additional low-rainfall season RPS^n result tables for each forecast option can be found in *Appendix D*.

Table 7-8 | Low-rainfall season - RPS^n results for S4_DA forecast option

Dry Season		RPS^n at end of Lead month						
SoS	ToF	0	1	2	3	4	5	6
2002-04-01	2002-10-01	0.02	0.03	0.07	0.12	0.16	0.47	0.44
2003-04-01	2003-10-01	0.02	0.07	0.02	0.02	0.00	0.00	0.00
2004-04-01	2004-10-01	0.19	0.19	0.01	0.04	0.02	0.01	0.01
RPS		0.08	0.10	0.03	0.06	0.06	0.16	0.15

Table 7-8 shows that excellent seasonal forecast accuracy was achieved by the S4_DA ensemble forecast for the 2003 and 2004 below-average precipitation years. Similar to the high-rainfall season, above-average precipitation years did not achieve good forecast accuracy. This is especially evident for latter lead months.

Table 7-9 | Low-rainfall season - RPS^n results for S4TP_DA_BC forecast option

Dry Season		RPS^n at end of Lead month						
SoS	ToF	0	1	2	3	4	5	6
2002-04-01	2002-10-01	0.01	0.12	0.14	0.15	0.13	0.06	0.07
2003-04-01	2003-10-01	0.04	0.29	0.28	0.27	0.23	0.11	0.13
2004-04-01	2004-10-01	0.11	0.07	0.14	0.15	0.15	0.10	0.10
RPS		0.05	0.16	0.19	0.19	0.17	0.09	0.10

Table 7-9 indicates that the introduction of bias corrected System 4 precipitation and temperature data greatly increases the forecast accuracy for the above-average precipitation year of 2002. The accuracy of below-average precipitation years 2003 and 2004 is however reduced, similar to results obtained for the high-rainfall season forecast period (see *Table 7-5*).

Table 7-10 presents a comparison of forecast option RPS values based on the 2003 and 2004 below-average precipitation years. From these results, it can be seen that the introduction of bias corrected System 4 precipitation data reduces forecast accuracy over these below-average precipitation years. The introduction of bias corrected temperature data (S4T_DA_BC) however has a positive effect on seasonal forecast accuracy, and overall accuracy is of this forecast option is found similar to the S4_DA forecast option.

Table 7-10 | Low-rainfall season RPS per forecast option (2003, 2004)

Forecast Option		RPS at end of Lead month						
No.	Name	0	1	2	3	4	5	6
4	S4	0.35	0.22	0.20	0.09	0.12	0.01	0.00
5	S4_DA	0.11	0.13	0.01	0.03	0.01	0.01	0.01
6	S4_DA_BC	0.08	0.19	0.22	0.21	0.18	0.14	0.16
7	S4T	0.46	0.33	0.30	0.26	0.22	0.08	0.02
8	S4T_DA	0.59	0.11	0.05	0.14	0.09	0.07	0.01
9	S4T_DA_BC	0.12	0.12	0.02	0.03	0.01	0.01	0.00
10	S4TP_DA_BC	0.08	0.18	0.21	0.21	0.19	0.11	0.12

7.2.3 General remarks on RPS

The RPS results indicate that the most accurate seasonal inflow forecast for the high-rainfall season were obtained with the use of bias corrected- precipitation and temperature forecasts. However, during periods of below-average precipitation, forecast accuracy is reduced due to overestimation of bias corrected precipitation data. Additional investigation of alternative precipitation bias correction methods could provide better representation of annual precipitation variability to improve bias correction and forecast performance over periods of below-average precipitation. During the low-rainfall season, the most accurate seasonal inflow forecasts are obtained with the use of bias corrected temperature data alone. This is due to the limited influence of low precipitation total over this period.

7.3 Ranked Probability Skill Score (RPSS)

The Ranked Probability Skill Score (RPSS) measures the RPS improvement of forecast to a reference forecast (see *Section 5.6.3*). In this study, the seasonal forecast option based on raw System 4 precipitation forecast ensemble (S4) was used as the RPS_{ref} reference forecast. This would allow for the assessment on forecast benefit for System 4 based forecast options. The RPSS results for high-rainfall and low-rainfall season forecasts are presented in *Table 7-11* and *Table 7-12* respectively. Positive RPSS scores indicated a forecast benefit over a raw System 4 precipitation forecast based approach (forecast option S4).

Table 7-11 | High-rainfall season RPSS per forecast option (2002-2005)

Forecast Option		RPSS at end of Lead month						
No.	Name	0	1	2	3	4	5	6
5	S4_DA	0.73	0.31	0.43	0.05	0.24	-0.34	-0.01
6	S4_DA_BC	0.83	0.34	0.21	0.02	0.35	0.22	0.43
7	S4T	-0.11	-0.17	-0.42	-0.68	-0.41	-0.35	-0.10
8	S4T_DA	-0.80	0.35	0.18	-0.63	-0.13	-0.64	-0.08
9	S4T_DA_BC	0.64	0.48	0.54	0.33	0.45	-0.17	0.12
10	S4TP_DA_BC	0.82	0.41	0.28	-0.01	0.39	0.52	0.57

Table 7-11 indicates an increase in forecast skill improvement over most lead months for 4 of the 6 forecast options. The introduction of temperature data (S4T and S4T_DA) indicates a reduction in forecast performance, which is however significantly improved with bias correction of temperature data. The introduction of bias corrected precipitation data however provides the greatest forecast benefits, with resultant forecast skill improvement over almost all lead months. A general reduction in forecast option skill can be seen with increasing lead month time, with a large decreases in forecast skill occurring at the end lead month 3.

Table 7-12 | Low-rainfall season RPSS per forecast option (2002-2004)

Forecast Option		RPSS at end of Lead month						
No.	Name	0	1	2	3	4	5	6
5	S4_DA	0.79	0.47	0.78	0.16	0.54	-1.07	-0.01
6	S4_DA_BC	0.85	0.13	-0.15	-1.39	-0.05	-0.56	0.10
7	S4T	0.12	-0.28	-0.66	-1.83	-0.85	-1.01	-0.20
8	S4T_DA	-0.17	0.46	0.41	-1.83	-0.23	-1.93	-0.16
9	S4T_DA_BC	0.73	0.51	0.82	0.47	0.72	-0.67	0.17
10	S4TP_DA_BC	0.85	0.12	-0.19	-1.82	-0.26	-0.17	0.30

Table 7-12 indicates the largest forecast benefit in the low-rainfall season was with the introduction of bias corrected temperature data. The inclusion of bias corrected precipitation forecasts reduces forecast skill. RPSS results for the remaining forecast options are mixed due to limited variation in forecast estimates and RPS results. A general reduction in forecast skill can be seen with increasing lead month time. A large decrease in forecast skill can be seen occurring for the majority of forecast options at lead month 3. The reduction corresponds to the end of January, where snowmelt contribution to runoff is significantly reduced and accumulated inflow per month decreases. The RPS value for the raw System precipitation forecast (S4), at the end of lead month 3 was 0.09, resulting in large negative RPSS values for the remaining forecast options.

7.4 General remarks on Forecast Verification

Seasonal forecast model bias during the high-rainfall season was reduced with the use of bias corrected System 4 forecasted precipitation data over ESP based approaches. This was especially evident over longer lead time periods. Due to low amount of precipitation and variability during the low-rainfall seasons, forecast bias is in general, considerably lower compared to high-rainfall season values. Limited variation in seasonal forecast bias occurs over the low-rainfall season for all forecast options. The introduction of bias corrected precipitation data does however reduce forecast bias over longer lead times.

For high-rainfall season forecasts, improved forecast skill for all lead month times is evident with the introduction of bias corrected precipitation data. Forecast skill can however be negatively effected over period of below-average precipitation where bias correction of precipitation overestimates precipitation totals. Introduction of temperature provide improved forecast skill up to the end of lead month 4. For low-rainfall season forecasts, introduction of bias corrected precipitation reduces forecast skill over periods of below-average precipitation. Use of bias corrected temperature data improved forecast skill up to the end of lead month 4. For both high-rainfall and low-rainfall seasons, incorporation of DA improves forecast accuracy and skill predominantly over the initial forecast lead months.

8 Discussion and Conclusions

8.1 Conclusions

This study presents an evaluation of the use of seasonal precipitation and temperature forecasts to predict inflow volumes to the Colbún Reservoir located at the outlet of the Upper Maule River Basin, Chile. The discussion and conclusions drawn throughout this study are summarised below.

The ESP-Q method provides valuable information in terms of historical ranges of accumulated seasonal inflow volumes. During the low-rainfall season however, ESP-Q based inflow ensembles create a wide forecast tercile range due to the natural annual variability of snowmelt volumes over this seasonal period. Seasonal inflow estimations based on the ESP-Q therefore are limited in terms of forecast accuracy due to the natural variability in the high-rainfall and low-rainfall seasons. If inflow estimations are to be based on the average value of forecast ensemble members, large volumes error can occur during periods of above- or below-normal inflow.

The Extended Streamflow prediction or ESP-P method was found to be effective and helpful to categorize ranges of possible future water volumes, however the quality of output data is heavily reliant on the rainfall-runoff model calibration. During the high-rainfall season, ESP-P based inflow ensembles span a wide range of predicted inflow volumes over the forecast period due to the high inherent variability of seasonal precipitation. ESP-P based forecast ensembles generally higher forecast accuracy in terms of predicted mean inflow compared to the ESP-Q based approach during this seasonal period, due to the continuous simulation of catchment water storages by the calibrated rainfall-runoff model used by the ESP-P approach.

During the low-rainfall season, the ESP-P method was found to greatly outperform the ESP-Q based approach. This was due to the continuous simulation of catchment conditions during the hindcast and forecast period. As accumulated inflow during the low-rainfall seasons was to be highly dependent on the preceding season's total precipitation, accurate simulation of accumulated snowfall would allow accurate predictions of inflow volumes during the snowmelt period. The limited average precipitation during the low-rainfall season also reduces ensemble variability over this period, providing a narrow inflow ensemble spread over the 7-month forecast period.

Data Assimilation (DA) of reservoir levels and streamflows over the hindcast period allows for increased accuracy in simulated initial hydrological conditions up to the ToF. Inclusion of DA results in improved forecast accuracy and skill predominantly over the initial forecast lead months. For hindcast periods where a good match between simulated and observed records are been obtained, inclusion of DA provides limited result improvement over the hindcast and forecast period. Although DA provides a more accurate representation of accumulated inflow volume at ToF, simulation model biases can however still be included in the forecast period.

The ensemble inflows generated by the raw System 4 precipitation forecasts resulted in reduced forecast accuracy over the high-rainfall season, due to the underestimation of observed precipitation. Higher accuracy in the low-rainfall season was however largely due to limited precipitation over this period and the strong influence of the initial conditions. The underestimation of forecast precipitation data may be due to coarse resolution of System 4 variable datasets compared to the size of the study area but is also a result of the limitations in the ability of the climate model to represent the processes affecting this area.

The introduction of bias corrected System 4 precipitation provided improved inflow forecast accuracy compared to raw System 4 precipitation forecast during high-rainfall seasonal periods with above-average precipitation. However, during high-rainfall seasonal periods of below-average precipitation, bias correction of System 4 data leads (or led) to the overestimation of precipitation and resultant seasonal inflow. The predominant source to forecast inaccuracy however is the inaccurate forecast of total seasonal precipitation by System 4, as bias correction scaling only adjusts the average of the precipitation time series. Introduction of bias corrected System 4 precipitation to low-rainfall season inflow forecasts results in marginal reduction in forecast model bias compared to a raw System 4 precipitation forecast, due to the limited amount of precipitation based runoff during this season.

The use of System 4 temperature forecasts appear to have a relatively limited effect on seasonal inflow forecast performance. Variation in estimated inflow volumes are predominantly caused by differences in the distribution of average monthly temperatures between System 4 forecast and observed values. Generally, average System 4 temperatures were found to be lower than observed values during the austral winter period and higher than observed values in spring. This results in the simulated overestimation of accumulated snow in the winter period and earlier onset of the snowmelt period, resulting in a general reduction of inflow volumes compared to the raw System 4 precipitation based forecast. Bias correction of System 4 temperature data reduced forecast model bias in the high-rainfall seasons compared to a raw System 4 temperature forecast, with comparable results in the low-rainfall season. The use of bias corrected System 4 temperature resulted in marginal improvement of forecast accuracy and skill up to lead month 4, when compared to a raw System 4 precipitation based forecasts.

Seasonal forecasts including bias-corrected System 4 values of both precipitation and temperature data provided the highest forecast accuracy and skill for above-average precipitation years during the high-rainfall season. Seasonal inflow was however. overestimated during below-average precipitation years due to the overcorrection of precipitation forecasts. Performance of System 4 based low-rainfall season forecast using both precipitation and temperature data, can be deemed comparable to the majority of forecast options with a general slight underestimation of seasonal inflow.

In summary, the study shows that the use of bias corrected seasonal precipitation and temperature forecasts from CGCM over resampled historical meteorological data, can improve seasonal hydrological forecast accuracy and skill over periods of above-

average rainfall typically associate with the El Niño-Southern Oscillation (ENSO). For reservoir managers, this improvement in forecast skill provides valuable information related to potential hydrological effects of ocean-atmosphere teleconnections, to aid long-term planning of water resources management and hydropower production. Due to increased predictability of predominantly snowmelt-based inflow during the low-rainfall season, accurate simulation of initial hydrological conditions such as reservoir water level and accumulated snow, can provide accurate low-rainfall seasonal hydrological forecasts for long lead times with the use of forecasted precipitation and temperature data. Increases in forecast accuracy and skill over an ESP based approach during the low-rainfall season was however marginal.

8.2 Study Limitations

In terms of observations data, constraints limiting accurate representation of the study area climatology are listed below:

- Limited historical observed precipitation and temperature data for large parts of the study area, especially for most southern portion of the basin. This makes accurate calibration challenging.
- Reservoir regulation is based on observed reservoir releases records and not on regulation rules. This may affect the response to forecasts especially in extreme years.

Aspects of limitations when applying forecast verification metrics are listed below:

- Seasonal forecast verification was applied to a limited number of study years (4) and seasonal forecast periods (2). Verification of additional years and simulation periods would provide valuable additional information.
- The seasonal forecast verification was implemented with regard to a multi-categorical approach of events three categories defined by ESP-P based terciles. Other possible approaches, such as binary events or continuous variables, were not tested in this study.
- Limited forecast verification methods were applied to seasonal forecasts. Additional methods such as the Relative Operating Characteristics (ROC) and Reliability diagrams could provide additional information on the forecast model performance.

8.3 Improvements and Future Work

This study investigated the potential performance of rainfall-runoff based forecasting system using precipitation and temperature data produced by a probabilistic-based global climate forecast system and corrected a simplistic downscaling method. Ideas for potential model improvements and further investigation are mentioned below:

- Simulation of additional study years and seasonal periods to assess model performance over varied conditions. More detailed assessment of forecast model performance as a function of lead month.

- Evaluation of uncertainty introduced with the use of reservoir regulation rules compared the observed reservoir releases records used in this study.

- The use and comparison of gridded climatic variable datasets from alternative seasonal forecasting models such as Glosea5 (MacLachlan, et al., 2015) and CFSv2 (Saha, et al., 2014).

- Data Assimilation (DA) of snow station observations could provide better estimates of seasonal snow cover depth and distribution at the start of the forecast period. This could potentially provide increased forecast accuracy of snowmelt based runoff and timing of snowmelt events.

- The use of additional downscaling methods such as Gamma Quantile Mapping (GQM) for precipitation data and Empirical Gamma Quantile Mapping (eQM) for temperature data. These methods apply linear transformation functions to each quantile of the forecasted data, potentially providing better representation of seasonal climate variability compared to single linear scaling values.

- Scaling factors used for the bias correction of forecasted precipitation data are dependent on the month of the year and forecast lead month number. The introduction of an additional dependency, amount of total forecasted precipitation, could potentially allow annual varying scaling factors to be applied to raw forecasted data. As found in this study, application of the scaling factors obtained from long term-averages, tend to overestimate (underestimate) seasonal periods of below-average (above-average) precipitation.

- A constant hindcast period of 6 months was used this his study. Shortening of the hindcast period could be tested to assess the impact of shorter model warm-up periods over different seasons.

References

Arenaa, C., Cannarozzo, M. & Mazzolaa, M., 2015. *Seasonal forecasts for reservoir systems operation with an over-year carryover capacity – what is their value?.* Broadbeach, Australia, 21st International Congress on Modelling and Simulation.

Bárdossy, A. & Pegram, G., 2011. Downscaling precipitation using regional climate models and circulation patterns toward hydrology. *Water Resources Research,* Volume 47, p. W04505.

Beven, K. & Freer, J., 2001. Equifinality, data assimilation and uncertainty estimation in mechanistic modelling of complex environmental systems using the GLUE methodology. *Journal of Hydrology,* Volume 249, pp. 11-29.

Bierkens, M. F. P. & Beek, L. P. H. v., 2009. Seasonal Predictability of European Discharge: NAO and Hydrological Response Time. *Journal of Hydrometeorology,* 10(4), pp. 953-968.

Brumbelow, K. & Georgakakos, A., 2001. Agricultural planning and irrigation management: The need for decision support. *The Climate Report,* 1(4), pp. 2-6.

Butts, M. B. et al., 2016. A regional approach to climate adaptation in the Nile Basin. *Proceedings of the International Association of Hydrological Sciences,* 374(3).

Butts, M. B. et al., 2007. Flood Forecasting for the Upper and Middle Odra River Basin. In: *Advances in Natural and Technological Hazards Research.* Begum, S.; Stive, Marcel J.F.; Hall, James W. (Eds.): 20067 ISBN: 1-4020-4199-3..

Butts, M. B., Payne, J. T., Kristensen, M. & Madsen, H., 2004. An Evaluation of the Impact of Model Structure on Hydrological Modelling Uncertainty for Streamflow Simulation. *Journal of Hydrology,* 298(1), pp. 242-266.

Cabreraa, V. E., Letsona, D. & Podestáb, G., 2007. The value of climate information when farm programs matter. *Agricultural Systems,* 93(1-3), pp. 25-42.

Clark, M. P. et al., 2006. Assimilation of snow covered area information into hydrologic and landsurface models. *Adv. Water Resour,* Volume 29, p. 1209–1221.

Cobo, B. & Hamilton, R., 1979. *History of the Inca Empire: an account of the Indians' customs and their origin, together with a treatise on Inca legends, history, and social institutions.* Austin Texas: University of Texas Press.

DHI, 2011. *Sistema de pronóstico de caudal a corto, mediano y largo plazo para la cuenca del Embalse de Colbún, Calibración modelo hidrológico* , s.l.: Prepared for Colbún S.A..

DHI, 2016. *MIKE OPERATIONS Release note 2016.* [Online]
Available at: http://releasenotes.dhigroup.com/2016/MIKEOPERATIONSrelinf.htm
[Accessed 28 May 2017].

DHI, 2017. *Hydrology.* [Online]
Available at: https://www.mikepoweredbydhi.com/products/mike-hydro-

river/hydrology
[Accessed 28 May 2017].

DHI, 2017. *MIKE OPERATIONS.* [Online]
Available at: https://www.mikepoweredbydhi.com/products/mike-operations
[Accessed 30 May 2017].

Dixon, S. & Wilby, R., 2015. Forecasting reservoir inflows using remotely sensed precipitation estimates: a pilot study for the River Naryn, Kyrgyzstan. *Hydrological Sciences Journal,* 61(1), pp. 107-122.

Draw, B., 2016. *Seasonal forecasting for multi-purpose reservoir management in Spain,* Cottbus - Senftenberg: Brandenburg University of Technology; DHI.

Etkin, D., 2009. *Utilizing Seasonal Forecasts to Improve Reservoir Operations in the Comoé River Basin* , Medford, US: (Master Thesis) Tufts University.

FAO, 2017. *CLIMWAT.* [Online]
Available at: http://www.fao.org/land-water/databases-and-software/climwat-for-cropwat/en/
[Accessed 26 February 2017].

Gelfan, A. N., Motovilov, Y. G. & Moreido, V. M., 2015. Ensemble seasonal forecast of extreme water inflow into a large reservoir. *Proceedings of the International Association of Hydrological Sciences,* Volume 369, pp. 115-120.

Goddard, L. et al., 2001. Current approaches to seasonal to interannual climate predictions. *International Journal of Climatology,* Volume 21, pp. 1111-1152.

Hay, L. & Clark, M., 2003. Use of statistically and dynamically downscaled atmospheric model output for hydrologic simulations in three mountainous basins in the western United States. *Journal of Hydrology,* Volume 282, pp. 57-75.

Higgins, S., 2015. *Limitations to Seasonal Weather Prediction and Crop Forecasting due to Nonlinearity and Model Inadequacy,* London: The London School of Economics and Political Science.

Jolli, I. T. & Stephenson, D. B., 2012. *Forecast Verificaiton: A Practitioner's Guide in Atmospheric Science.* Second Edition ed. s.l.:John Wiley & Sons, Ltd.

Lenderink, G., Buishand, A. & van Deursen, W., 2007. Estimates of future discharges of the river Rhine using two scenario methodologies: direct versus delta approach. *Hydrol. Earth Syst. Sci,* Volume 11, pp. 1145-1159.

Leung, L., Mearns, L., Giorgi, F. & Wilby, R., 2003. Regional Climate Research: Needs an Opportunities. *American Meteorological Society,* Volume 84, pp. 89-95.

MacLachlan, C. et al., 2015. Global Seasonal forecast system version 5 (GloSea5): a high-resolution seasonal forecast system. *Q.J.R. Meteorol. Soc.,* Volume 141, p. 1072–1084.

MacLachlan, C. et al., 2015. Global Seasonal forecast system version 5 (GloSea5): a high-resolution seasonal forecast system. *Quarterly Journal of the Royal Meteorological Society,* Volume 141, pp. 1072-1084.

Madsen, H., 2000. Automatic calibration of a conceptual rainfall–runoff model using multiple objectives. *Journal of Hydrology,* 235(3-4), pp. 276-288.

Madsen, H., 2003. Parameter estimation in distributed hydrological catchment modelling using automatic calibration with multiple objectives. *Advances in Water Resources,* 26(2), p. 205–216.

Maurer, E. P. & Lettenmaier, D. P., 2003. Predictability of seasonal runoff in the Mississippi River basin. *J. Geophys. Res.*, 108(D16).

Met Office UK , 2016. *El Niño, La Niña and the Southern Oscillation.* [Online] Available at: http://www.metoffice.gov.uk/research/climate/seasonal-to-decadal/gpc-outlooks/el-nino-la-nina/enso-description [Accessed 12 Feb 2017].

Mo, K. & Lettenmaier, D., 2014. Hydrologic prediction over the conterminous United States using the national multi-model ensemble. *Journal of Hydrometeorology,* Volume 15, p. 1457–1472.

Molteni, F. et al., 2011. *The new ECMWF seasonal (System 4),* Berkshire: ECMWF Technical Memorandum, 656.

Montecinos, A. & Aceituno, P., 2003. Seasonality of the ENSO-Related Rainfall Variability in Central Chile and Associated Circulation Anomalies. *Journal of Climate,* 16(2), pp. 281-296.

Montecinos, A., Díaz, A. & Aceituno, P., 2000. Seasonal Diagnostic and Predictability of Rainfall in Subtropical South America Based on Tropical Pacific SST. *Journal of Climate,* Volume 13, pp. 746-758.

Najafi, M. R., Moradkhani, H. & Piechota, T. C., 2012. Ensemble Streamflow Prediction: Climate signal weighting methods vs. Climate Forecast System Reanalysis. *Journal of Hydrology,* Volume 442-443, pp. 105-116.

Nielsen, S. A. & Hansen, E., 1973. Numerical simulation of the rainfall-runoff process on a daily basis. *Nordic Hydrol.,* 4(3), pp. 171-190.

NOAA, 2014. *What is the El Niño–Southern Oscillation (ENSO) in a nutshell?.* [Online] Available at: https://www.climate.gov/news-features/blogs/enso/what-el-ni%C3%B1o%E2%80%93southern-oscillation-enso-nutshell [Accessed 15 February 2017].

NOAA, 2016. *What are El Niño and La Niña?.* [Online] Available at: http://oceanservice.noaa.gov/facts/ninonina.html [Accessed 12 February 2017].

NOAA, 2017. *Equatorial Pacific Sea Surface Temperatures.* [Online] Available at: https://www.ncdc.noaa.gov/teleconnections/enso/indicators/sst.php [Accessed 12 March 2017].

Pagano, T. & Garen, D., 2004. Evaluation of Official Western U.S. Seasonal Water Supply Outlooks, 1922–2002. *Journal of Hydrometeorology,* 5(5), pp. 896-909.

Panthi, B. M., 2016. *Seasonal Forecasting for a snow-fed Hydropower Reservoir in Chile,* Cottbus - Senftenberg: Brandenburg University of Technology; DHI.

Peng, Z. et al., 2014. Statistical calibration and bridging of ECMWF System4 outputs for forecasting seasonal precipitation over China. *J. Geophys. Res. Atmos.,* Volume 119, p. 7116–7135.

Pizarro-Tapia, R., Valdés-Pineda, R., Olivares, C. & González, P., 2014. Development of Upstream Data-Input Models to Estimate Downstream Peak Flow in Two Mediterranean River Basins of Chile. *Open Journal of Modern Hydrology,* Volume 4, pp. 132-143.

Rivera, D. et al., 2012. Forecasting monthly precipitation in Central Chile: a self-organizing map approach using filtered sea surface temperature. *Theoretical and Applied Climatology,* 107(1), pp. 1-13.

Rivera, D. et al., 2012. Forecasting monthly precipitation in Central Chile: a self-organizing map approach using filtered sea surface temperature. *Theoretical and Applied Climatology,* Volume 107, pp. 1-13.

RStudio, 2017. *RStudio Products.* [Online]
Available at: https://www.rstudio.com/products/rstudio/
[Accessed 30 May 2017].

Rubio-Álvarez, E. & McPhee, J., 2010. Patterns of spatial and temporal variability in streamflow records in south central Chile in the period 1952–2003. *Water Resources Research*, 46(5), p. W05514.

Saha, S. et al., 2014. The NCEP Climate Forecast System Version 2. *Journal of Climate,* 27(6), pp. 2185-2208.

Santander Meteorology Group, 2017. *Santander Meteorology Group - Repositories.* [Online]
Available at: https://github.com/SantanderMetGroup
[Accessed 10 February 2017].

Sene, K., 2010. *Hydrometeorology: Forecasting and Applications.* 1 ed. Dordrecht: Springer Netherlands.

Shukla, S. & Lettenmaier, D. P., 2011. Seasonal hydrologic prediction in the United States: understanding the role of initial hydrologic conditions and seasonal climate forecast skill. *Hydrology and Earth System Sciences,* 15(11), p. 3529–3538.

Shukla, S., Sheffield, J., Wood, E. & Lettenmaier, D., 2013. On the sources of global land surface hydrological predictability. *Hydrol Earth Syst Sci,* Volume 17, p. 2781–2796.

Solomon, S. et al., 2007. *Contribution of Working Group I to the Fourth Assessment Report of the Intergovernmental Panel on Climate Change,* Cambridge: Cambridge University Press.

Sudheer, C., Maheswaran, R., Panigrahi, B. K. & Mathur, S., 2014. A hybrid SVM-PSO model for forecasting monthly streamflow. *Neural Computing and Applications,* 24(6), pp. 1381-1389.

Twedt, T. M., Schaake Jr, J. C. & and Peck, E. L., 1977. *National weather service extended streamflow prediction.* Albuquerque, New Mexico, Western Snow Conference.

UCMG, 2016. *The ECOMS User Data Gateway.* [Online]
Available at: https://meteo.unican.es/trac/wiki/udg/ecoms
[Accessed 10 February 2017].

USGS, 2017. *Earth Explorer.* [Online]
Available at: http://earthexplorer.usgs.gov/
[Accessed March 2017].

Waylen, P. R., Caviedes, C. N. & Juricic, C., 1993. El Niño-southern oscillation and the surface hydrology of Chile: a window on the future?. *Canadian Water Resources Journal / Revue canadienne des ressources hydriques,* 18(4), pp. 425-441.

Weigel, A. P., Liniger, M. A. & Appenzeller, C., 2007. The Discrete Brier and Ranked Probability Skill Scores. *Monthly Weatehr Review,* 135(1), pp. 118-124.

Wetterhall, F., Pappenberger, F., He, Y. & Cloke, H. L., 2012. Conditioning model output statistics of regional climate model precipitation on circulation patterns. *Nonlinear Processes in Geophysics,* Volume 19, pp. 623-633.

Wilks, D. S., 2005. *Statistical Methods in Atmospherical Sciences.* Second Edition ed. s.l.:Elsevier.

Williams, J. & Null, J., 2015. What You Need to Know to Understand the Current El Niño. *Weatherwise,* 68(6), pp. 12-19.

WMO, 2009. *Guide to Hydrological Practices Volume 2: Management of Water Resources and Application of Hydrological Practices. WMO-No. 168.* 6th Edition ed. Geneva, Switzerland: World Meteorological Organization.

Wood, A. W. & Lettenmaier, D. P., 2006. A Test Bed for New Seasonal Hydrologic Forecasting Approaches in the Western United States. *Bulletin of the American Meteorological Society (BAMS),* 87(12), pp. 1699-1712.

Wood, A. W. & Lettenmaier, D. P., 2008. An ensemble approach for attribution of hydrologic prediction uncertainty. *Geophysical Research Letters,* 35(14).

Yao, H. & Georgakakos, A. P., 2001. Assessment of Folsom Lake response to historical and potential future climate scenarios, 2. Reservoir management. *Journal of Hydrology,* Volume 249, pp. 176-196.

Yuan, X., Wood, E. F. & Ma, Z., 2015. A review on climate-model-based seasonal hydrologic forecasting: physical understanding and system development. *WIREs Water,* Volume 2, pp. 523-536.

Yuan, X., Wood, E. F., Roundy, J. K. & Pan, M., 2013. CFSv2-Based Seasonal Hydroclimatic Forecasts over the Conterminous United States. *Journal of Climate,* Volume 26, pp. 4828-4847.

Zhao, T. et al., 2015. Quantifying predictive uncertainty of streamflow forecasts based on a Bayesian joint probability model. *Journal of Hydrology,* Volume 528, pp. 329-340.

Appendices

Appendix A: Analysis year selection – Hydrological analysis

Appendix B: Additional seasonal forecast model output plots for selected forecast options

Appendix C: Results tables of accumulated inflow and percentage volume error per forecast option

Appendix D : RPS^n result tables per forecast option and seasonal forecast period

Appendix A | *Analysis year selection – Hydrological analysis*

The average monthly precipitation and Colbún Reservoir inflow for selected analysis years (2002, 2003, 2004, 2005) are presented in *Figure A-1* and *Figure A-2* respectively.

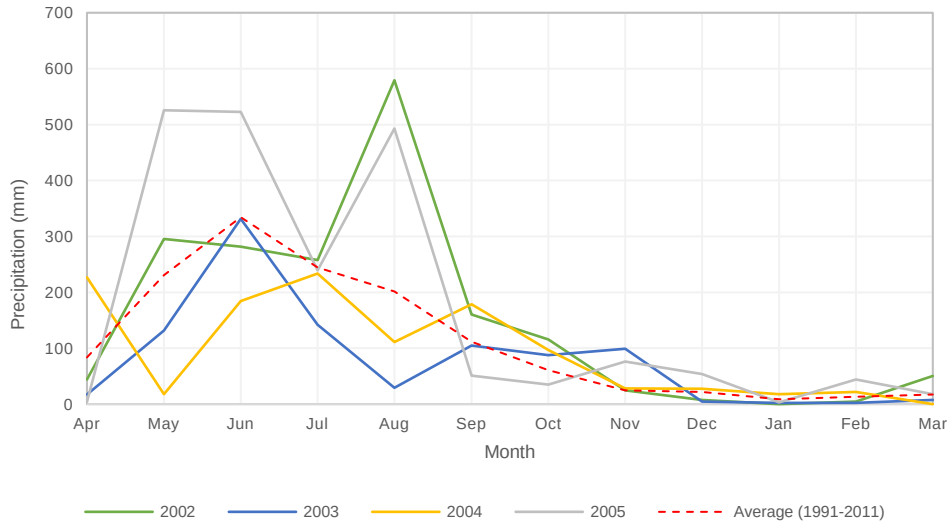

Figure A-1 | Catchment-based total monthly precipitation per selected analysis year

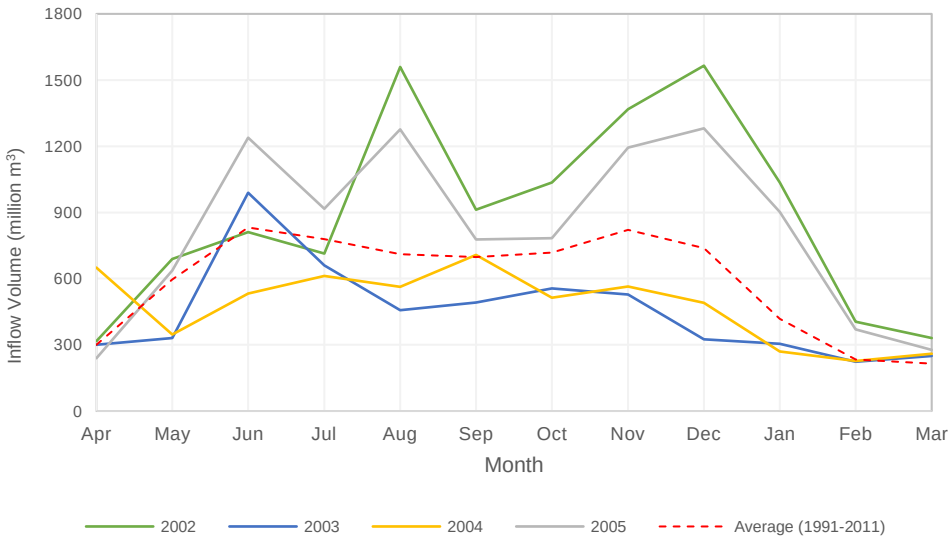

Figure A-2 | Colbún Reservoir monthly accumulated inflow per selected analysis year

Figure A-2 illustrates the two seasonal inflow peaks experienced over the high-rainfall and snowmelt periods for the above average-precipitation years of 2002 and 2005 (see *Figure A-1*). Early seasonal forecast of above-average seasonal inflow would provide reservoir managers with valuable temporal information related to reservoir filling, optimisation of hydropower generation and water management between upstream reservoirs. The relationship between high-rainfall season precipitation totals and subsequent low-rainfalls seasonal reservoir inflow (see *Section 4.6.3*), could also provide reservoir managers with an initial estimate of seasonal inflow over the low-rainfall season.

Figure A-2 also shows greatly reduced seasonal inflow peaks were experienced during 2003 and 2004, due to the below-average precipitation experienced over the preceding high-rainfall seasons (see *Figure A-1)*. This two-year period of below-average reservoir inflow would be critical for reservoir management due to limited water supply and carry over storage for the subsequent years.

Figure A-3 compares average monthly observed temperatures for selected analysis at the *LoAguirre* temperature station.

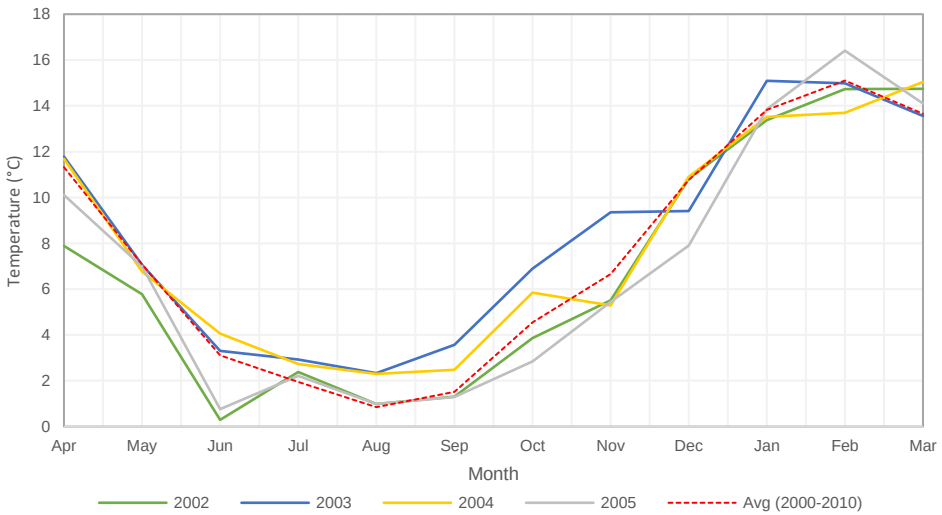

Figure A-3 | LoAguirre Average monthly temperatures for selected analysis years

Figure A-3 indicates similar below-average temperatures were experienced for above-average precipitation years 2002 and 2005. During the below-average precipitation years of 2003 and 2004, above-average temperatures were experienced over the winter and spring period.

Appendix B | *Additional seasonal forecast model output plots for selected forecast options*

Forecast Option 5: S4_DA

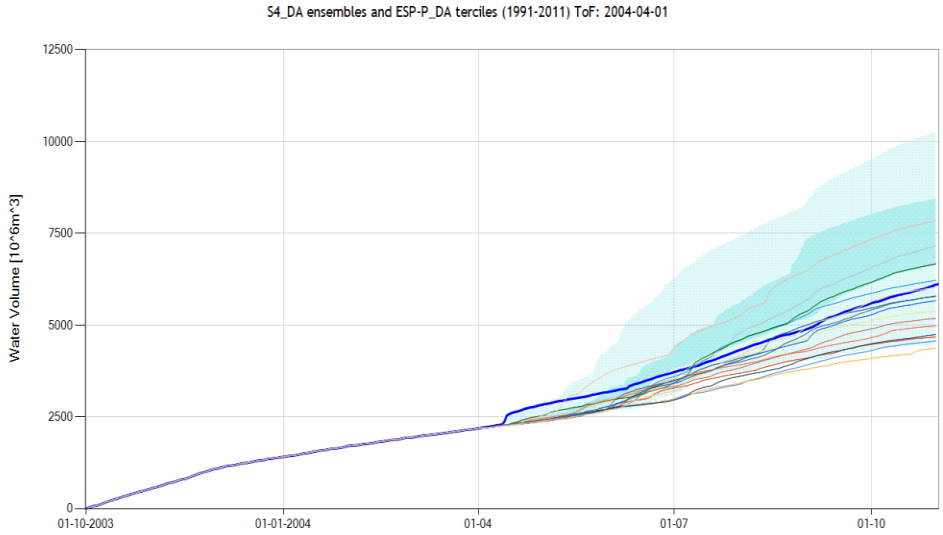

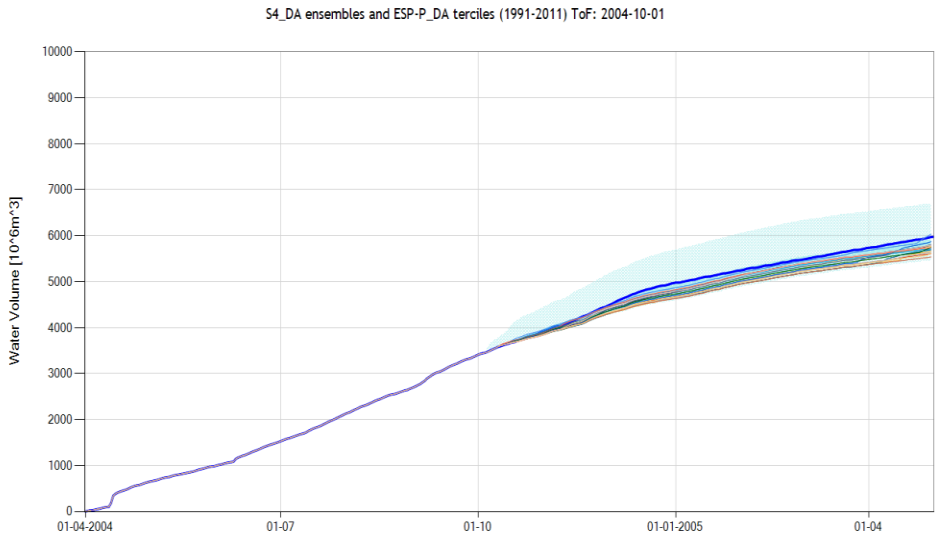

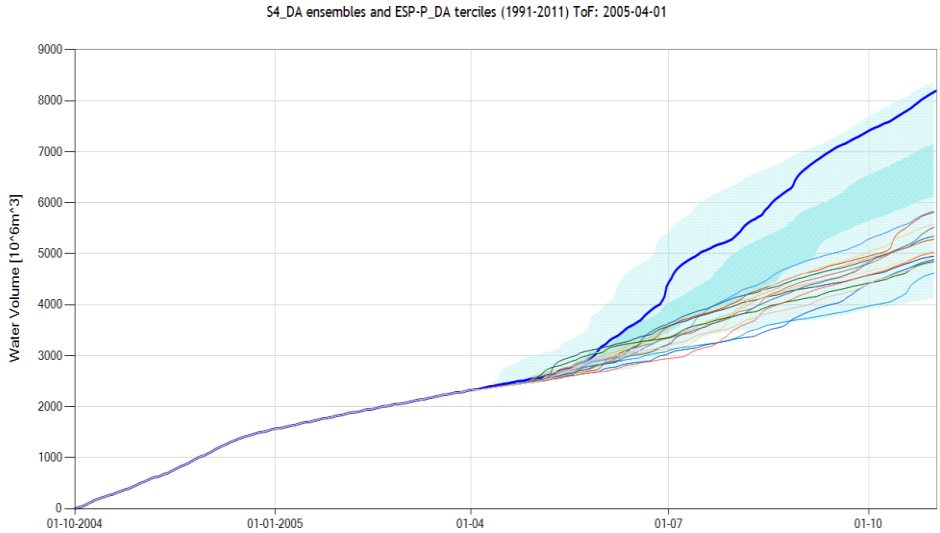

Forecast Option 6: S4_DA_BC

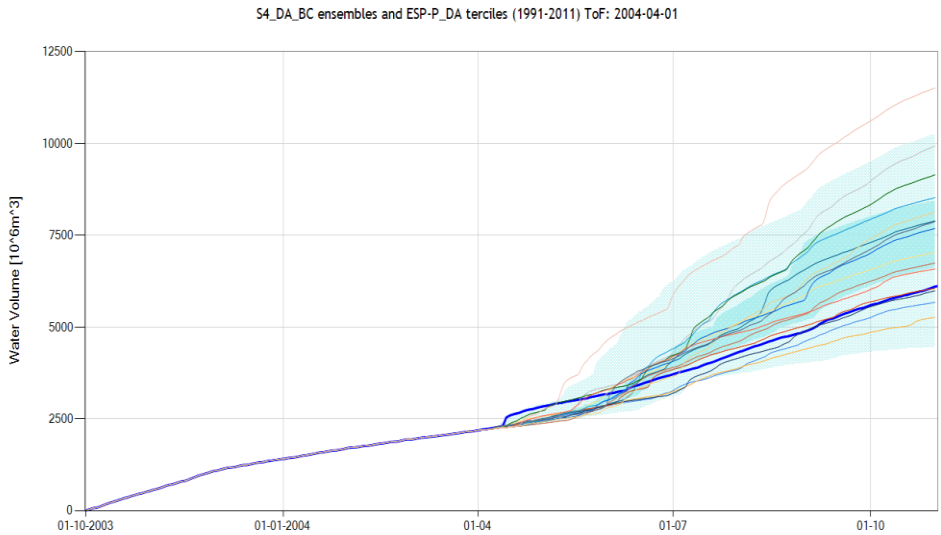

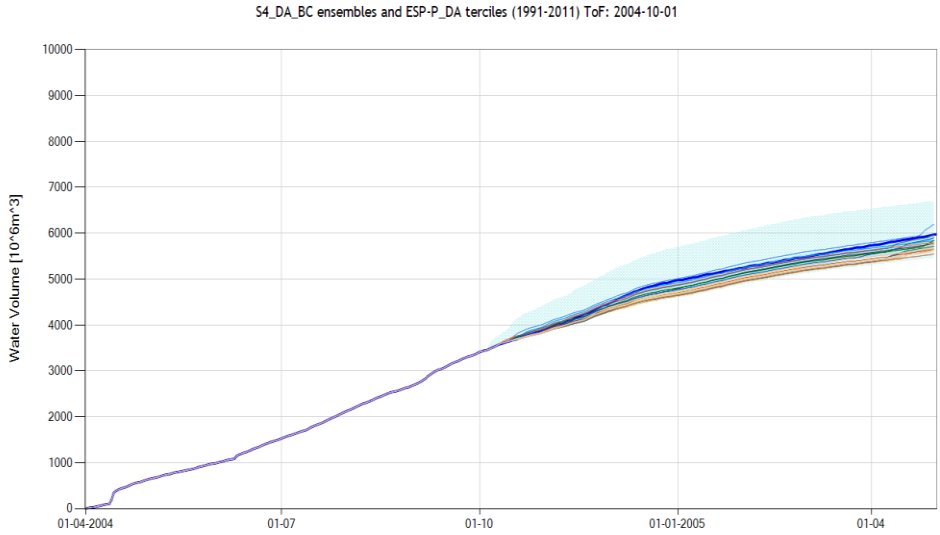
S4_DA_BC ensembles and ESP-P_DA terciles (1991-2011) ToF: 2004-10-01
Water Volume [10^6m^3]
10000
9000
8000
7000
6000
5000
4000
3000
2000
1000
0
01-04-2004
01-07
01-10
01-01-2005
01-04

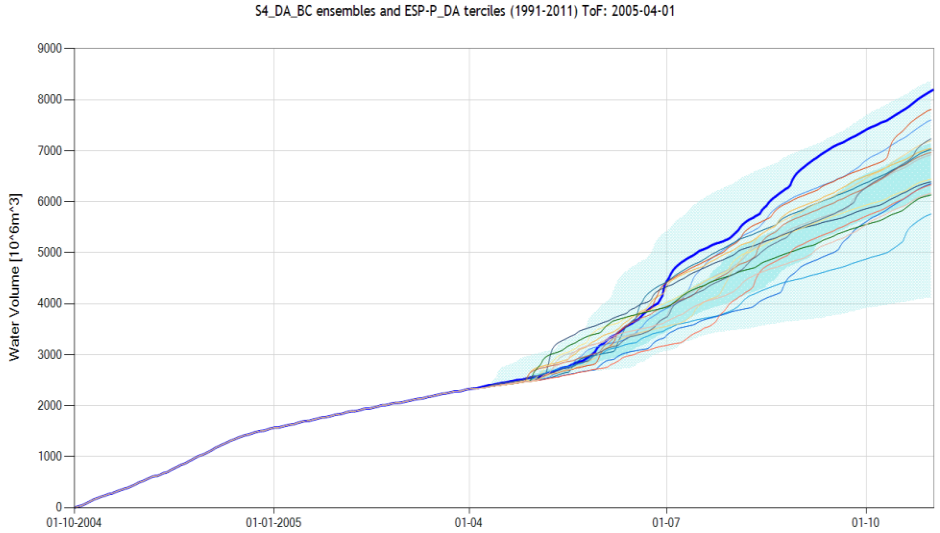
S4_DA_BC ensembles and ESP-P_DA terciles (1991-2011) ToF: 2005-04-01
Water Volume [10^6m^3]
9000
8000
7000
6000
5000
4000
3000
2000
1000
0
01-10-2004
01-01-2005
01-04
01-07
01-10

Forecast Option 10: S4TP_DA_BC

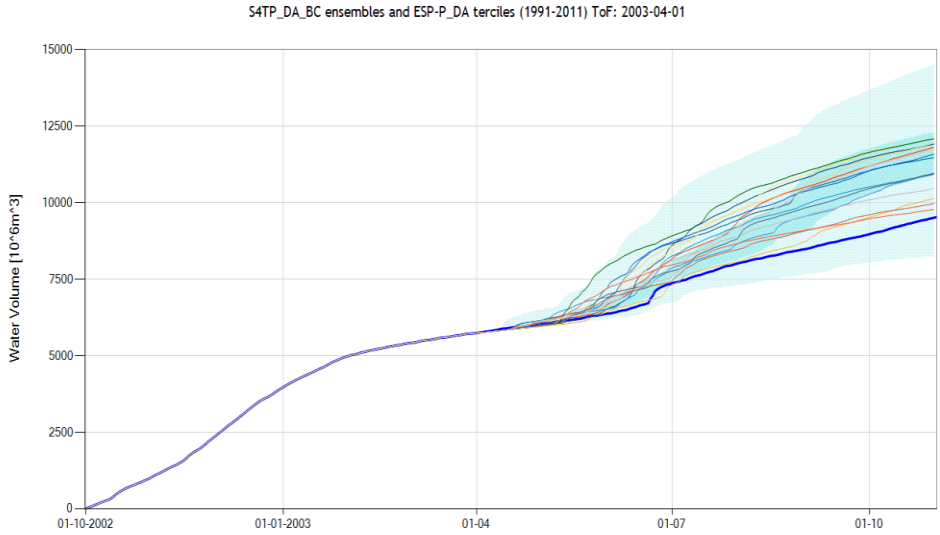

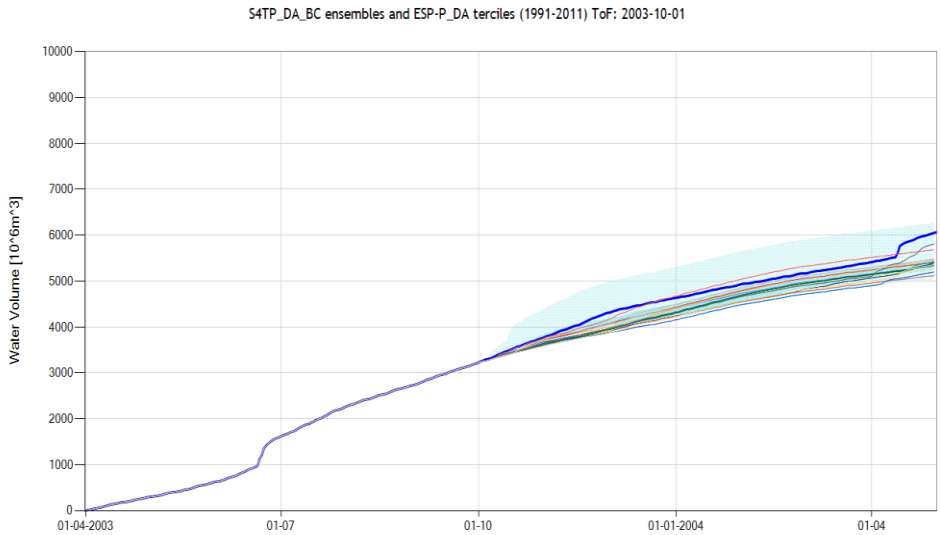

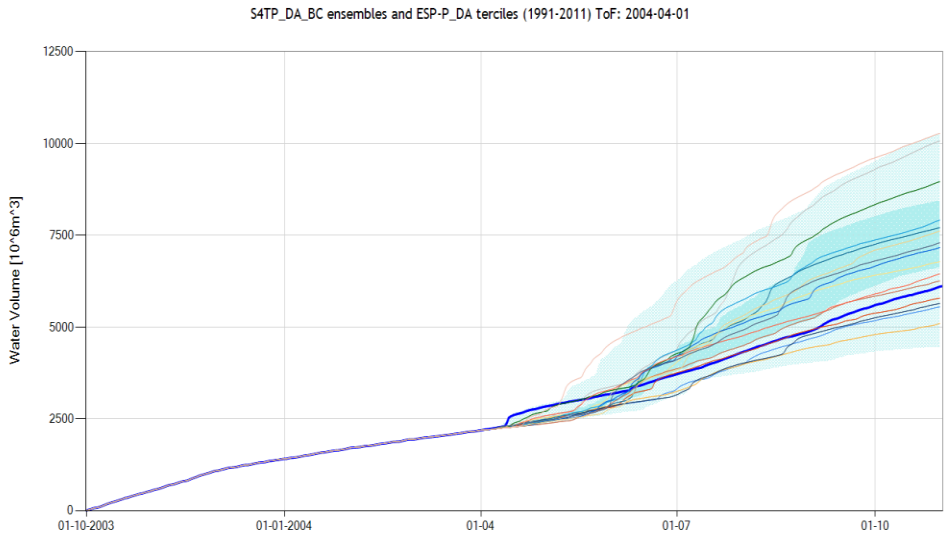
S4TP_DA_BC ensembles and ESP-P_DA terciles (1991-2011) ToF: 2004-04-01
Water Volume [10^6m^3]
12500
10000
7500
5000
2500
0
01-10-2003
01-01-2004
01-04
01-07
01-10

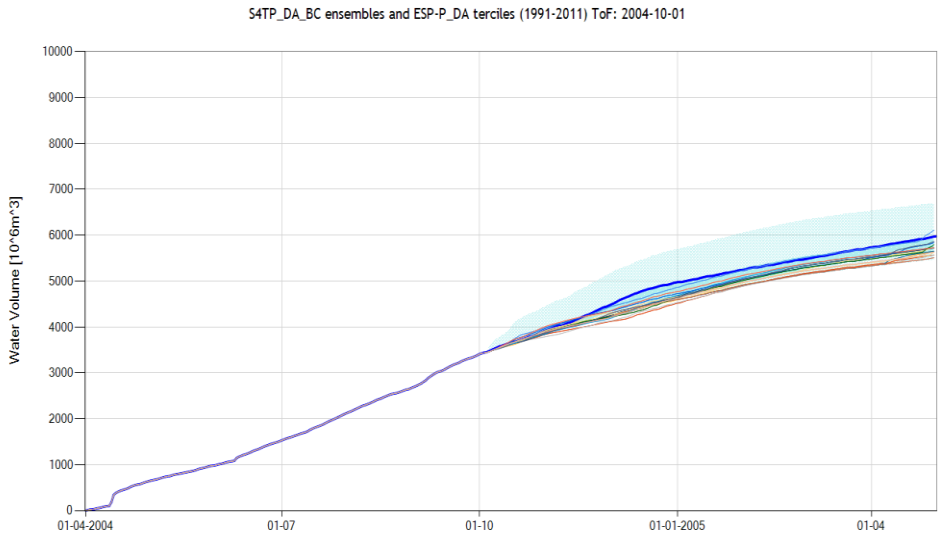
S4TP_DA_BC ensembles and ESP-P_DA terciles (1991-2011) ToF: 2004-10-01
Water Volume [10^6m^3]
10000
9000
8000
7000
6000
5000
4000
3000
2000
1000
0
01-04-2004
01-07
01-10
01-01-2005
01-04

Appendix C | *Results tables of accumulated inflow and percentage volume error per forecast option*

Table B-1 | Summary of selected Seasonal Forecast options

Forecast Option		Inflows before ToF based on		Inflows after ToF based on						
		Historical Streamflows	Historical Precipitation (Rainfall-runoff Model)	Ensemble Streamlow prediction based on						
				Historical Streamflows ESP-Q	Historical Precipitation ESP-P	System 4 forecast variable (15 member ensemble)		Includes DA of discharge and water levels	Includes Downscaling of Precip Data	Includes Downscaling of Temp Data
No.	Name					Precipitation	Temperature			
1	ESP-Q	x		x						
2	ESP-P		x		x					
3	ESP-P_DA		x		x			x		
4	S4		x			x				
5	S4_DA		x			x		x		
6	S4_DA_BC		x			x		x	x	
7	S4T		x			x	x			
8	S4T_DA		x			x	x	x		
9	S4T_DA_BC		x			x	x	x		x
10	S4TP_DA_BC		x			x	x	x	x	x

High Rainfall Season 2002		Ensemble member average: Total accumulated inflow volume (million m^3) and %error							
SoS	01/10/2001								
ToF	01/04/2002	at end of Lead Month 0-6							
EoS	31/10/2002	at ToF		0		1		2	
Forecast Option									
No.	Name								
-	Observed Inflow	**3439.5**	-	**3744.3**	-	**4409.4**	-	**5238.1**	-
1	ESP-Q	3439.5	0.0%	3722.7	-0.6%	4275.5	-3.0%	5032.4	-3.9%
2	ESP-P	3728.4	8.4%	4133.6	10.4%	4796.2	8.8%	5643.2	7.7%
3	ESP-P_DA	3442.8	0.1%	3812.1	1.8%	4473.9	1.5%	5320.6	1.6%
4	S4	3728.4	8.4%	4038.0	7.8%	4609.0	4.5%	5211.1	-0.5%
5	S4_DA	3439.6	0.0%	3719.7	-0.7%	4288.1	-2.8%	4890.1	-6.6%
6	S4_DA_BC	3442.8	0.1%	3777.5	0.9%	4663.6	5.8%	5648.0	7.8%
7	S4T	3672.2	6.8%	3973.4	6.1%	4462.2	1.2%	4958.4	-5.3%
8	S4T_DA	3442.8	0.1%	3704.5	-1.1%	4193.1	-4.9%	4689.3	-10.5%
9	S4T_DA_BC	3442.8	0.1%	3709.5	-0.9%	4327.7	-1.9%	5089.9	-2.8%
10	S4TP_DA_BC	3442.8	0.1%	3764.9	0.5%	4725.6	7.2%	6014.6	14.8%
		3		4		5		6	
Forecast Option									
No.	Name								
-	Observed Inflow	**5945.5**	-	**7486.0**	-	**8412.3**	-	**9439.4**	-
1	ESP-Q	5781.2	-2.8%	6475.1	-13.5%	7155.2	-14.9%	7857.2	-16.8%
2	ESP-P	6497.9	9.3%	7345.7	-1.9%	7992.9	-5.0%	8635.1	-8.5%
3	ESP-P_DA	6174.9	3.9%	7022.5	-6.2%	7669.6	-8.8%	8209.7	-13.0%
4	S4	5844.7	-1.7%	6382.6	-14.7%	6818.5	-18.9%	7301.4	-22.6%
5	S4_DA	5523.5	-7.1%	6061.4	-19.0%	6497.2	-22.8%	6993.7	-25.9%
6	S4_DA_BC	6571.1	10.5%	7411.9	-1.0%	8120.5	-3.5%	8841.0	-6.3%
7	S4T	5386.4	-9.4%	5724.7	-23.5%	6047.1	-28.1%	6617.7	-29.9%
8	S4T_DA	5117.3	-13.9%	5455.6	-27.1%	5778.0	-31.3%	6348.5	-32.7%
9	S4T_DA_BC	5840.0	-1.8%	6376.2	-14.8%	6782.1	-19.4%	7195.3	-23.8%
10	S4TP_DA_BC	7160.3	20.4%	8061.3	7.7%	8769.4	4.2%	9397.6	-0.4%

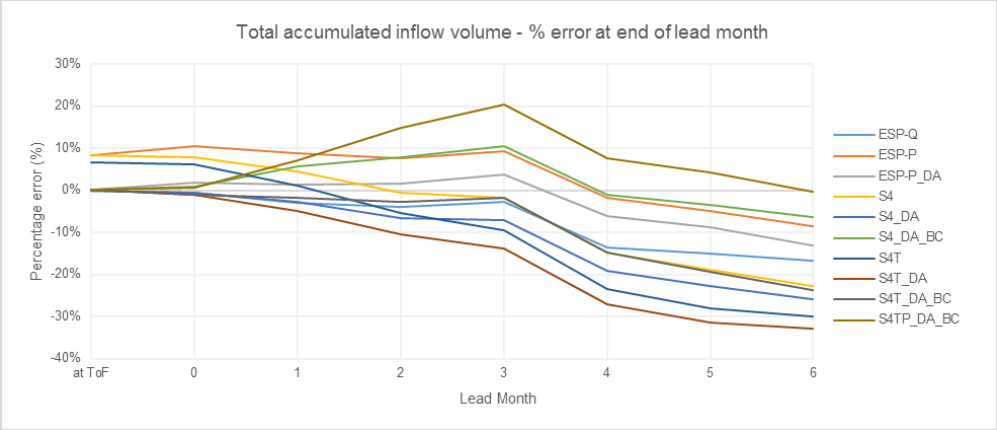

Low Rainfall Season 2002 / 2003		Ensemble member average: Total accumulated inflow volume (million m^3) and %error							
SoS	01/04/2002								
ToF	01/10/2002	at end of Lead Month 0-6							
EoS	01/04/2003	at ToF		0		1		2	
Forecast Option									
No.	Name								
-	Observed Inflow	**5001.4**	-	**5999.9**	-	**7348.2**	-	**8927.4**	-
1	ESP-Q	5001.4	0.0%	5694.2	-5.1%	6495.7	-11.6%	7209.1	-19.2%
2	ESP-P	5025.2	0.5%	5916.6	-1.4%	7005.3	-4.7%	8411.4	-5.8%
3	ESP-P_DA	5001.4	0.0%	5848.2	-2.5%	6922.5	-5.8%	8328.0	-6.7%
4	S4	5025.2	0.5%	5924.3	-1.3%	7034.2	-4.3%	8456.6	-5.3%
5	S4_DA	5001.4	0.0%	5856.1	-2.4%	6951.5	-5.4%	8373.3	-6.2%
6	S4_DA_BC	5001.4	0.0%	5932.1	-1.1%	7043.8	-4.1%	8499.7	-4.8%
7	S4T	4705.2	-5.9%	5621.8	-6.3%	7267.6	-1.1%	8558.9	-4.1%
8	S4T_DA	5001.4	0.0%	5864.7	-2.3%	7501.9	2.1%	8791.6	-1.5%
9	S4T_DA_BC	5001.4	0.0%	5678.0	-5.4%	6547.7	-10.9%	7847.7	-12.1%
10	S4TP_DA_BC	5001.4	0.0%	5724.8	-4.6%	6616.0	-10.0%	7965.9	-10.8%
		3		4		5		6	
Forecast Option									
No.	Name								
-	Observed Inflow	**9979.4**	-	**10400.7**	-	**10731.2**	-	**11036.3**	-
1	ESP-Q	7617.4	-23.7%	7854.8	-24.5%	8072.1	-24.8%	8359.8	-24.3%
2	ESP-P	9159.9	-8.2%	9514.6	-8.5%	9812.9	-8.6%	10159.8	-7.9%
3	ESP-P_DA	9076.0	-9.1%	9430.5	-9.3%	9728.8	-9.3%	9950.1	-9.8%
4	S4	9219.0	-7.6%	9562.5	-8.1%	9843.9	-8.3%	10142.3	-8.1%
5	S4_DA	9135.0	-8.5%	9478.5	-8.9%	9759.8	-9.1%	10058.3	-8.9%
6	S4_DA_BC	9277.9	-7.0%	9624.8	-7.5%	9901.1	-7.7%	10229.6	-7.3%
7	S4T	9115.8	-8.7%	9441.1	-9.2%	9703.6	-9.6%	9961.8	-9.7%
8	S4T_DA	9348.1	-6.3%	9673.4	-7.0%	9935.9	-7.4%	10194.1	-7.6%
9	S4T_DA_BC	8931.0	-10.5%	9395.7	-9.7%	9737.6	-9.3%	10056.4	-8.9%
10	S4TP_DA_BC	9080.4	-9.0%	9557.1	-8.1%	9898.7	-7.8%	10247.7	-7.1%

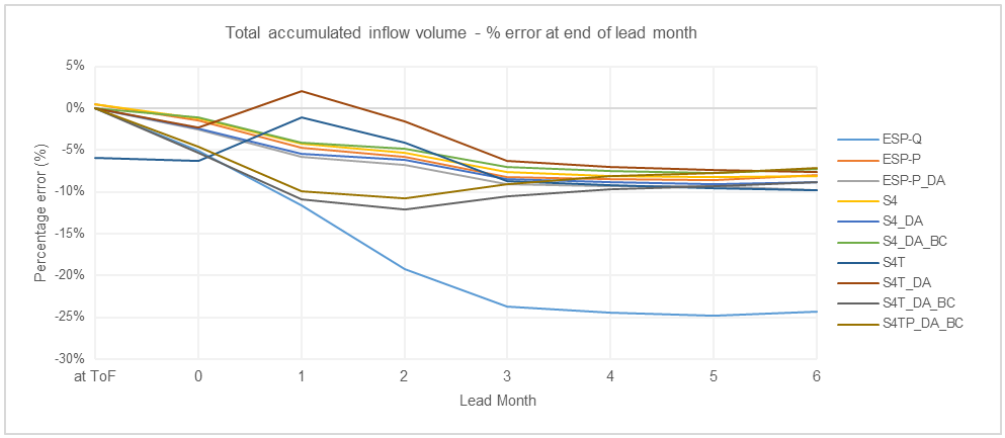

High Rainfall Season 2003		Ensemble member average: Total accumulated inflow volume (million m^3) and %error							
SoS	01/10/2002								
ToF	01/04/2003	at end of Lead Month 0-6							
EoS	31/10/2003	at ToF		0		1		2	
Forecast Option									
No.	Name								
-	Observed Inflow	**5741.2**	-	**6034.9**	-	**6363.6**	-	**7335.0**	-
1	ESP-Q	5741.2	0.0%	6024.1	-0.2%	6577.0	3.4%	7333.9	0.0%
2	ESP-P	4834.9	-15.8%	5168.0	-14.4%	5846.6	-8.1%	6945.5	-5.3%
3	ESP-P_DA	5741.2	0.0%	6061.9	0.4%	6742.7	6.0%	7842.8	6.9%
4	S4	4834.9	-15.8%	5090.7	-15.6%	5597.7	-12.0%	6320.3	-13.8%
5	S4_DA	5741.2	0.0%	5983.5	-0.9%	6495.1	2.1%	7218.2	-1.6%
6	S4_DA_BC	5741.2	0.0%	6047.0	0.2%	6857.2	7.8%	8107.9	10.5%
7	S4T	4827.3	-15.9%	5069.8	-16.0%	5463.6	-14.1%	5913.2	-19.4%
8	S4T_DA	5741.2	0.0%	5968.5	-1.1%	6366.0	0.0%	6817.5	-7.1%
9	S4T_DA_BC	5741.2	0.0%	5979.0	-0.9%	6501.8	2.2%	7240.2	-1.3%
10	S4TP_DA_BC	5741.2	0.0%	6035.2	0.0%	6854.9	7.7%	8127.6	10.8%
		3		4		5		6	
Forecast Option									
No.	Name								
-	Observed Inflow	**7999.8**	-	**8469.3**	-	**8949.5**	-	**9505.0**	-
1	ESP-Q	8082.7	1.0%	8776.5	3.6%	9456.7	5.7%	10158.7	6.9%
2	ESP-P	7972.5	-0.3%	9052.0	6.9%	9977.6	11.5%	10731.6	12.9%
3	ESP-P_DA	8870.0	10.9%	9949.5	17.5%	10875.1	21.5%	11503.2	21.0%
4	S4	6984.2	-12.7%	7619.0	-10.0%	8181.0	-8.6%	8627.3	-9.2%
5	S4_DA	7882.5	-1.5%	8517.4	0.6%	9079.4	1.5%	9525.7	0.2%
6	S4_DA_BC	9097.9	13.7%	10064.1	18.8%	10928.2	22.1%	11652.2	22.6%
7	S4T	6329.6	-20.9%	6725.4	-20.6%	7125.1	-20.4%	7662.3	-19.4%
8	S4T_DA	7233.9	-9.6%	7629.7	-9.9%	8029.4	-10.3%	8566.6	-9.9%
9	S4T_DA_BC	7934.7	-0.8%	8483.1	0.2%	8909.9	-0.4%	9248.9	-2.7%
10	S4TP_DA_BC	9189.4	14.9%	10033.8	18.5%	10690.5	19.5%	11189.9	17.7%

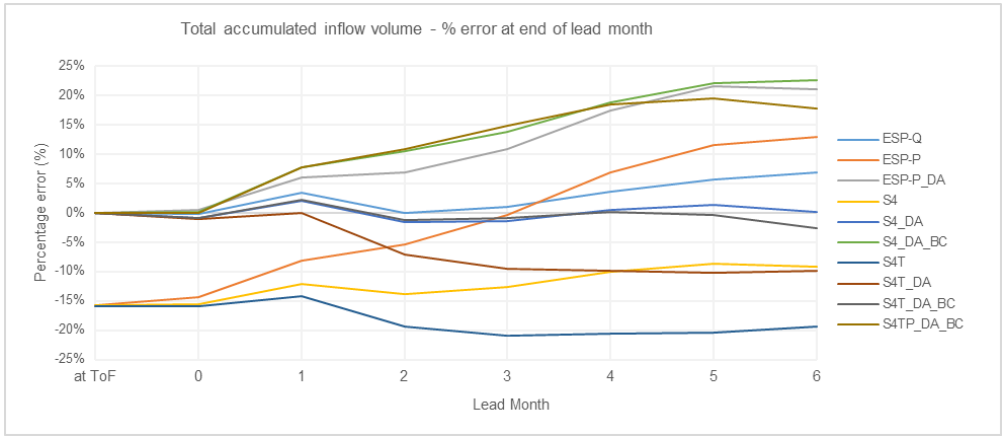

Low Rainfall Season 2003 / 2004		Ensemble member average: Total accumulated inflow volume (million m^3) and %error							
SoS	01/04/2003								
ToF	01/10/2003	at end of Lead Month 0-6							
EoS	01/04/2004	at ToF		0		1		2	
Forecast Option									
No.	Name								
-	Observed Inflow	**3229.2**	-	**3763.8**	-	**4309.9**	-	**4631.0**	-
1	ESP-Q	3229.2	0.0%	3920.6	4.2%	4722.1	9.6%	5435.5	17.4%
2	ESP-P	3485.5	7.9%	4111.3	9.2%	4516.1	4.8%	4787.7	3.4%
3	ESP-P_DA	3229.2	0.0%	3810.7	1.2%	4179.9	-3.0%	4449.8	-3.9%
4	S4	3485.5	7.9%	4077.2	8.3%	4464.2	3.6%	4710.8	1.7%
5	S4_DA	3229.2	0.0%	3780.1	0.4%	4126.2	-4.3%	4371.2	-5.6%
6	S4_DA_BC	3229.2	0.0%	3844.2	2.1%	4211.3	-2.3%	4462.9	-3.6%
7	S4T	3260.5	1.0%	3803.7	1.1%	4249.5	-1.4%	4522.3	-2.3%
8	S4T_DA	3229.2	0.0%	3719.4	-1.2%	4123.0	-4.3%	4393.8	-5.1%
9	S4T_DA_BC	3229.2	0.0%	3607.5	-4.2%	3914.5	-9.2%	4254.9	-8.1%
10	S4TP_DA_BC	3229.2	0.0%	3656.0	-2.9%	3981.6	-7.6%	4347.0	-6.1%
		3		4		5		6	
Forecast Option									
No.	Name								
-	Observed Inflow	**4931.1**	-	**5164.3**	-	**5406.8**	-	**6050.3**	-
1	ESP-Q	5843.8	18.5%	6081.2	17.8%	6306.2	16.6%	6593.9	9.0%
2	ESP-P	5113.1	3.7%	5362.4	3.8%	5570.6	3.0%	5862.7	-3.1%
3	ESP-P_DA	4774.9	-3.2%	5024.1	-2.7%	5231.9	-3.2%	5410.1	-10.6%
4	S4	5032.7	2.1%	5273.6	2.1%	5466.2	1.1%	5717.4	-5.5%
5	S4_DA	4692.8	-4.8%	4933.7	-4.5%	5126.3	-5.2%	5376.3	-11.1%
6	S4_DA_BC	4779.5	-3.1%	5013.3	-2.9%	5198.4	-3.9%	5474.6	-9.5%
7	S4T	4838.2	-1.9%	5074.7	-1.7%	5262.9	-2.7%	5491.3	-9.2%
8	S4T_DA	4709.2	-4.5%	4945.7	-4.2%	5133.9	-5.0%	5362.3	-11.4%
9	S4T_DA_BC	4606.3	-6.6%	4857.3	-5.9%	5050.2	-6.6%	5295.8	-12.5%
10	S4TP_DA_BC	4701.9	-4.6%	4957.2	-4.0%	5145.9	-4.8%	5415.2	-10.5%

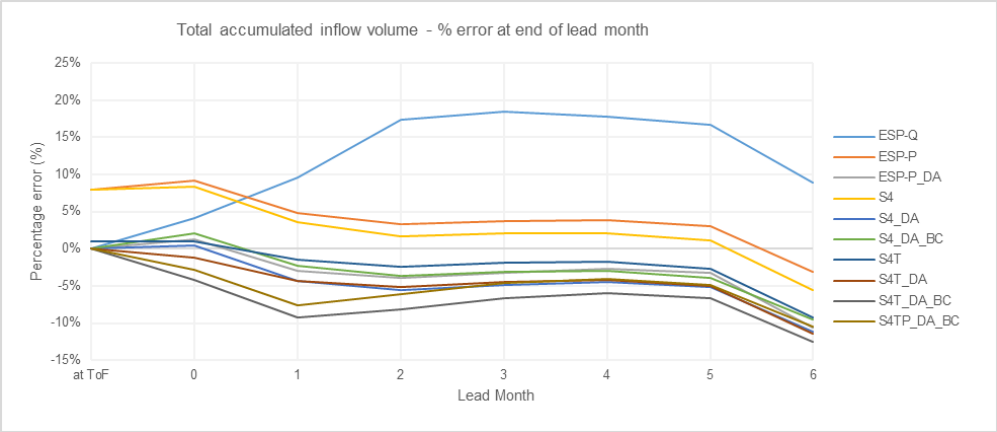

High Rainfall Season 2004		Ensemble member average: Total accumulated inflow volume (million m^3) and %error							
SoS	01/10/2003								
ToF	01/04/2004	at end of Lead Month 0-6							
EoS	31/10/2004	at ToF		0		1		2	
Forecast Option									
No.	Name								
-	Observed Inflow	**2186.1**	-	**2821.2**	-	**3169.7**	-	**3696.3**	-
1	ESP-Q	2186.1	0.0%	2468.8	-12.5%	3021.6	-4.7%	3778.5	2.2%
2	ESP-P	2318.1	6.0%	2649.9	-6.1%	3322.2	4.8%	4361.9	18.0%
3	ESP-P_DA	2188.0	0.1%	2490.6	-11.7%	3164.7	-0.2%	4208.9	13.9%
4	S4	2318.1	6.0%	2587.8	-8.3%	3006.0	-5.2%	3538.9	-4.3%
5	S4_DA	2188.0	0.1%	2427.5	-14.0%	2849.1	-10.1%	3383.2	-8.5%
6	S4_DA_BC	2188.0	0.1%	2503.5	-11.3%	3121.9	-1.5%	4012.7	8.6%
7	S4T	2299.6	5.2%	2547.9	-9.7%	2894.1	-8.7%	3272.9	-11.5%
8	S4T_DA	2188.0	0.1%	2411.6	-14.5%	2759.0	-13.0%	3139.4	-15.1%
9	S4T_DA_BC	2188.0	0.1%	2423.2	-14.1%	2838.4	-10.5%	3394.2	-8.2%
10	S4TP_DA_BC	2188.0	0.1%	2494.9	-11.6%	3099.5	-2.2%	4016.9	8.7%
		3		4		5		6	
Forecast Option									
No.	Name								
-	Observed Inflow	**4306.1**	-	**4871.3**	-	**5574.4**	-	**6099.2**	-
1	ESP-Q	4527.3	5.1%	5221.2	7.2%	5901.3	5.9%	6603.3	8.3%
2	ESP-P	5341.0	24.0%	6313.6	29.6%	7148.4	28.2%	7768.4	27.4%
3	ESP-P_DA	5196.0	20.7%	6172.9	26.7%	7010.8	25.8%	7532.3	23.5%
4	S4	4243.9	-1.4%	4890.8	0.4%	5458.4	-2.1%	5816.5	-4.6%
5	S4_DA	4090.7	-5.0%	4737.6	-2.7%	5305.3	-4.8%	5669.6	-7.0%
6	S4_DA_BC	5074.3	17.8%	6073.0	24.7%	6973.8	25.1%	7601.5	24.6%
7	S4T	3688.8	-14.3%	4099.6	-15.8%	4434.4	-20.4%	4964.0	-18.6%
8	S4T_DA	3555.4	-17.4%	3971.3	-18.5%	4307.3	-22.7%	4837.0	-20.7%
9	S4T_DA_BC	4134.4	-4.0%	4731.6	-2.9%	5138.0	-7.8%	5455.5	-10.6%
10	S4TP_DA_BC	5131.5	19.2%	6074.0	24.7%	6732.3	20.8%	7238.2	18.7%

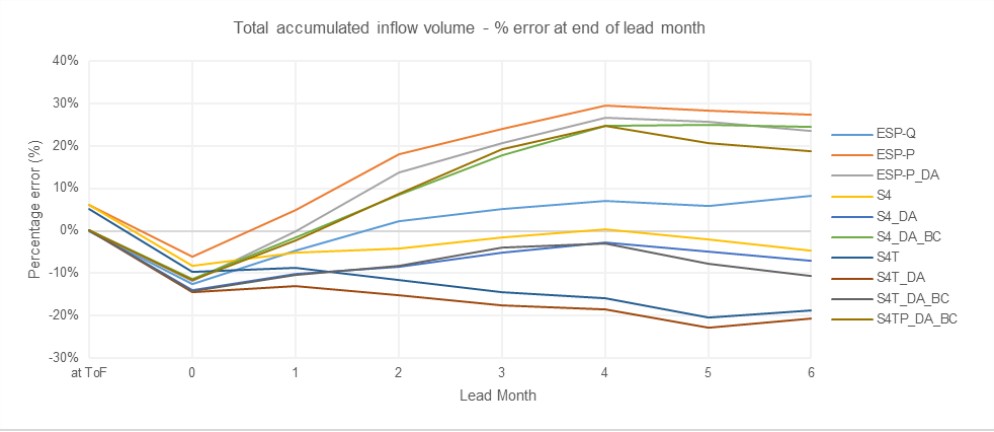

Low Rainfall Season 2004 / 2005		Ensemble member average: Total accumulated inflow volume (million m^3) and %error							
SoS	01/04/2004								
ToF	01/10/2004	at end of Lead Month 0-6							
EoS	01/04/2005	at ToF		0		1		2	
Forecast Option									
No.	Name								
-	Observed Inflow	**3411.8**	-	**3913.1**	-	**4467.1**	-	**4968.3**	-
1	ESP-Q	3411.8	0.0%	4102.2	4.8%	4903.6	9.8%	5617.1	13.1%
2	ESP-P	3766.1	10.4%	4325.1	10.5%	4843.1	8.4%	5245.5	5.6%
3	ESP-P_DA	3411.8	0.0%	3937.1	0.6%	4452.2	-0.3%	4850.0	-2.4%
4	S4	3766.1	10.4%	4257.6	8.8%	4751.7	6.4%	5114.9	2.9%
5	S4_DA	3411.8	0.0%	3870.0	-1.1%	4361.6	-2.4%	4720.7	-5.0%
6	S4_DA_BC	3411.8	0.0%	3898.3	-0.4%	4394.8	-1.6%	4762.4	-4.1%
7	S4T	3526.7	3.4%	4150.6	6.1%	4696.8	5.1%	4965.3	-0.1%
8	S4T_DA	3411.8	0.0%	4007.1	2.4%	4521.0	1.2%	4788.1	-3.6%
9	S4T_DA_BC	3411.8	0.0%	3862.9	-1.3%	4213.6	-5.7%	4596.7	-7.5%
10	S4TP_DA_BC	3411.8	0.0%	3890.1	-0.6%	4249.6	-4.9%	4644.0	-6.5%
		3		4		5		6	
Forecast Option									
No.	Name								
-	Observed Inflow	**5242.2**	-	**5468.1**	-	**5731.5**	-	**5970.8**	-
1	ESP-Q	6025.4	14.9%	6262.8	14.5%	6480.0	13.1%	6767.7	13.3%
2	ESP-P	5577.5	6.4%	5836.8	6.7%	6052.5	5.6%	6345.1	6.3%
3	ESP-P_DA	5181.8	-1.2%	5441.1	-0.5%	5656.8	-1.3%	5832.7	-2.3%
4	S4	5440.6	3.8%	5684.0	3.9%	5885.9	2.7%	6129.2	2.7%
5	S4_DA	5046.3	-3.7%	5289.6	-3.3%	5491.5	-4.2%	5734.1	-4.0%
6	S4_DA_BC	5084.1	-3.0%	5323.9	-2.6%	5515.7	-3.8%	5776.0	-3.3%
7	S4T	5265.2	0.4%	5494.9	0.5%	5686.5	-0.8%	5903.7	-1.1%
8	S4T_DA	5087.7	-2.9%	5317.4	-2.8%	5508.9	-3.9%	5726.2	-4.1%
9	S4T_DA_BC	4948.3	-5.6%	5207.6	-4.8%	5408.3	-5.6%	5646.3	-5.4%
10	S4TP_DA_BC	5001.0	-4.6%	5261.0	-3.8%	5456.1	-4.8%	5713.6	-4.3%

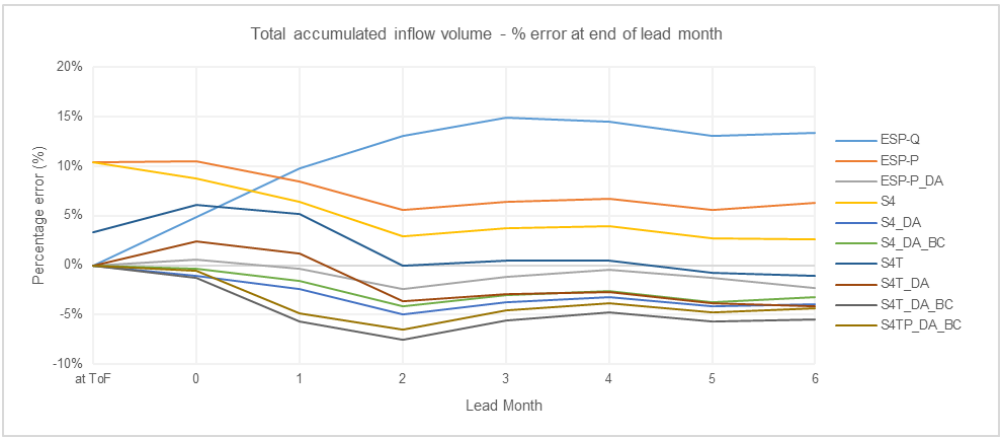

High Rainfall Season 2005		Ensemble member average: Total accumulated inflow volume (million m^3) and %error							
SoS	01/10/2004								
ToF	01/04/2005	at end of Lead Month 0-6							
EoS	31/10/2005	at ToF		0		1		2	
Forecast Option									
No.	Name								
-	Observed Inflow	**2324.0**	-	**2559.0**	-	**3171.2**	-	**4353.1**	-
1	ESP-Q	2324.0	0.0%	2606.3	1.8%	3159.1	-0.4%	3916.0	-10.0%
2	ESP-P	2315.7	-0.4%	2590.1	1.2%	3063.4	-3.4%	3808.0	-12.5%
3	ESP-P_DA	2325.2	0.1%	2593.1	1.3%	3067.0	-3.3%	3812.4	-12.4%
4	S4	2315.7	-0.4%	2494.4	-2.5%	2891.2	-8.8%	3292.7	-24.4%
5	S4_DA	2325.2	0.1%	2497.9	-2.4%	2895.6	-8.7%	3297.0	-24.3%
6	S4_DA_BC	2325.2	0.1%	2531.4	-1.1%	3144.6	-0.8%	3849.3	-11.6%
7	S4T	2279.5	-1.9%	2455.9	-4.0%	2886.7	-9.0%	3174.6	-27.1%
8	S4T_DA	2325.2	0.1%	2495.1	-2.5%	2926.9	-7.7%	3214.9	-26.1%
9	S4T_DA_BC	2325.2	0.1%	2497.0	-2.4%	3016.7	-4.9%	3467.5	-20.3%
10	S4TP_DA_BC	2325.2	0.1%	2529.4	-1.2%	3360.1	6.0%	4166.1	-4.3%
		3		4		5		6	
Forecast Option									
No.	Name								
-	Observed Inflow	**5316.6**	-	**6594.7**	-	**7384.0**	-	**8171.1**	-
1	ESP-Q	4664.8	-12.3%	5358.7	-18.7%	6038.9	-18.2%	6740.8	-17.5%
2	ESP-P	4595.6	-13.6%	5349.9	-18.9%	5950.7	-19.4%	6575.3	-19.5%
3	ESP-P_DA	4601.3	-13.5%	5357.0	-18.8%	5958.6	-19.3%	6484.3	-20.6%
4	S4	3800.6	-28.5%	4307.5	-34.7%	4689.6	-36.5%	5200.7	-36.4%
5	S4_DA	3804.9	-28.4%	4311.9	-34.6%	4694.5	-36.4%	5206.1	-36.3%
6	S4_DA_BC	4627.2	-13.0%	5440.0	-17.5%	6033.6	-18.3%	6757.1	-17.3%
7	S4T	3495.7	-34.2%	3793.0	-42.5%	4092.4	-44.6%	4643.4	-43.2%
8	S4T_DA	3536.0	-33.5%	3833.3	-41.9%	4133.5	-44.0%	4684.9	-42.7%
9	S4T_DA_BC	4063.5	-23.6%	4558.4	-30.9%	4907.1	-33.5%	5273.5	-35.5%
10	S4TP_DA_BC	5113.8	-3.8%	5955.0	-9.7%	6526.1	-11.6%	7055.4	-13.7%

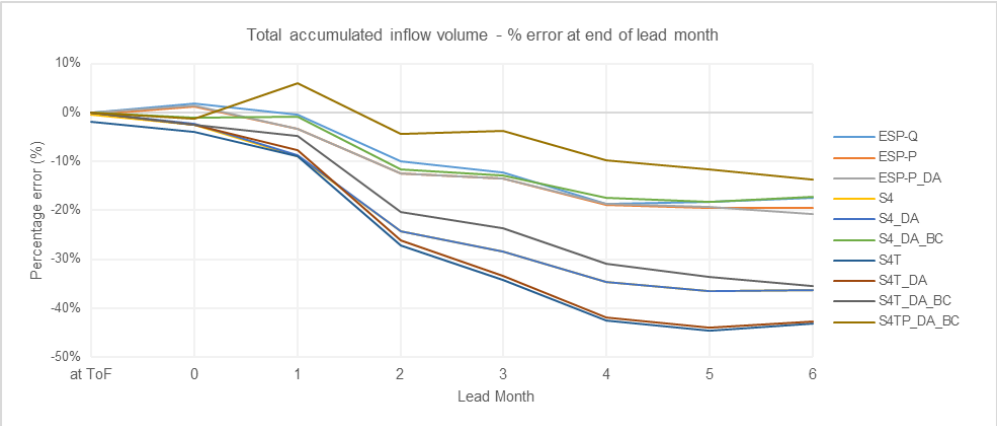

Appendix D | *RPS^n result tables per forecast option and seasonal forecast period*

1. High-rainfall season

S4

High-rainfall season		RPS^n at end of Lead month						
SoS	ToF	0	1	2	3	4	5	6
2001-10-01	2002-04-01	0.36	0.11	0.07	0.03	0.16	0.22	0.44
2002-10-01	2003-04-01	0.52	0.27	0.38	0.14	0.22	0.00	0.00
2003-10-01	2004-04-01	0.19	0.16	0.01	0.04	0.02	0.01	0.01
2004-10-01	2005-04-01	0.09	0.29	0.39	0.44	0.50	0.50	0.50
RPS		0.29	0.21	0.21	0.16	0.23	0.18	0.24

S4_DA

High-rainfall season		RPS^n at end of Lead month						
SoS	ToF	0	1	2	3	4	5	6
2001-10-01	2002-04-01	0.02	0.03	0.07	0.12	0.16	0.47	0.44
2002-10-01	2003-04-01	0.02	0.07	0.02	0.02	0.00	0.00	0.00
2003-10-01	2004-04-01	0.19	0.19	0.01	0.04	0.02	0.01	0.01
2004-10-01	2005-04-01	0.09	0.29	0.39	0.44	0.50	0.50	0.50
RPS		0.08	0.14	0.12	0.15	0.17	0.25	0.24

S4_DA_BC

High-rainfall season		RPS^n at end of Lead month						
SoS	ToF	0	1	2	3	4	5	6
2001-10-01	2002-04-01	0.01	0.09	0.09	0.08	0.06	0.08	0.08
2002-10-01	2003-04-01	0.04	0.29	0.31	0.26	0.22	0.16	0.19
2003-10-01	2004-04-01	0.11	0.09	0.14	0.15	0.14	0.12	0.13
2004-10-01	2005-04-01	0.03	0.08	0.14	0.14	0.16	0.21	0.14
RPS		0.05	0.14	0.17	0.16	0.15	0.14	0.13

S4T

High-rainfall season		RPS^n at end of Lead month						
SoS	ToF	0	1	2	3	4	5	6
2001-10-01	2002-04-01	0.01	0.04	0.18	0.05	0.30	0.30	0.50
2002-10-01	2003-04-01	0.58	0.44	0.53	0.36	0.30	0.05	0.00
2003-10-01	2004-04-01	0.34	0.22	0.07	0.16	0.13	0.11	0.03
2004-10-01	2005-04-01	0.35	0.28	0.44	0.51	0.53	0.52	0.50
RPS		0.32	0.24	0.30	0.27	0.32	0.25	0.26

S4T_DA

High-rainfall season		RPS^n at end of Lead month						
SoS	ToF	0	1	2	3	4	5	6
2001-10-01	2002-04-01	0.07	0.07	0.18	0.30	0.30	0.54	0.50
2002-10-01	2003-04-01	0.62	0.00	0.03	0.11	0.05	0.05	0.00
2003-10-01	2004-04-01	0.55	0.22	0.07	0.16	0.13	0.09	0.01
2004-10-01	2005-04-01	0.83	0.25	0.43	0.48	0.53	0.52	0.50
RPS		0.52	0.14	0.18	0.26	0.26	0.30	0.25

S4T_DA_BC

High-rainfall season		RPS^n at end of Lead month						
SoS	ToF	0	1	2	3	4	5	6
2001-10-01	2002-04-01	0.04	0.04	0.05	0.05	0.09	0.36	0.36
2002-10-01	2003-04-01	0.04	0.04	0.03	0.02	0.00	0.00	0.00
2003-10-01	2004-04-01	0.21	0.19	0.01	0.04	0.02	0.03	0.01
2004-10-01	2005-04-01	0.13	0.16	0.31	0.33	0.38	0.47	0.47
RPS		0.10	0.11	0.10	0.11	0.12	0.21	0.21

S4TP_DA_BC

High-rainfall season		RPS^n at end of Lead month						
SoS	ToF	0	1	2	3	4	5	6
2001-10-01	2002-04-01	0.01	0.12	0.14	0.15	0.13	0.06	0.07
2002-10-01	2003-04-01	0.04	0.29	0.28	0.27	0.23	0.11	0.13
2003-10-01	2004-04-01	0.11	0.07	0.14	0.15	0.15	0.10	0.10
2004-10-01	2005-04-01	0.05	0.01	0.06	0.08	0.05	0.08	0.09
RPS		0.05	0.12	0.15	0.16	0.14	0.09	0.10

2. Low-rainfall Season

S4

Dry Season		RPS^n at end of Lead month						
SoS	ToF	0	1	2	3	4	5	6
2002-04-01	2002-10-01	0.36	0.11	0.07	0.03	0.16	0.22	0.44
2003-04-01	2003-10-01	0.52	0.27	0.38	0.14	0.22	0.00	0.00
2004-04-01	2004-10-01	0.19	0.16	0.01	0.04	0.02	0.01	0.01
RPS		0.36	0.18	0.16	0.07	0.13	0.08	0.15

S4_DA

Dry Season		RPS^n at end of Lead month						
SoS	ToF	0	1	2	3	4	5	6
2002-04-01	2002-10-01	0.02	0.03	0.07	0.12	0.16	0.47	0.44
2003-04-01	2003-10-01	0.02	0.07	0.02	0.02	0.00	0.00	0.00
2004-04-01	2004-10-01	0.19	0.19	0.01	0.04	0.02	0.01	0.01
RPS		0.08	0.10	0.03	0.06	0.06	0.16	0.15

S4_DA_BC

Dry Season		RPS^n at end of Lead month						
SoS	ToF	0	1	2	3	4	5	6
2002-04-01	2002-10-01	0.01	0.09	0.09	0.08	0.06	0.08	0.08
2003-04-01	2003-10-01	0.04	0.29	0.31	0.26	0.22	0.16	0.19
2004-04-01	2004-10-01	0.11	0.09	0.14	0.15	0.14	0.12	0.13
RPS		0.05	0.16	0.18	0.16	0.14	0.12	0.13

S4T

Dry Season		RPS^n at end of Lead month						
SoS	ToF	0	1	2	3	4	5	6
2002-04-01	2002-10-01	0.01	0.04	0.18	0.05	0.30	0.30	0.50
2003-04-01	2003-10-01	0.58	0.44	0.53	0.36	0.30	0.05	0.00
2004-04-01	2004-10-01	0.34	0.22	0.07	0.16	0.13	0.11	0.03
RPS		0.31	0.23	0.26	0.19	0.25	0.16	0.18

S4T_DA

Dry Season		RPS^n at end of Lead month						
SoS	ToF	0	1	2	3	4	5	6
2002-04-01	2002-10-01	0.07	0.07	0.18	0.30	0.30	0.54	0.50
2003-04-01	2003-10-01	0.62	0.00	0.03	0.11	0.05	0.05	0.00
2004-04-01	2004-10-01	0.55	0.22	0.07	0.16	0.13	0.09	0.01
RPS		0.42	0.10	0.09	0.19	0.16	0.23	0.17

S4T_DA_BC

Dry Season		RPS^n at end of Lead month						
SoS	ToF	0	1	2	3	4	5	6
2002-04-01	2002-10-01	0.04	0.04	0.05	0.05	0.09	0.36	0.36
2003-04-01	2003-10-01	0.04	0.04	0.03	0.02	0.00	0.00	0.00
2004-04-01	2004-10-01	0.21	0.19	0.01	0.04	0.02	0.03	0.01
RPS		0.10	0.09	0.03	0.04	0.04	0.13	0.12

S4TP_DA_BC

Dry Season		RPS^n at end of Lead month						
SoS	ToF	0	1	2	3	4	5	6
2002-04-01	2002-10-01	0.01	0.12	0.14	0.15	0.13	0.06	0.07
2003-04-01	2003-10-01	0.04	0.29	0.28	0.27	0.23	0.11	0.13
2004-04-01	2004-10-01	0.11	0.07	0.14	0.15	0.15	0.10	0.10
RPS		0.05	0.16	0.19	0.19	0.17	0.09	0.10